AD-A128 470 JOINT SERVICES ELECTRONICS PROGRAM(U) OHIO STATE UNIV 1/2
COLUMBUS ELECTROSCIENCE LAB DEC 82 ESL-710816-12
N00014-78-C-0049

UNCLASSIFIED F/G 20/14 NL

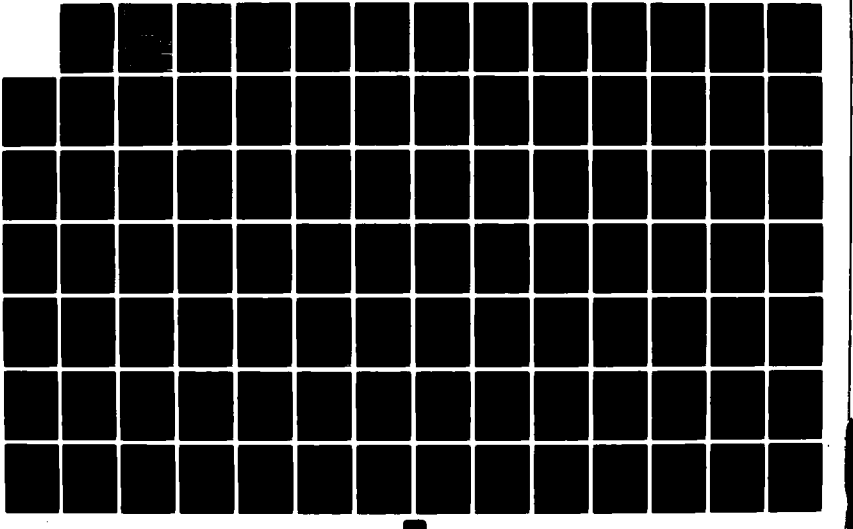

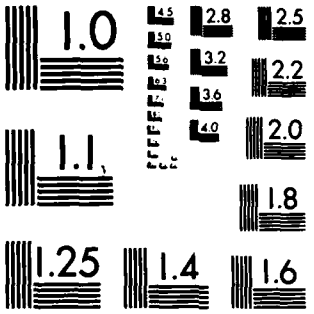

(12)

OSU

The Ohio State University

JOINT SERVICES ELECTRONICS PROGRAM

The Ohio State University

ElectroScience Laboratory

Department of Electrical Engineering
Columbus, Ohio 43212

Fifth Annual Report 710816-12

Contract N00014-78-C-0049

December 1982

Department of the Navy
Office of Naval Research
800 Quincy Street
Arlington, Virginia 22217

NOTICES

When Government drawings, specifications, or other data are used for any purpose other than in connection with a definitely related Government procurement operation, the United States Government thereby incurs no responsibility nor any obligation whatsoever, and the fact that the Government may have formulated, furnished, or in any way supplied the said drawings, specifications, or other data, is not to be regarded by implication or otherwise as in any manner licensing the holder or any other person or corporation, or conveying any rights or permission to manufacture, use, or sell any patented invention that may in any way be related thereto.

50272-101

REPORT DOCUMENTATION PAGE	1. REPORT NO.	2.	3. Recipient's Accession No.

4. Title and Subtitle

JOINT SERVICES ELECTRONICS PROGRAM

5. Report Date

December 1982

6.

7. Author(s)

8. Performing Organization Rept. No.

ESL 710816-12

9. Performing Organization Name and Address

The Ohio State University ElectroScience Laboratory
Department of Electrical Engineering
Columbus, Ohio 43212

10. Project/Task/Work Unit No.

11. Contract(C) or Grant(G) No

(C)

(G) N00014-78-C-0049

12. Sponsoring Organization Name and Address

Department of the Navy, Office of Naval Research
800 North Quincy Street
Arlington, Virginia 22217

13. Type of Report & Period Covered

Annual Report
11/81 - 11/82

14.

15. Supplementary Notes

16. Abstract (Limit: 200 words)

This report presents the fifth annual review of research at Ohio State University sponsored by the Joint Services Electronics Program (JSEP). The research is in the area of electromagnetics and the specific topics are: (1) Diffraction Studies; (2) Hybrid Techniques; (3) Antenna Studies; (4) Time Domain Studies; (5) Transient Signature Measurements of Radar Targets for Inverse Scattering Research.

17. Document Analysis a. Descriptors

b. Identifiers/Open-Ended Terms

Electromagnetics
Diffraction
Hybrid Techniques
Surface Current
Antennas
Time Domain
Polarization
Radar Target
Inverse Scattering
Transient Signature

c. COSATI Field/Group

18. Availability Statement	19. Security Class (This Report) Unclassified	21. No. of Pages 142
	20. Security Class (This Page) Unclassified	22. Price

(See ANSI-Z39.18) *See Instructions on Reverse* OPTIONAL FORM 272 (4-77)
(Formerly NTIS-35)
Department of Commerce

TABLE OF CONTENTS

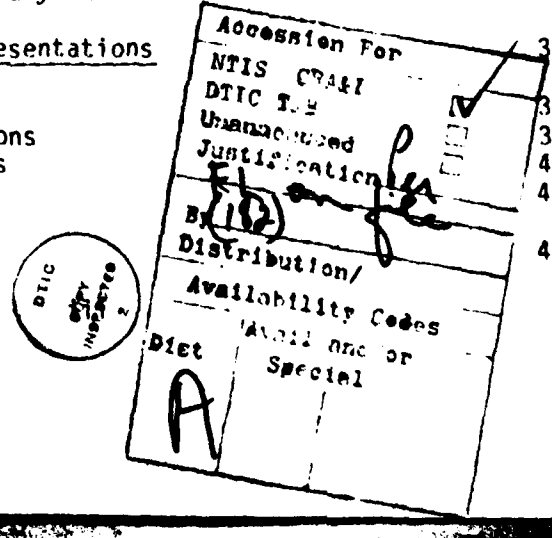

LIST OF FIGURES

I. INTRODUCTION

This report presents the fifth annual summary of research at Ohio State sponsored by the Joint Services Electronics Program (JSEP). The research is in the area of electromagnetics and the specific topics are: (1) Diffraction Studies; (2) Hybrid Techniques; (3) Antenna Studies; (4) Time Domain Studies; and (5) Transient Signature Measurements of Radar Targets for Inverse Scattering Research.

The following sections summarize the significant accomplishments of the program (Section II) and the research by work unit (Section III). Researchers and their publications are listed under each work unit. A listing of the present research programs at the Laboratory and all reports and papers published by the Laboratory during the past year are given in the appendices.

II. SIGNIFICANT ACCOMPLISHMENTS

The study of the Uniform Geometrical Theory of Diffraction continues to be one of our major efforts. This work is basic to the development of computer codes for calculating the patterns of reflector antennas and antennas on aircraft, missiles, satellites, ships and in other environments, and for calculating the radar cross section of a wide range of objects. In the present period, significant contributions were made in analyzing the diffraction from the edges of a surface impedance patch on a planar perfectly conducting surface; the radiation, scattering and diffraction from dielectric coated and impedance surfaces which are curved; the diffraction of plane, cylindrical, and surface waves by a moderately thick dielectric half plane; and the radiation from antennas mounted close to perfectly-conducting edges (and also the scattering from objects positioned at edges), as well as the problem of paraxial edge diffraction and the problem of slope diffraction by perfectly-conducting convex cylinders. The radiation studies are helping us to develop more general computer codes on other programs for the analysis of antennas on or near complex structures (e.g., aircraft and ships). The scattering work is helping on programs involving radar cross section studies and target identification.

Using a hybrid method which combines the best features of the uniform geometrical theory of diffraction and the numerical moment method technique, a numerically derived solution was previously obtained

for the diffraction by a perfectly-conducting planar surface which is smoothly terminated by a circular cylinder. This solution is very useful in optimizing practical terminations to flat plate structures such as horn antennas, and also in matching the feed waveguide to the horn resulting in substantially improved bandwidth and VSWR compared to a conventional horn. Furthermore, that numerical solution provided important clues as to the manner in which a partially uniform analytical solution for the diffraction by a discontinuity in curvature could be obtained. Recently, the latter analytical solution has been improved and a new uniform analytical expression for the diffraction by discontinuity in curvature has been developed. Also, a hybrid combination of multiple scattering and moment method techniques has been employed to arrive at a very efficient and physically appealing solution for predicting the diffraction and transmission through an aperture in a thick perfectly-conducting screen, and for the scattering by a rectangular notch in a perfectly-conducting plane surface. The latter problems are of importance in EMP studies (for calculating electromagnetic penetration through cracks) and in radar cross section studies. Additional improvements are currently being investigated.

Many practical antenna applications involve a support structure such as a ship, plane, tank, etc. One of our goals is to develop techniques for the design and analysis of antennas including support structure. We currently are employing method of moment (MM) techniques where the antennas are modelled by wire segments and/or conducting

patches and the support structure is modelled by conducting plates (patches). Existing numerical techniques only permit the modelling of perfectly conducting support structures. Our current work seeks to remove this limitation so that structures made of composite material or metal structures with absorber coating can be analyzed. During the past year, we have derived the coupled integral equations for a thin plate with a surface impedance and have begun to evaluate the self and mutual reactions required to solve these equations.

In the area of time domain studies, we have demonstrated the synthesis of K-pulse and associated response waveforms for finite-length non-uniform transmission lines. Results indicate that the inverse problem of synthesizing the parameters of the non-uniform line from measured K-pulse and response waveforms is equally tractable. The key roll of the K-pulse in factoring the system response before attempting synthesis has been clearly established in this approach, which differs from other one-dimensional inversion techniques.

In the area of transient signature measurements, the measured complex radar cross sections of several canonical targets have been assembled into the broadest coherent spectral data known to the personnal at this Laboratory. The measured transfer function, $F(j\omega)$, has been inverse Fast Fourier Transformed to obtain impulse responses of high resolution. The measurements were made for all three polarizations of the transmit and receive radar and for look angles of every 15° from 0° - 180°.

The measured results have been compared to theoretical results obtained from first-order Uniform Theory of Diffraction (UTD) solutions. Comparisons were made in both the frequency and time domains. In the impulse response, the close relation between the time axis and target geometry can be utilized to identify specific radiating mechanisms on the target. Such comparisons show great promise for a complete understanding of the scattering properties of a target.

Nine graduate students have been involved in the above research over the past year. Over the past four years, with the support of the JSEP at Ohio State, there have been 8 students granted the M.Sc. degree in Electrical Engineering and 8 students granted the Ph.D. degree in Electrical Engineering.

III. RESEARCH SUMMARY

A. Diffraction Studies

Researchers: R.G. Kouyoumjian, Professor (Phone: (614) 422-7302)
P.H. Pathak, Assistant Professor
N. Wang, Senior Research Associate
R. Tiberio, Visiting Professor and Consultant
T. Jirapunth, Graduate Research Associate
M. Buyukdura, Graduate Research Associate

Accomplishments

During the present contract period, the work accomplished in extending the uniform geometrical theory of diffraction (UTD) has been substantial. This research, and the technical papers based on this research which have recently appeared (or have been accepted for publication) are described below.

1. Diffraction by Non-Conducting Surfaces

a. Smooth dielectric covered and impedance convex surface

A study of the electromagnetic radiation and scattering from a conducting surface with dielectric loading is of great interest in that it provides an understanding of the effects of the loading on the scattered fields. An interesting application of coating is to control the electromagnetic scattering characteristics from conducitng bodies such as an aircraft, missile, satellite, etc. Also, it is useful in predicting the radar cross-section of structures made of composite materials or conducting bodies coated with dielectric materials.

In the case of a conducting surface coated with a thin layer of dielectric with a uniform thickness, the surface can be conveniently viewed as an impedance surface with a constant surface impedance. We have developed a high frequency solution for the problem and were able to predict the resonance phenomena of the radar cross-section of a circular cylinder with a constant surface impedance. It was found that surface waves with almost pure imaginary propagation constant traverse around the cylinder surface with diminishing attenuation, and interfere with each other constructively such that they add in phase to give the distinctive resonance phenomena in the radar cross-section. Numerical values for the propagation constant of the surface wave, which are related to the Regge poles of the impedance cylinder, have been found. Also, a criterion for predicting resonance has been established and

the correlations between the resonance, the Regge poles, and the natural frequencies of the impedance cylinder have been demonstrated.

It should be noted that the surface-impedance model is valid only for low-loss, thin dielectric sheets over the conducting surfaces. For a coating with moderate thickness, a more accurate approach is being pursued. More recently, work has been carried out on the investigation of the radar cross-section of a conducting cylinder coated by a dielectric layer of uniform thickness.

Using the standard Watson's transformation technique, the rigorous eigenfunction solution for the coated circular cylinder is cast into a ray solution. The backscattered field from the coated cylinder, illuminated with an incident plane wave, is obtained by summing the geometrical-optics contribution and the surface-wave contributions which include all the multiply-encircled surface waves. The parameter of fundamental importance associated with surface-wave fields is the propagation constant of the surface wave. The propagation constant is related to the Regge poles of the coated cylinder. By a combination of numerical procedures, these Regge poles were obtained by solving the high frequency approximation of the resonance equation for the dielectric coated conducting cylinder.

For thick enough coatings the surface waves moving around the cylinder resemble those trapped in a planar, grounded, dielectric slab. It is found that the dominant surface waves have a small attenuation rate so that all the multiply-encircled waves must be taken into

consideration in a self-consistent fashion. As a consequence, resonances appear in the scattering cross section. The surface wave interpretation of the resonance phenomenon and the condition for predicting the resonance frequencies are now understood. The normalized radar cross section of the coated cylinder obtained from the high frequency ray solution has been shown to compare well with the eigenfunction result.

As a continuation and extension of the work involving the backscattering from the coated cylinder, efforts have been directed to the problems of radiation and bistatic scattering from smooth, dielectric covered and/or impedance convex surfaces. The ultimate goal here is to develop a uniform high-frequency solution for the electromagnetic fields due to an antenna radiating in the presence of a loaded convex surface. This solution could be expressed in terms of an integral representation similar to the Fock-type integrals which appeared in the solution for the perfectly-conducting, smooth, convex surfaces [1,2,3] except that the Fock integral now contains a denominator in the Fock integrand which yields a resonant condition in terms of the impedance or dielectric loading. Far from the geometrical shadow boundaries, the integrals can be well approximated by the geometrical optics (GO) solution in the illuminated region and by the surface (creeping) or ray modal residue series solution in the shadow region, respectively. However, within the transition region, i.e., in the neighborhood of the shadow boundaries, only the integral representation provides the correct solution. Furthermore, this

transition integral joins smoothly with the GO solution in the lit region and reduces to the surface ray modal or residue series solution in the shadow region. Thus, the essential task is to develop an efficient method for evaluating this Fock-type transition integral associated with the smooth, dielectric-covered and impedance type convex surface.

During the previous year, the Fock (transition) integral g(x,q), associated with the canonical problem of the radiation by a two dimensional (2-D) magnetic line source on a circular cylinder with a constant surface impedance type boundary condition, has been derived and evaluated. Some preliminary numerical results for g(x,q) are presented in Figure A-1. Referring to Figure A-1, our results for a lossy curved surface (A = 0.5, 1.0) compare well with those obtained by Wait and Conda [4]. Note that g(x,q) represents the field radiated by the line source on the cylinder, or it also represents the field induced on the surface of the cylinder by a distant line source (located off the surface) via reciprocity. For a reactive surface that supports a surface wave, our results (q>0) confirm the fact that a reactive surface is more efficient than the conducting surface for guiding the electromagnetic energy. Notice that in Figure A-1, the curve denoted by q=0 is for the case of a perfectly conducting curved surface. Here, q is a parameter related to the value of the surface impedance and the cylinder radius. The shadow boundary is located at x=0 in Figure A-1.

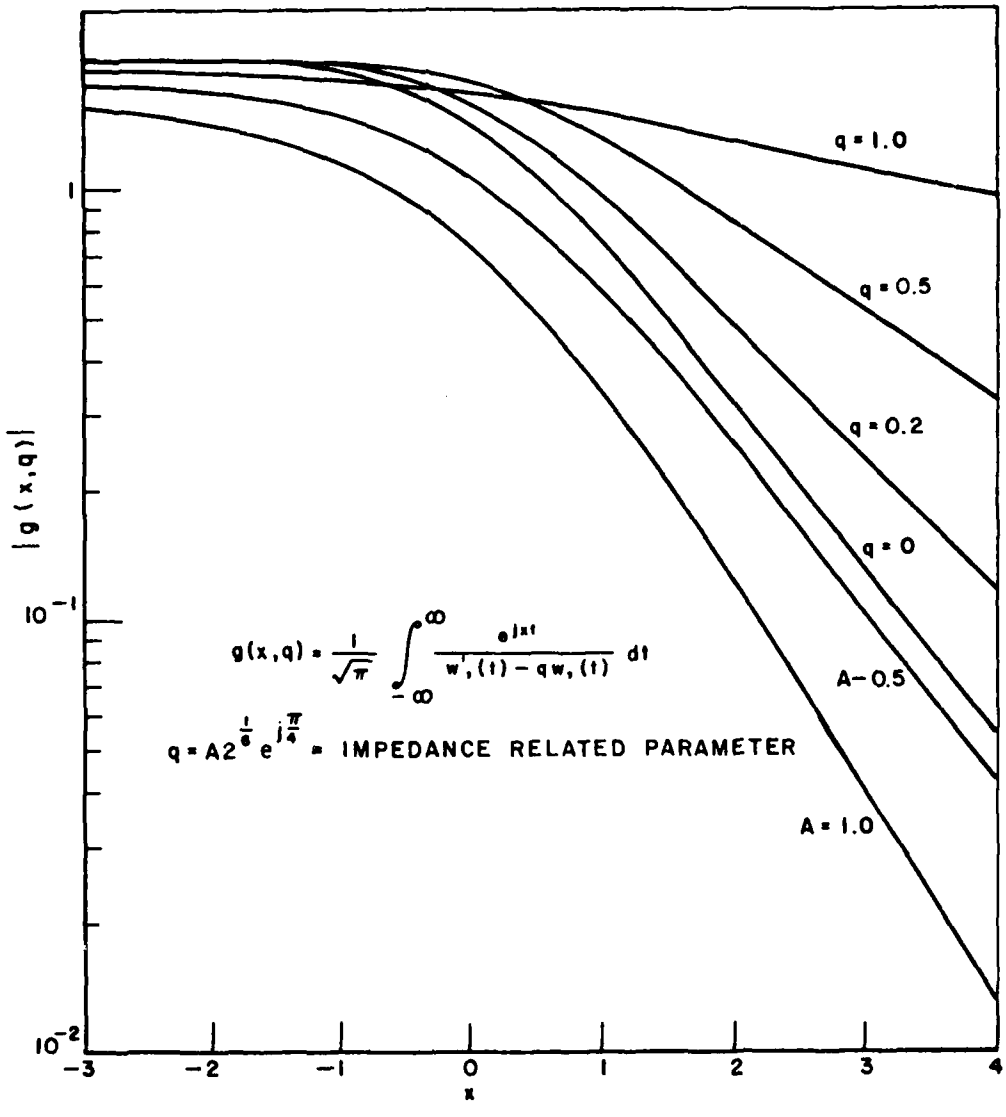

Figure A-1. The transition integral $|g(x,q)|$.

Work is now in progress to investigate the accuracy of the newly-developed high frequency solution for the canonical problem of the radiation by a 2-D magnetic line source on a circular cylinder with a reactive surface impedance boundary condition.

b. Discontinuity of surface impedance

Two papers are being prepared on the subject of asymptotic high-frequency radiation from a magnetic line source or a magnetic line dipole located on a uniform impedance surface which partially covers a perfectly-conducting surface. This work is of interest, for example, in the study of fuselage mounted airborne slot antennas for the purposes of increasing the field radiated near the horizon or shadow boundary over that which would exist in the absence of any coating. These papers which will be submitted shortly for publication are:

"An Approximate Asymptotic Analysis of the Radiation from Sources on Perfectly-Conducting Convex Cylinders with an Impedance Surface Patch", by L. Ersoy and P.H. Pathak; to be submitted for publication to the IEEE Transactions on Antennas and Propagation.

"Ray Analysis of the Radiation from Sources on Planar and Cylindrical Surfaces with an Impedance Surface Patch", by P.H. Pathak and L. Ersoy; to be submitted to J. Radio Science.

In the second paper, the impedance surface is assumed to be such that it always supports a surface wave mode* for a given source. The surface wave diffraction effects are calculated via the Uniform GTD (or UTD) which employs uniform diffraction coefficients. The latter are found from the Wiener-Hopf solutions to canonical problems of surface wave diffraction by a planar two-part surface. The first paper removes the limitations placed in the analysis pertaining to the second paper in that it is also valid for impedance surfaces which do not support a surface wave-type mode.

A natural extension of the work reported in the first paper which is proposed for future study is to treat the corresponding scattering problem where the source is no longer positioned on the surface with the impedance patch (or, alternatively, this structure may be illuminated by a plane wave). A study of the scattering from such a surface is of value in that it provides an understanding of the effect of the impedance loading on the scattered fields. An interesting application is to control the electromagnetic scattering from conducting bodies such as an aircraft, missile, or a satellite, etc. Also, it is useful in the radar cross section calculations of structures made of composite materials or of conducting bodies coated with absorber materials.

---

*Here the surface wave mode could be "strongly" trapped on the impedance boundary; this mode reduces to the "totally" trapped (or bound) surface wave mode on a planar reactive surface as the surface curvature vanishes.

An additional topic of interest which has been analyzed via ray methods is the diffraction by a strip with two face impedances when illuminated at grazing. An analysis of the backscattering from a strip with two face impedances has been performed elsewhere for special cases; on the other hand, the present analysis is valid for all aspects including the forward scatter direction when the strip is illuminated at grazing (or at edge on). It is noted that the analysis in the forward scatter direction for grazing incidence is complicated because the diffraction from the leading edge produces a non-ray optical field at the trailing edge; consequently, the diffraction of this non-ray optical field from the trailing edge which contributes to the field diffracted in the forward direction must be handled carefully. Here, the diffraction of the non-ray optical field is analyzed via a spectral extension of the geometrical theory of diffraction. A paper has been written recently which describes this work; namely:

"Scattering by a Strip with Two Face Impedances at Edge-On Incidence", by R. Tiberio, F. Bessi, G. Manara, and G. Pelosi, submitted for publication to J. Radio Science.

A second configuration of interest which has also been investigated recently, and which is somewhat related to the previous one, deals with the problem of diffraction of an electromagnetic plane wave by the edges of an impedance surface patch on a planar perfectly-conducting boundary of infinite extent. In this investigation, an asymptotic high frequency solution for the surface field is obtained. Both the TE and TM

polarizations are considered in this two-dimensional problem, and the contribution from the bound surface waves (on the impedance surface) is included in the solution. Furthermore, this analysis is further extended to treat the diffraction by a planar three-part impedance surface in which diffracted rays are produced by the illumination at the edges of the impedance surface patch that lies in the middle of that planar three-part impedance surface. A paper describing this work has been written recently, namely:

> "High Frequency Scattering From the Edges of Impedance Discontinuities on a Flat Plane", by R. Tibereo and G. Pelosi, submitted to the IEEE Transactions on Antennas and Propagation.

In the future, it is planned to extend this work to treat the diffraction by an impedance surface patch on an otherwise perfectly-conducting smooth convex surface with a source and a receiver that are located on the perfectly-conducting portions but on opposite sides of the impedance surface patch. This work would be useful in calculating the mutual coupling between a pair of antennas which are located on a perfectly-conducting planar or convex structure with a surface impedance patch that is inserted between these two antennas. The latter configuration is commonly encountered on aircraft and spacecraft structures where absorber panels are introduced between two nearby fuselage mounted antennas to increase their isolation over that which would exist without the absorber panel.

c. Diffraction by the edge of a thin dielectric half plane

The diffraction by a thin dielectric half plane is an important canonical problem in the study of the diffraction of electromagnetic waves by penetrable bodies with edges. The excitation chosen for studying this problem is either an electromagnetic plane wave, or a surface wave incident along the dielectric surface; both types of excitation are considered. For sufficiently thin dielectric half planes, solutions based on the Wiener-Hopf technique have been obtained where one initially approximates the effect of the thin dielectric slab by an equivalent impedance boundary condition. This analysis begins by bisecting the semi-infinite dielectric half plane by an electric wall in the first case, and by a magnetic wall in the second case. The problem of plane (or surface) wave diffraction by the dielectric half plane is then constructed by appropriately superimposing the corresponding solutions for the electric and magnetic wall bisections, respectively. This procedure is expected to yield a dielectric half plane diffraction coefficient which is more accurate than the one obtained recently by Anderson for the case of an incident plane wave electric field which is parallel to the edge of the thin dielectric half plane [5], because the latter analysis employs an approximate "equivalent" polarization current sheet model for the thin dielectric half plane. The approximation in [5] contains only a part of the information present in the more general approach being employed in our work; consequently, it is found that the

previous analysis in [5] yields a diffraction coefficient which is valid only for an extremely thin dielectric half plane. Furthermore, the equivalent polarization current approximation leads to a rather complicated Wiener-Hopf analysis when the magnetic field is parallel to the edge; the latter case has not been treated by Anderson [5]. It is also noted that the Wiener-Hopf factors for the case treated by Anderson [5] do not appear to be well behaved for near edge on plane wave incidence. In contrast, the Wiener-Hopf factors being employed in our work are based on Weinstein's factorization procedure [6] which appears to overcome the difficulties present in [5].

At the present time, the diffraction coefficients for the two-dimensional case of both, TE and TM, plane and surface wave excitation of the thin dielectric half-plane have been obtained, and they have been tested for accuracy. Also, these results have been extended to treat a moderately thick dielectric half plane which is excited not only by plane and surface wave fields, but also by a cylindrical wave (or line source excited) field. The Uniform GTD (UTD) solution obtained for the thin dielectric half plane suggests an ansatz upon which the aforementioned extensions to the moderately thick dielectric half plane and also cylindrical wave illumination are based.

A typical numerical result for the diffraction of a cylindrical wave by a moderately thick dielectric strip that is based on the present UTD solution is shown in Figure A-2. The UTD based result in Figure A-2 is compared with an independent numerical moment-method solution of an integral equation pertaining to this line source excited dielectric

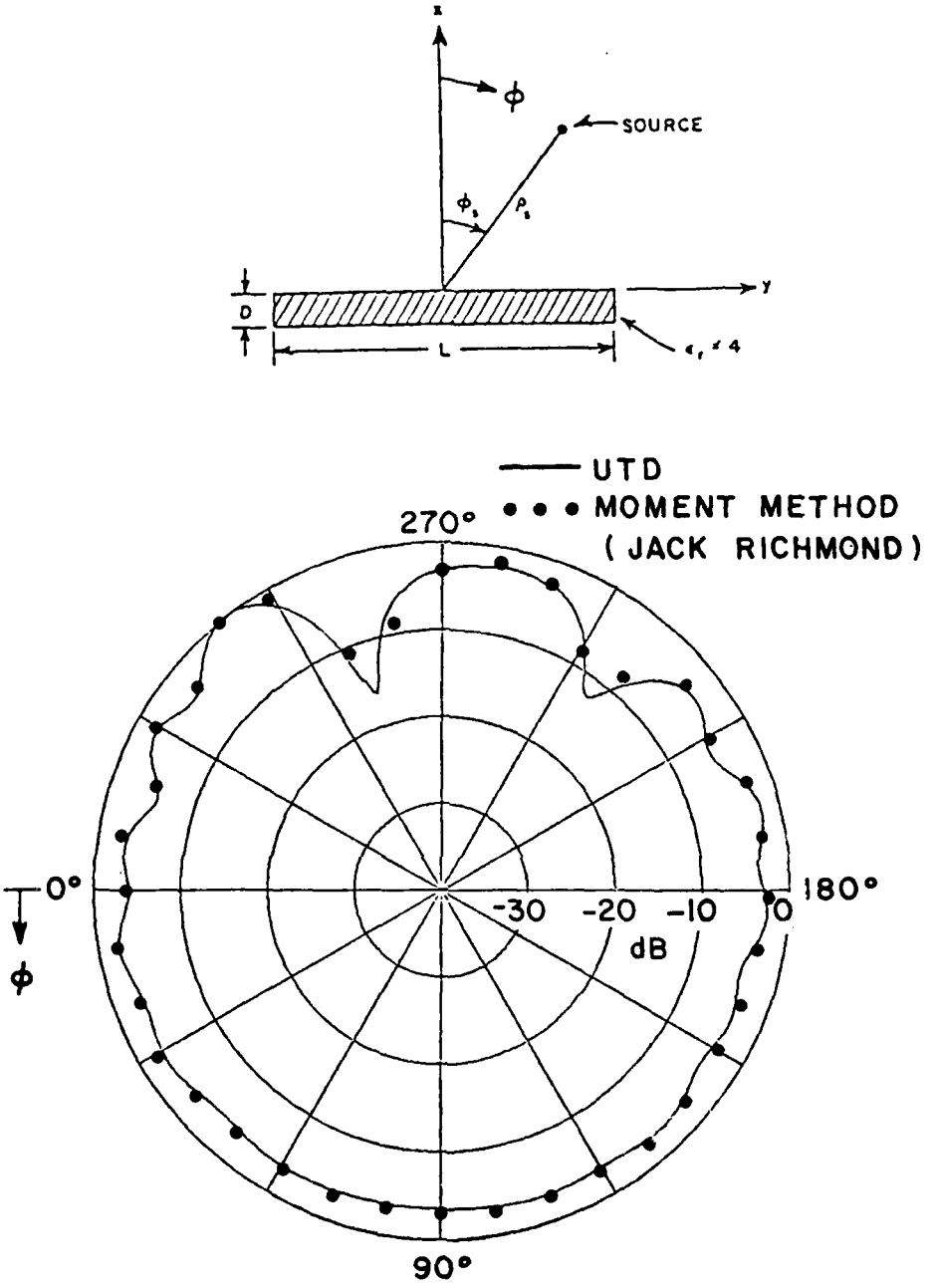

Figure A-2. Electric line source above a thin dielectric strip of $\epsilon_r=4$; $L=2\lambda$; $D=0.05\lambda$; $\phi_S=80°$; $\rho_S=1\lambda$.

strip geometry. Since the line source illuminates the strip at near grazing angles of incidence in Figure A-2, it is especially important in this near grazing incidence case to include surface wave diffraction effects as well. Figure A-3 shows all the dominant singly and multiply diffracted rays whose contributions are included for calculating the pattern in Figure A-2. It is noted from the pattern in Figure A-2 that the total UTD field is continuous at the reflection and transmission shadow boundaries as it should be; furthermore, the very close agreement between the totally independent UTD and moment method solution in Figure A-2 (and also in other cases which are not shown here) is indeed gratifying.

In the next phase of this study, the two-dimensional (2-D) solutions obtained recently will be generalized to treat the three-dimensional (3-D) problems of the diffraction of obliquely incident plane, conical, and spherical waves, and obliquely incident surface waves by a thin (or at most moderately thick) dielectric half-plane. These important generalizations are not trivial because an obliquely incident plane wave is expected to launch both TE and TM type surface waves at the edge of the dielectric half plane. In other words, a mode coupling between TE and TM surface waves obliquely incident on the edge of a dielectric half plane is possible. Consequently, the generalization of the two dimensional (2-D) solutions to treat the corresponding three dimensional (3-D) problems is not expected to be straightforward. It is also noted that even though a relationship

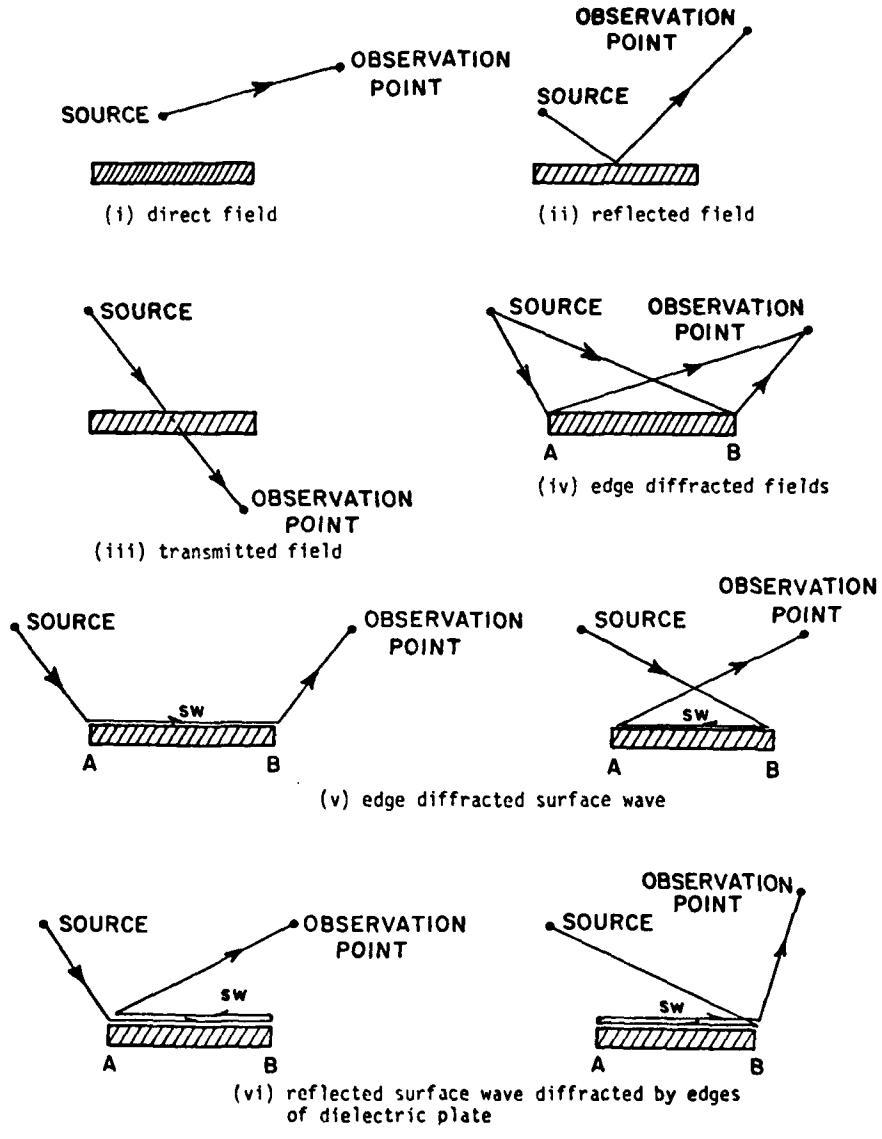

Figure A-3. Dominant rays whose field contributions are included in calculating the pattern of Figure A-2.

exists between the 2-D and 3-D solutions, this is not a direct relationship of the type which would allow the 3-D solutions to be constructed in a simple way from the 2-D solutions as is possible for the case of a perfectly conducting half plane. The 3-D dielectric half plane diffraction solution may also be of interest in the area of integrated optics and millimeter wave integrated circuits where open dielectric guide structures are employed.

A paper describing the 2-D solution which has been obtained for the problem of the diffraction of a plane, cylindrical or a surface wave field by a thin (or moderately thick) dielectric half plane is currently in preparation.

2. Perfectly-Conducting Surfaces

a. Vertex diffraction

In many practical antenna problems one encounters situations where an antenna radiates in the presence of finite, planar structures with edges which terminate in a vertex (or corner), e.g., an antenna radiating in the presence of a finite, rectangular ground plane. Also, flat plates with edges are used in the modeling of aircraft wings and vertical or horizontal stabilizers for analyzing on-aircraft antenna patterns. In the above problems, the antenna pattern is affected by the diffraction of electromagnetic waves not only by the edges, but also by the vertices or corners. Thus, the analysis of vertex diffraction is an important problem.

A formally exact eigenfunction solution has been obtained earlier at the ElectroScience Laboratory [7]; however, this solution is not given in terms of simple functions and it is, therefore, quite difficult to implement in the GTD format. Nevertheless, this convergent solution is of great value in numerically checking approximate high-frequency solutions obtained by asymptotic methods. More will be said about this later in this section.

Approximate, asymptotic high-frequency solutions to the vertex or corner diffraction problem have been presented for the acoustic case [8,9]. While these solutions constitute a first step in obtaining useful solutions, they are not uniform in that the vertex diffraction coefficient obtained is not valid along the vertex and edge shadow boundaries where the edge and vertex diffracted fields assume their greatest magnitude and importance. Some initial work on vertex diffraction recently pursued at the ElectroScience Laboratory has led to a simple, approximate vertex diffraction coefficient which appears to work reasonably well for certain cases. However, this result has been obtained heuristically, and it needs to be improved in order for it to be useful in the general situations encountered in practice; nevertheless, this diffraction coefficient offers some clues for constructing the more refined and useful vertex diffraction coefficient, which we expect to obtain from asymptotic analysis.

The canonical geometry presented in Figure A-4 locally models a typical vertex in a finite, planar, perfectly-conducting surface. In general, a vertex in a planar surface is formed by the intersection of

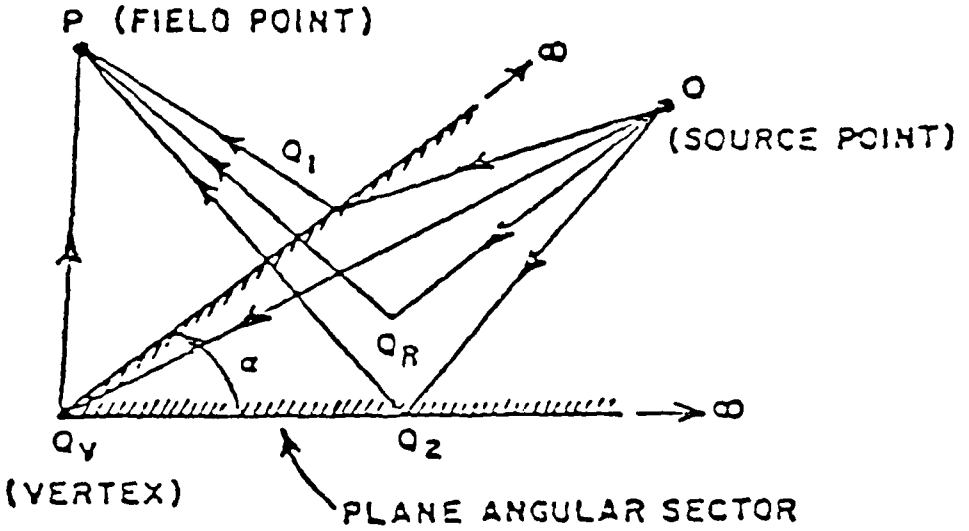

Figure A-4. Various rays associated with the diffraction of waves by a plane angular sector.

two otherwise smooth, curved edges which constitute two of the other boundaries of the surface. The angle α, shown in Figure A-4, is the internal angle enclosed by the tangents at the vertex to each of the two intersecting curved edges.

The asymptotic high-frequency analysis of electromagnetic vertex diffraction is rather complicated. Vertices not only shadow the incident field, but they also shadow the edge diffracted fields. The shadow boundary of an edge diffracted field is a conical surface whose tip coincides with the vertex and whose axis is an extension of the shadowed edge. The vertex introduces a diffracted ray which penetrates

the shadow regions; moreover, the vertex diffracted field must also compensate the discontinuties in the incident and edge diffracted fields at their shadow boundaries. At these boundaries the vertex diffracted field assumes its largest magnitude and, hence, its greatest importance. If the vertex diffracted field is omitted in the GTD solution, then substantial discontinuities connected with the shadowing of the incident and edge diffracted fields may occur in the calculated radiation pattern.

The high frequency solution to this canonical problem may be carried out by asymptotically evaluating an integral representation for the fields scattered by the plane angular sector. The current on the plane angular sector which appears in the integral for the scattered field may be approximated by the local half-plane currents near the edges, by the geometrical optics currents in the interior region, and, near the vertex, by the first few terms of the eigenfunction solution [7] or an approximate quasi-static solution. The asymptotic evaluation of the integral representation for the scattered field would be based on the method of stationary phase. Three types of critical points shown in Figure A-4 are involved; an interior point Q_R associated with the geometrical optics reflected field, edge points Q_1 and Q_2 associated with the edge diffracted fields, and a critical point at the vertex Q_v associated with the vertex diffracted field. During the past year, we employed this approach starting with the geometrical optics current. A uniform asymptotic approximation of the integral representation of the

scattered field, which is valid at a confluence of the aforementioned critical points, has not yet been obtained. It may be necessary to settle for a solution which is partially uniform, i.e., there would be one solution for the transition regions of the shadow and reflection boundaries, and a second solution valid outside the transition regions where the critical points are isolated. To be useful, the two solutions must overlap.

As was mentioned earlier, a convergent solution would be valuable in checking the diffraction coefficient obtained by asymptotic methods. Therefore an effort has been made to accurately determine the dyadic Green's function for the plane angular sector. As explained below the problem largely reduces to finding the eigenvalues and eigenfunctions of the Lame' equations.

To find the dyadic Green's function we begin by expanding it in terms of a complete set of vector wave functions which are solutions of the vector wave equation along with the radiation condition and the boundary conditions at the surface of the sector. The vector wave functions, in turn, are expressed in terms of scalar wave functions which are solutions to the scalar wave equation with the appropriate boundary conditions. Both Neumann and Dirichlet type boundary conditions must be satisfied to yield a complete set of vector wave functions. The final step of the solution involves separating the scalar wave equation in the sphero-conal coordinate system. The resulting separated equations include the spherical Bessel equation and

two Lame' equations (one with periodic boundary conditions and the other with nonperiodic boundary conditions) which are coupled through the two eigenvalues which are actually the separation constants. It is precisely these eigenvalue pairs which serve as the summation index of the free space dyadic Green's function solution.

The solution is thus ultimately reduced to solving for the eigenvalues and eigenfunctions of the separated Lame' equations. It is then a straightforward procedure to construct the vector wave functions and hence the dyadic Green's function. Once this is found one can proceed to investigate a wide variety of problems because of the versatility and general nature of the Greens's function solutions.

There is no known closed form solution to the Lame' equations and one is therefore attracted to an infinite series solution. Earlier work used Fourier sine and cosine series representations, but these resulted in the need to solve two simultaneous infinite continued fraction equations for the eigenvalues and eigenvectors. This solution proves to be numerically formidable, and indeed, almost impossible for higher order eigenvalues because of the rapidly varying nature of the continued fractions. Therefore, during the past year, we employed Legendre functions as a basis set for one of the Lame equations. At first, this approach seemed promising, but later, difficulties were encountered in attempting to implement it numerically. The sine and cosine series representations are better suited for this purpose, and recently, Saholos [10] has used these functions to develop a method of calculation

which is more efficient and accurate than the one mentioned earlier. We plan to study his method before doing further work on this problem; it may be adequate for purpose of calculating the dyadic Green's function for the plane angular sector.

During the past year we have worked on the special case of the dyadic Green's function where $\alpha = \pi$ and the plane angular sector reduces to a half plane. This is discussed in the following section.

b. Paraxial diffraction (grazing incidence to the axis)

i) At edges

In the case of grazing incidence to the edge of a wedge, convergent representations for the electromagnetic field in the paraxial region in terms of cylindrical wave functions [11] or other representation based thereon (such as the UTD) fail. As was mentioned in the last section, the dyadic Green's function for the plane angular sector can be applied to the half-plane by letting the sector angle go to 180°. The Lame differential equations decouple and the eigenvalues and eigenfunctions are easily found; furthermore, this solution can be extended to the wedge without difficulty. An advantage of this solution for the dyadic Green's function of the wedge is that it can be used when the field and the source point are close to the edge. This should make it possible to extend the UTD solution [12] to the paraxial region, i.e., to grazing incidence on the edge, and to study the propagation of edge waves. These waves are important in analyzing the scattering from plates

illuminated at or near grazing incidence or in treating the coupling between monopoles or slots near the edge of a wedge.

The spherical wave functions used to construct this dyadic Green's function are products of spherical Bessel (or Hankel) functions, trigonometric functions and Ferrer type associated Legendre functions. A fast, accurate algorithm for calculating Ferrer type functions has been developed. Furthermore, the new dyadic Green's function is complete in the sense that it remains valid when the field and source points coincide.

The above solution was checked numerically by calculating the far-zone fields due to a dipole near the edge and comparing the results with those obtained from the UTD [12]. Aspects sufficiently far from grazing were chosen so that the UTD [12] would be valid. The patterns calculated by the two methods were found to be in excellent agreement. Examples of this comparison appear in Figures A-5 and A-6. The location of the dipole is defined by r', θ', ϕ'; the relevant geometry is shown in the insert of Figure A-5. To compare the θ-and ϕ-components, the pattern in Figure A-6 should be lowered by 3.65 dB.

It should be noted that the eigenfunction solution was checked against a more accurate (improved) version of the UTD solution [13] in which the matrix form of the diffraction coefficient contains non-zero off-diagonal elements, i.e., $\hat{\phi}'\hat{\theta}$ and $\hat{\theta}'\hat{\phi}$ terms, together with $\hat{r}'\hat{\phi}$ and $\hat{r}'\hat{\theta}$ elements due to the radial components of the incident field. These elements were determined by retaining all the derivatives of the longitudinal (edge directed) components of the field used to obtain the

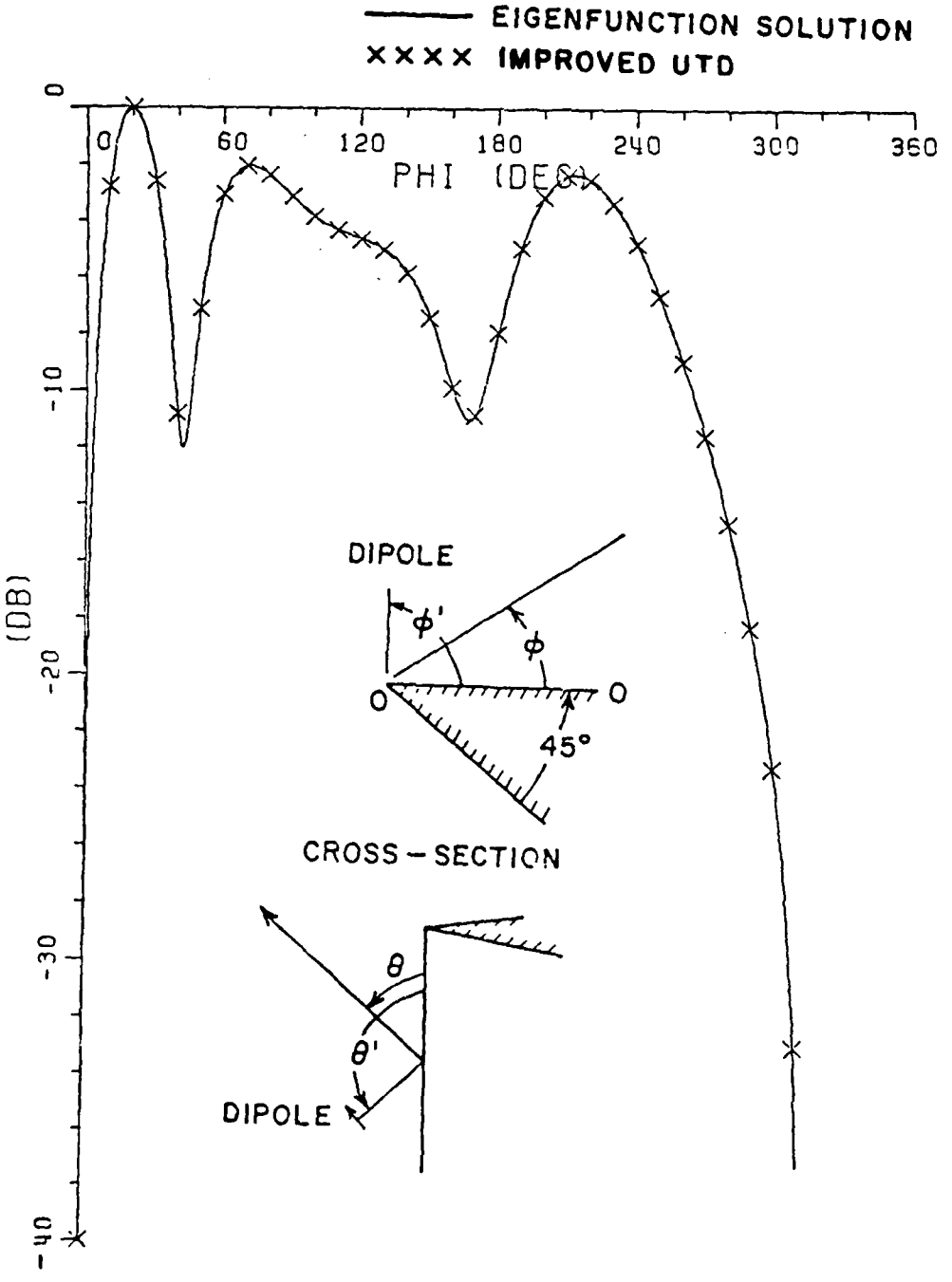

Figure A-5. θ-component of the total electric field due to a θ' directed dipole at $R'=\lambda$, $\phi'=90°$, $\theta'=120°$, $\theta=60°$.

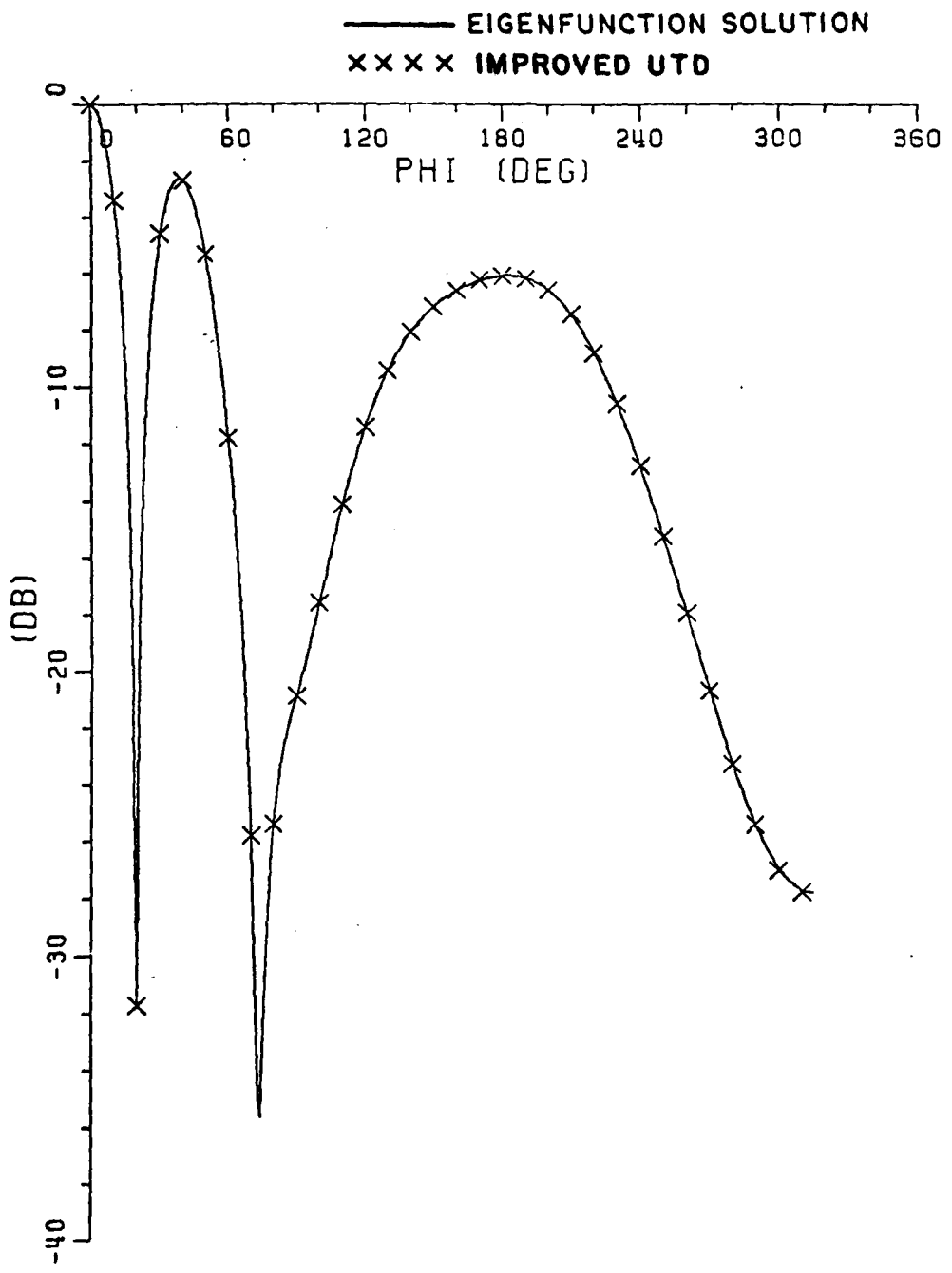

Figure A-6. ϕ-component of the total electric field due to a θ' directed dipole at $R'=\lambda$, $\phi'=90°$, $\theta'=120°$, $\theta=60°$.

transverse components. Then two asymptotic methods were used to determine the improved UTD solution; one of these is described in [13]. Thus, a dipole close to the edge gives rise to a diffracted field which is cross polarized with respect to the orientation of the dipole in the ray-fixed coordinate system, as well as a co-polarized component given by the ordinary UTD [12].

Expressions for the electromagnetic field in the paraxial region of the edge were obtained from the new dyadic Green's function, and as expected, a wave guided by the edge is evident when the interior wedge angle is less than 180°. The form of this wave is independent of the orientation of the exciting dipole, and its strength increases as the wedge angle decreases.

The solution for the wedge was then extended to the case where there is a spherical boss at the edge. Again, a complete dyadic Green's function was found which is expressed in terms of the same transcendental functions. Expressions obtained from this solution show that for the case of an electrically small boss. The paraxial region field is the sum of the field of the dipole source radiating in the presence of the wedge and a field scattered directly from the boss. The form of the latter field is exactly the same as that obtained previously for the field and source points close to the edge.

An irregular shaped object placed on the edge was considered next. A generalized T-Matrix method was developed which makes use of the dyadic Green's function for the wedge. This method was then applied to the problem of the scattering from a spherical boss as a special case

of an irregular object at the edge. The results were compared with the solution using the exact dyadic Green's function for this problem, which was mentioned in the preceding paragraph, and were found to be identical. This approach may be useful in treating the diffraction from a rough edge.

ii) At smooth, quasi-cylindrical surfaces

Several papers were written (under the JSEP program) and published [1,2,3] which describe Uniform GTD (UTD) solutions for the diffraction by perfectly-conducting convex surfaces. In particular, efficient UTD solutions for the problems of the radiation from sources both off and on a convex surface and the mutual coupling between sources on a convex surface were presented in [1,2,3]. These UTD solutions, for the problems of scattering, radiation, and mutual coupling, which are associated with the radiation by antennas in the presence of an arbitrary, smooth perfectly-conducting convex surface that is electrically large represent an important and useful contribution to the area of ray methods for analyzing the EM radiation and scattering from complex structures. It is noted that the effects of surface ray torsion on the diffracted fields are explicitly identified in these solutions. Here, the diffracted fields are associated with surface rays as well as with rays shed from the surface rays. It is noted that these surface rays on a convex surface traverse geodesic paths which in general are torsional; i.e., the surface ray paths are twisted (or they do not lie in a plane).

While the above mentioned UTD solutions for sources on or off a smooth perfectly-conducting convex surface are valid under very general conditions, they must be modified within the paraxial regions. For example, these solutions must be modified for an observation point (either on or off the surface) which lies in the paraxial region of an elongated or cigar shaped (quasi-cylindrical) convex surface whenever the rays from the source to that observation point traverse paths which lie within the paraxial zone. Presently, useful expressions for the field within the paraxial region of a quasi-cylindrical smooth convex surface which is electrically large are not available. Consequently, work has been initiated on this subject so that the proper paraxial field expressions can be found. An analysis of this problem involves the use of special asymptotic high frequency approximations for the integral representation of the field within the paraxial region of a point source excited canonical circular cylinder geometry. The results for the canonical circular cylinder case would then be generalized to treat the quasi-cylindrical smooth convex surface according to the usual geometrical theory of diffraction prescription.

Presently, the solution in [3] for the surface fields of a source on a convex surface (as in the mutual coupling problem for antennas on a convex surface) has been generalized so that it remains accurate within the paraxial zone. That generalized surface field solution offers clues as to the manner in which the radiation solution in [2] may be generalized so that it remains valid in the paraxial zone; this aspect is presently under study and some progress is being made. When the

latter study is completed, then the solution in [1] for the scattering problem will also be generalized as a next step so that it remains valid within the paraxial zone of elongated (quasi-cylindrical) convex bodies.

c. Slope diffraction

If the field incident at the edge of a wedge or the shadow boundary of a convex surface has a rapid spatial variation, a slope diffraction term must be added to the ordinary UTD. The slope diffraction term is proportional to the spatial derivatives of the incident field. It ensures that the spatial derivatives of the resulting radiation pattern are continuous at the shadow and reflection boundaries so that there are no "kinks" in the calculated pattern.

The derivation of slope diffraction terms for wedges and circular cylinders was described in the preceding annual report. Since that time, a dissertation based on this work has been written [14], and the slope diffraction analysis of the circular cylinder has been extended to the convex cylinder.

In Figure A-7, the total electric field of an electric line dipole illuminating a perfectly conducting convex cylinder is shown. The electric field incident from this line source vanishes at shadow boundary SB_I so that only the slope diffracted field is excited at this boundary. The pattern calculated from the UTD with slope diffraction included is seen to be in very good agreement with that calculated from a moment method solution.

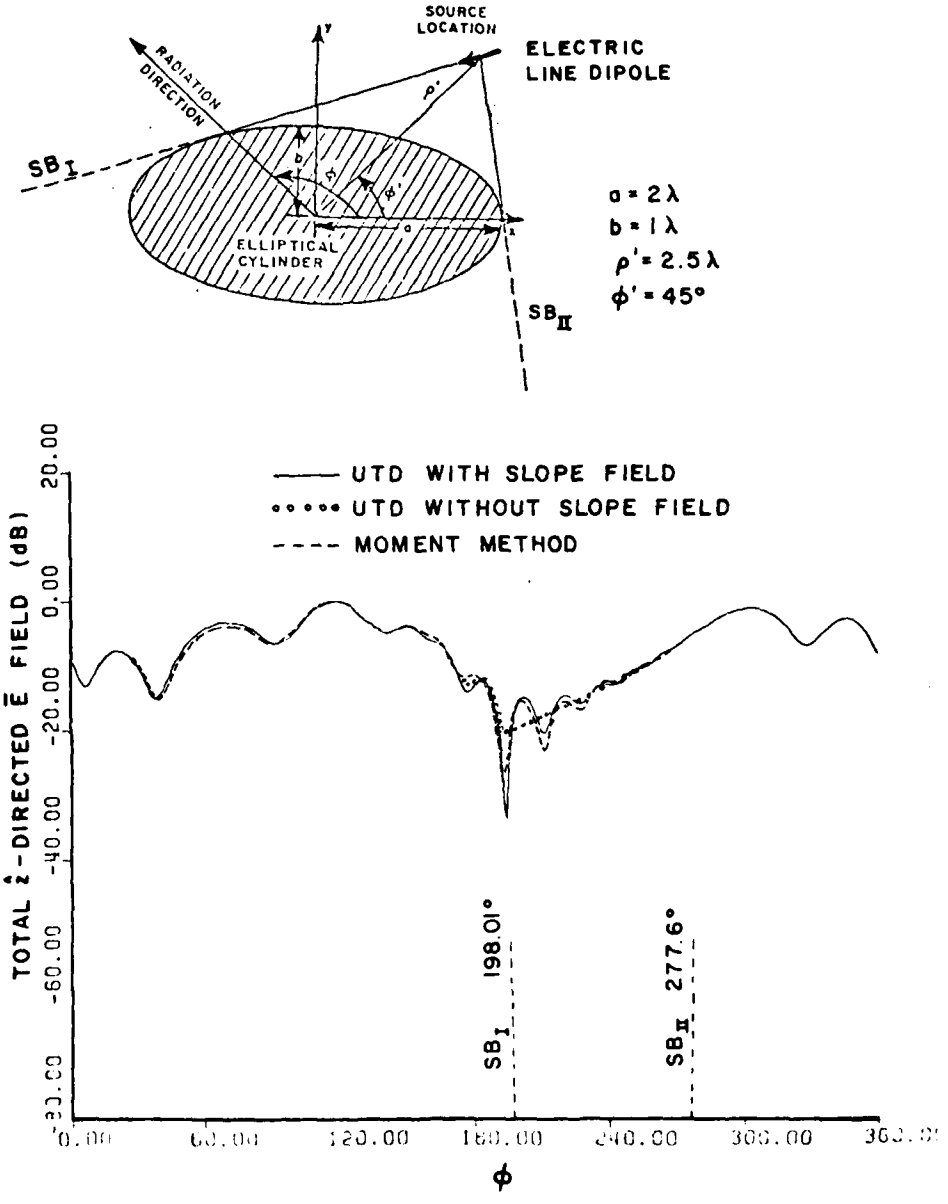

Figure A-7. Effects of the slope diffraction of an incident electric line dipole field by a perfectly-conducting elliptic cylinder.

3. Diffraction of Non-Ray Optical Fields

a. Shadow boundary field incident

Two papers have been written on the diffraction by a pair of nearby, parallel edges, where one edge lies on the shadow boundary of the other; they are:

"An Analysis of Diffraction at Edges Illuminated by Transition Region Fields", by R. Tiberio and R.G. Kouyoumjian, Journal of Radio Science, Vol. 17, No. 2, March-April 1982, pp. 323-336.

"Calculation of the High-Frequency Diffraction by Two Nearby Edges Illuminated at Grazing Incidence", by R. Tiberio and R.G. Kouyoumjian, accepted for publication in IEEE Transactions on Antennas and Propagation.

The configurations treated in these papers may be a part of practical antenna and scattering geometries. The solution of this problem requires an extension of the uniform GTD, which is valid only for ray-optical fields incident on the edge, because the shadow boundary field illuminating the second edge is not a ray-optical field. The analysis and calculations described in the two papers were restricted to perfectly-conducting surfaces; however, this work has since been extended to non-conducting surfaces as described in Section 1b.

b. Source close to an edge

In the conventional form of the Uniform GTD, it is assumed that the incident field is a ray-optical field, which implies that it is polarized in a direction perpendicular to the incident ray. In general, this requires that the source of the incident field be sufficiently far from the point of diffraction so that the component of the incident field parallel to its ray path (the component in the radial direction from the source) is negligible at the diffraction point. However, in some applications this is not the case, e.g., a monopole antenna may be mounted at or very close to the edge of a ship or the edges of wings and stabilizers. This case is also of interest in the development of the Hybrid GTD/Moment Method solution, where it is desired to calculate the input impedance of a wire antenna close to an edge. Recently, the UTD solution has been extended so that it may be used to calculate the fields of dipoles which are only a few tenths of a wavelength from the edge [13]. That paper [13] is also listed below for completeness:

R.G. Kouyoumjian, G. Pelosi and R. Tiberio, "An Extension of The Uniform GTD for the Diffraction by a Wedge Illuminated by a Dipole Close to It's Edge", to appear in Alta Frequenza

4. Caustic Field Analysis

The GTD is a very convenient and accurate procedure for analyzing high frequency radiation, scattering, and diffraction problems. However, the GTD suffers from a limitation inherent in ray methods; namely, it cannot be employed directly to evaluate fields at and near focal points or caustics of ray systems. The field at caustics must, therefore, be found from separate considerations [15,16].

In certain problems such as in the diffraction by smooth, closed convex surfaces or by surfaces with a ring-type edge discontinuity, it is possible to employ the GTD indirectly to evaluate the fields in the caustic regions via the equivalent ring current method [17,18]. However, even the equivalent ring current method fails if the incident or reflection shadow boundaries are near or on a caustic.

The recently developed uniform GTD (or UTD) solution for the scattering and diffraction of waves by a convex surface [1,2,3] offers clues as to how it may be employed indirectly to obtain the far zone fields in caustic regions where the surface is illuminated by a distant source. In the latter case, the shadow boundary and caustic transition regions tend to overlap. The far zone fields in the near axial direction of a closed surface of revolution illuminated by an axially directed plane wave can be expressed in terms of an equivalent ring current contribution plus a dominant term which may be interpreted as an "effective aperture integral". The latter integral can be evaluated in

closed form. In the near zone, where the shadow boundary and caustic directions are sufficiently far apart, only the equivalent ring current contribution must remain significant. Presently, such a solution has been developed for the special case of axial incidence on a rotationally symmetric convex surface (or revolution). The generalization of that solution to treat non-axial incidence and also closed convex surfaces which are not necessarily surfaces of revolution forms the subject of future investigation.

Publications and Presentations

1. Articles

Please refer to the section entitled "Accomplishments", which describes the progress to date on the research topics together with the list of publications.

2. Oral Presentations

a. "Ray Analysis of EM Scattering by a Finite Length Hollow Circular Cylinder", C.C. Huang and P.H. Pathak; 1982 International IEEE AP-S/URSI Symposium held 24-28 May, 1982 at Albuquerque, New Mexico.

b. "Slope Diffraction for Convex Surfaces and Wedges", R.G. Kouyoumjian, T. Veruttipong and P.H. Pathak; 1982 International IEEE AP-S/URSI Symposium held 24-28 May, 1982 at Albuquerque, New Mexico.

3. Invited Lectures

a. "A Uniform GTD Approach to EM Scattering and Radiation", by R.G. Kouyoumjian and P.H. Pathak presented at the Workshop/ Symposium on Research Techniques in Wave Propagation and Scattering, sponsored by U.S. Army Research Office, U.S. Office of Naval Research, and the Ohio State University at The Ohio State University, October 18-21, 1982.

b. "EM Diffraction by a Thin Dielectric Half Plane", by P.H. Pathak and R. Rojas-Teran, presented at the Workshop/ Symposium on Research Techniques in Wave Propagation and Scattering, sponsored by U.S. Army Research Office, U.S. Office of Naval Research, and the Ohio State University at The Ohio State University, October 18-21, 1982.

c. "Uniform Geometrical Theory of Diffraction", by P.H. Pathak, presented at the Meeting of the International Society for Optical Engineering, San Diego, California, August 24-25, 1982.

4. Dissertations

"Diffraction at Edges and Convex Surfaces Illuminated by Fields with a Rapid Spatial Variation", Ph.D. Dissertation by Thavath Veruttipong, The Ohio State University, 1982.

References

[1] Pathak, P.H., W.D. Burnside and R.J. Marhefka, "A Uniform GTD Analysis of the Scattering of Electromagnetic Waves by a Smooth Convex Surface", IEEE Transactions on Antennas and Propagation, Vol. AP-28, No. 5, September 1980, pp. 631-642.

[2] Pathak, P.H., N.N. Wang, W.D. Burnside and R.G. Kouyoumjian, "A Uniform GTD Solution for the Radiation from Sources on a Perfectly-Conducting Convex Surface", IEEE Transactions on Antennas and Propagation, Vol. AP-29, No.4, July 1982, pp. 609-621.

[3] Pathak, P.H. and N.N. Wang, "Ray Analysis of mutual Coupling Between Antennas on a Convex Surface", IEEE Transactions on Antennas and Propagation, Vol. AP-29, No. 6, November 1981, pp. 911-922.

[4] Wait, J.R. and A. M. Conda, "Pattern of an Antenna on a Curved Lossy Surface", IEEE Transactions on Antennas and Propagation, Vol. AP-6, No. 4, October 1958, pp. 348-359.

[5] Anderson, I., "Plane Wave Diffraction by a Thin Dielectric Half Plane", IEEE Trans. Antennas and Propagation, Vol. AP-27, pp. 584-589, September 1979.

[6] Weinstein, L.A., The Theory of Diffraction and the Factorization Method, The Golem Press, Boulder, Colorado, 1969.

[7] Satterwhite, R., and R.G. Kouyoumjian, "Electromagnetic Diffraction by a Perfectly-Conducting Plane Angular Sector", Report 2183-2, 1970, The Ohio State University ElectroScience Laboratory, Department of Electrical Engineering; prepared under Contract AF 19(628)-5929 for Air Force Cambridge Research Laboratories.

[8] Keller, J.B., R.M. Lewis, and B.D. Seckler, "Diffraction by an Aperture II", Journal of Appl. Physics, Vol. 28, No. 5, May 1957.

[9] Braumbek, W., Z. Physik; 127, p. 381 (1950).

[10] Sahalos, J., Private Communication.

[11] Tai, C.T., Dyadic Green's Functions in Electromagnetic Theory, Intext Educational Pulbishers, 1971.

[12] Kouyoumjian, R.G. and P.H. Pathak, "A Uniform Geometrical Theory of Diffraction for an Edge in a Pefectly-Conducting Surface", Proc. IEEE, Vol. 62, pp. 1448-1461, 1974.

[13] Kouyoumjian, R.G., G. Pelosi and R. Tibereo, "An Extension of the Uniform GTD for the Diffractin by a Wedge Illuminated by a Dipole Close to Its Edge", Alta Frequenza (to appear).

[14] Veruttipong, Thavath, "Diffraction at Edges and Convex Surfaces Illuminated by Fields with a Rapid Spatial Variation", Ph.D. Dissertation, The Ohio State University, 1982.

[15] Kay, I. and J.D. Keller, "Asymptotic Evaluation of the Field at a Casutic", J. Appl. Physics, Vol. 25, No. 7, pp. 876-886, July 1954.

[16] Ludwig, D., "Uniform Asymptotic Expansions at a Caustic", Commun. Pure Appl. Math, 19, pp. 215-25, 1966.

[17] Burnside, W.D. and L. Peters, Jr., "Radar Cross Section of Finite Cones by the Equivalent current Concept with Higher Order Diffraction", J. Radio Science, Vol. 7, No. 10, pp. 943-948, October 1972.

[18] Knott, E.F. and T.B.A. Senior, "A Comparison of Three High-Frequency Diffraction Techniques", Proc. IEEE, Vol. 62, No. 11, pp. 1468-1474, November 1974.

B. Hybrid Techniques

Researchers: P.H. Pathak, Assistant Professor
(Phone: (614) 422-6097)
C.D. Chuang, Senior Research Associate
S. Shrikanth, Graduate Research Associate

A General Description of Research Topics and Accomplishments

The method of moments (MM) provides a means of solving electromagnetic boundary value problems in terms of a set of simultaneous linear equations. In general, the electromagnetic boundary value problem is formulated as an integral equation for the unknown surface fields on the antenna or scatterer and the integral equation is then reduced to a system of equations by expanding the unknown in terms of a basis set and by enforcing this expansion to satisfy the boundary conditions in some average sense through the use of testing functions. However, the MM procedure can become inefficient and cumbersome if the number of unknowns (coefficient of the expansion or basis functions) becomes large as is the case for antennas or scatterers which are not small in terms of wavelength. On the other hand, the geometrical theory of diffraction (GTD) exploits the local nature of high frequency wave propagation, diffraction, and radiation, thereby reducing the antenna radiation or scattering problem to calculating the fields associated with just a few rays emanating from edges, tips, and shadow boundaries (of smooth convex surfaces), and also from other discontinuities in the geometrical and electrical properties of the antenna or scatterer. Although the GTD

is a high frequency technique, it works rather well, even for structures which are only moderately large in terms of the wavelength. However, the use of the GTD is limited by the number of available diffraction coefficients for characterizing a particular type of electrical and/or geometrical discontinuity. It is obvious that a procedure is desirable which would overcome the limitations of the individual MM and GTD approaches. Such a procedure, referred to as the "hybrid" GTD-MM procedure, can indeed overcome the limitations of the individual MM and GTD approaches by actually combining the best features of both methods. In particular, GTD provides the form of the local field over any part of the antenna or scattering structure, which is at least moderately large in terms of the wavelength; hence, the form of the GTD field could be viewed as a set of basis functions for the expansion of the unknowns in the MM formulation. The unknown coefficient associated with this type of GTD basis or expansion functions is then the diffraction coefficient for the surface field calculations if the unknown in the integral equation happens to be the surface field. Thus, by using the local GTD field form outside the region where the structure is small in terms of the wavelength, the number of unknowns is thereby vastly reduced in the MM procedure. The expansion for the unknown within regions (of the structure) which are small in terms of wavelength, is of course, done according to the conventional MM approach (perhaps using a subsectional basis set such as rectangular pulses, etc). Clearly, the hybrid GTD-MM procedure can solve problems far more efficiently than the MM procedure

as the frequency increases. Also, it can provide a useful check on future diffraction coefficients as and when they become available.

While the hybrid GTD-MM procedure will in general be employed to obtain diffraction coefficients, other hybrid techniques which combine ray methods and numerical methods different from the MM procedure will also be studied. Thus, in a broader sense, the area of hybrid techniques will emphasize useful combinations of high frequency or ray techniques with numerical methods for solving a variety of interesting and useful electromagnetic radiation and scattering problems.

Presently, two classes of diffraction problems are being investigated; namely, the diffraction by perfectly-conducting structures involving special edge or tip type discontinuities, and the diffraction by discontinuities associated with the junction of dielectric and perfectly-conducting structures which are connected in special ways. In particular, the problems in the first catagory are the problems of diffraction by a discontinuity in surface curvature (e.g., the smooth join of a half plane and a cylinder); by an edge type discontinuity in an otherwise smooth convex surface; by the tip of a cone type structure; by the tip of a semi-infinite wire; and by an aperture in a thick screen (and related configurations). The problems in the second catagory are the problems of diffraction by a truncated dielectric slab recessed in a perfectly-conducting structure as in Figure B-1(a), by the junction of a dielectric half plane which is joined to a thick perfectly-conducting half plane as in Figure B-1(b); and the problem

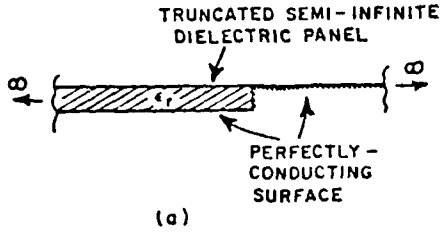

(a)

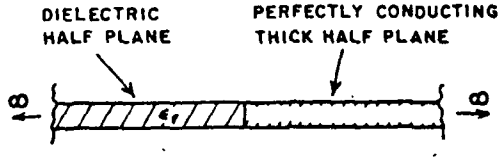

(b)

Figure B-1. Discontinuity formed by the junction of a dielectric and perfectly-conducting structure.

of the radiation of a single element or an array of electrically small microstrip patch antennas which are placed conformally on an electrically large perfectly-conducting smooth convex surface (such as the fuselage of an aircraft or a missile). The latter problem, as depicted in Figure B-2, requires a combination of low frequency techniques (for handling the electrically small microstrip patches) with the high frequency ray technique (for handling the electrically large convex surface).

During the present period, progress has been made in arriving at a new and improved diffraction coefficient for a discontinuity in surface curvature; this contribution which is valid for a perfectly-conducting surface, is described in more detail in the following section. Also,

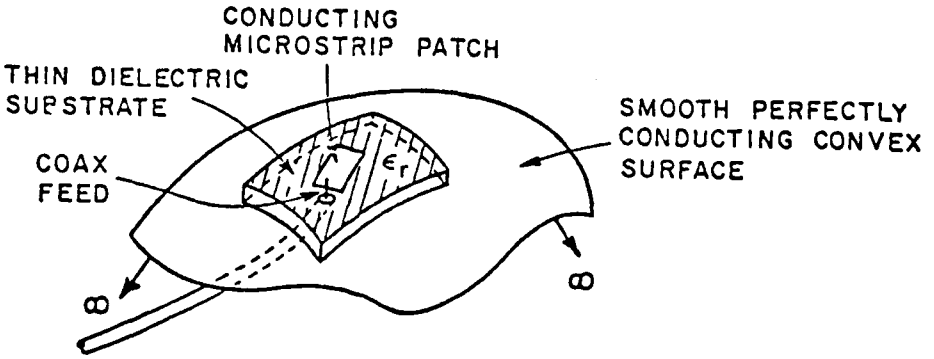

Figure B-2. Microstrip antenna element on a convex surface.

work has been initiated and some progress has been made in treating the problems of the diffraction by an edge in an otherwise smooth perfectly-conducting convex surface; by an aperture in a thick conducting screen (and a related configuration); and by the dielectric-conductor junction of Figure B-1(b). The work on the diffraction by an aperture in a thick screen is also described in some detail in the next section. Research on the problem of the diffraction by an edge in an otherwise smooth convex surface will be reported in more detail in the future as more complete results on this topic become available. Work on the problem in Figure B-1(b) will also be reported in more detail at a later time as that problem is currently under investigation. It is noted that the problems in Figures B-1(a) and B-2 are of great interest; however, time does not permit one to attempt to solve all of these problems simultaneously. The order in which these problems are to be completed will depend partly on their complexity. It is clear that the problems being addressed in both catagories, namely, in the catagory dealing with perfectly-conducting surfaces with special types of edge and tip type discontinuities, and the catagory dealing with the junction of dielectric and conducting structures, are of importance in the areas of antenna design and scattering (RCS) calculations which one needs to deal with in real world situations.

The following section summarizes in some detail the results obtained on the work dealing with the diffraction by a discontinuity in surface curvature, and with the diffraction by an aperture in a thick screen.

1. Diffraction by a Perfectly-Conducting Surface with a Discontinuity in Surface Curvature

We reported in our last (1981) Annual Report on JSEP [1], a diffraction coefficient for a curved surface/curved surface junction which has a discontinuity in curvature. The appropriate two-dimensional geometry is shown in Figure B-3. The curvature is discontinuous at 0, such that a jump in the reflected ray field occurs at the reflection boundary where $\phi+\phi'=\pi$. The diffracted ray field via the diffraction coefficient has the desired feature at the boundary of reflection, i.e., that it is discontinuous across the reflection boundary and compensates the discontinuity in the reflected ray field. However, away from the reflection boundary, the approximate solution of the diffraction coefficient does not agree with that obtained by Senior [2]. It is noted that the solution in [2] is not valid at and near the reflection boundary ($\phi+\phi'=\pi$). An improved version of the diffraction coefficient which shows agreement with [2] where [2] is valid, and which also remains valid within the reflection boundary transition region (around $\phi+\phi'=\pi$) has been obtained recently; that diffraction coefficient is given by

$$D_{\substack{s\\h}} = \frac{e^{-j\pi/4}}{\sqrt{2\pi k}} \frac{C_{\substack{s\\h}}(\xi_1)F(X_1)-C_{\substack{s\\h}}(\xi_2)F(X_2)}{\cos\phi+\cos\phi'}$$

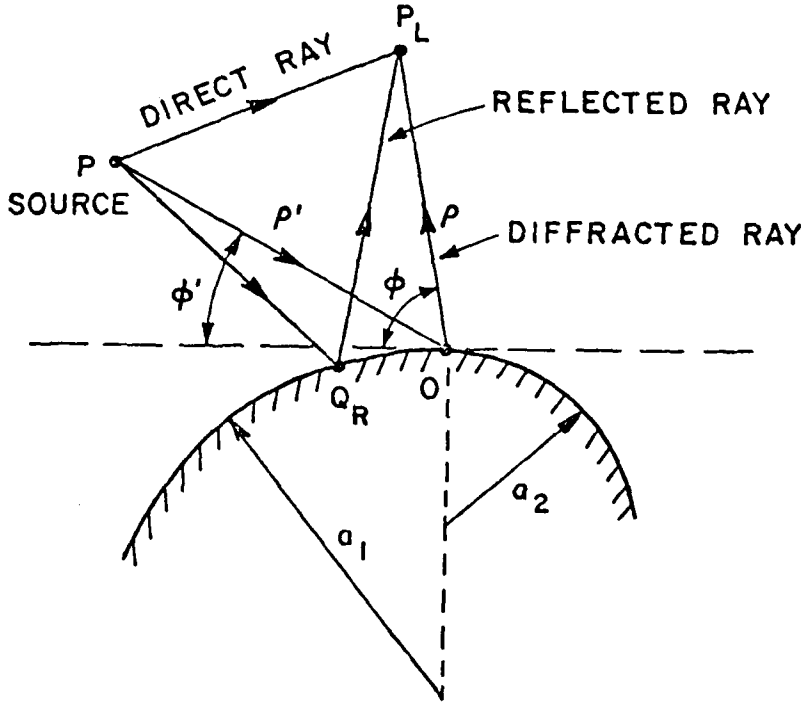

Figure B-3. Diffraction due to curvature discontinuity.

where

$$C_{s,h}(\xi_{1,2}) = \frac{2\cos\left(\frac{\phi-\phi'}{2}\right)}{a_{1,2}} \left\{\frac{1}{2} \sqrt{\frac{L}{\pi X}}\, F(X) + M_{1,2} \sqrt{\frac{2}{k}}\, q^{*}_{s,h}(\xi_{1,2})\right\}$$

$$e^{-j\pi/4 - j(\xi_{1,2})^3/13}$$

$$\xi_{1,2} = -2M_{1,2} \cos\left(\frac{\phi-\phi'}{2}\right)$$

$$M_{1,2} = (ka_{1,2}/2)^{1/3}$$

$$L = \frac{\rho\rho'}{\rho+\rho'}$$

$$X = 2kL \cos^2\left(\frac{\phi-\phi'}{2}\right)$$

$$X_{1,2} = \frac{ka_{1,2}(\cos\phi+\cos\phi')^2}{4\cos\left(\frac{\phi-\phi'}{2}\right)\left[1+\left(\frac{1}{\rho}+\frac{1}{\rho'}\right)\frac{a_{1,2}}{2}\cos\left(\frac{\phi-\phi'}{2}\right)\right]}$$

$$F(X) = 2j\sqrt{x}\, e^{jx} \int_{\sqrt{x}}^{\infty} e^{-jt^2}\, dt$$

$q_{s,h}(\xi)$ = a Pekeris function.

This diffraction coefficient is derived for the case where the source is off the conducting cylinder. When the source is moved close to the cylinder, as in the case where a_1 becomes infinite and $\phi'=0$, a more accurate diffraction coefficient should be applied; the latter

diffraction coefficient has been obtained previously using the GTD-MM hybrid technique under JSEP, and it has been published, along with its applications, in two papers [3,4]. In addition, we have also obtained a more efficient analytical expression of this diffraction coefficient for the ($a_1 \to \infty$; $\phi'=0$) case; it is given below.

In Figure B-3, let $a_1 \to \infty$, $a_2=a$ and a plane wave (hard case) is incident from the direction $\phi'=0$. Then the asymptotic approximation of the diffraction coefficient is

$$D_h = \frac{e^{-j\pi/4}}{2\sqrt{2\pi k}}\left\{-\tan\frac{\phi}{2}F(2k\rho\cos^2\frac{\phi}{2})+j\xi e^{j\xi^3/3}\begin{bmatrix}\bar{\xi}\tan\frac{\phi}{2}\int_{\xi}^{\infty}J(\alpha-\xi)e^{-j\alpha^3/3}d\alpha \\ -2\cot\phi\int_{\xi}^{\infty}(\alpha-\xi)J(\alpha-\xi)e^{-j\alpha^3/3}d\alpha\end{bmatrix}\right\}$$

where $\xi = 2M\left(\sin\frac{\phi}{2}\right)^{2/3}\cot\frac{\phi}{2}$

$$M = (ka/2)^{1/3}$$

and $J(X)$ satisfies

$$J(X) = e^{-jX^3/6}\left[1 - \frac{2}{\sqrt{\pi}}e^{-j\pi/4}\int_0^{\varepsilon}e^{jz^2}\,dz\right]$$

$$- \frac{e^{-j\pi/4}}{4}\sqrt{\frac{2}{\pi}}\int_0^{X}(X-\tau)^{1/2}J(\tau)e^{-j(x-\tau)^3/24}\,d\tau$$

with

$$\varepsilon = \left(\frac{x}{2}\right)^{3/2} .$$

A paper will be prepared to publish this formula.

2. Diffraction by an Aperture in a Thick Perfectly-Conducting Screen (and by a Related Configuration)

Figure B-4(a) illustrates an aperture in a thick perfectly-conducting screen excited by a line source; whereas, Figure B-4(b) illustrates the same configuration as in Figure B-4(a) but with a short circuit (closed) back end so that there can be no transmission of energy through the aperture onto the other side of the screen. Both of these problems in Figures B-4(a) and B-4(b) are of interest not only because they constitute basic diffraction problems, but also because of their relevance to technology. For example, the configuration of Figure B-4(a) is useful in the design of optical devices, and in the estimation of electromagnetic coupling through apertures for electromagnetic pulse (EMP) applications. Also, the configurations in Figures B-4(a) and B-4(b) are of significant interest in electromagnetic scattering and radar cross section (RCS) studies. In EMP and RCS applications, it is not uncommon to require one to consider a wide frequency band over which the scattering and transmission through apertures is of interest. Clearly, at high frequencies, ray methods can be employed, whereas at moderately large and low frequencies, a hybrid combination of ray and moment-method techniques would be more efficient and accurate. It is noted that even at moderately high frequencies, a moment method solution of this problem by itself would become extremely cumbersome and costly; thus, the need for a hybrid solution which combines the efficiency and the best features of low and high frequency techniques.

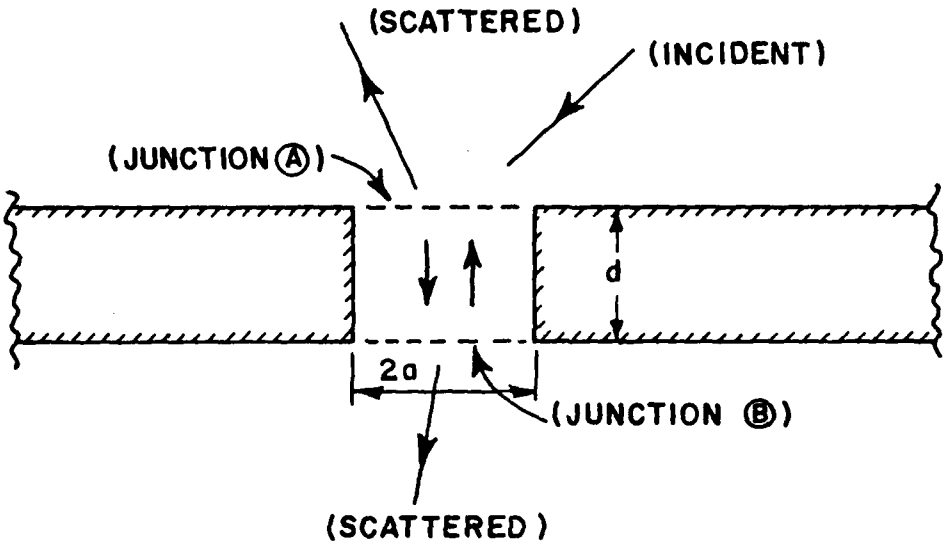

Figure B-4(a). Diffraction by an aperture in a thick perfectly-conducting screen.

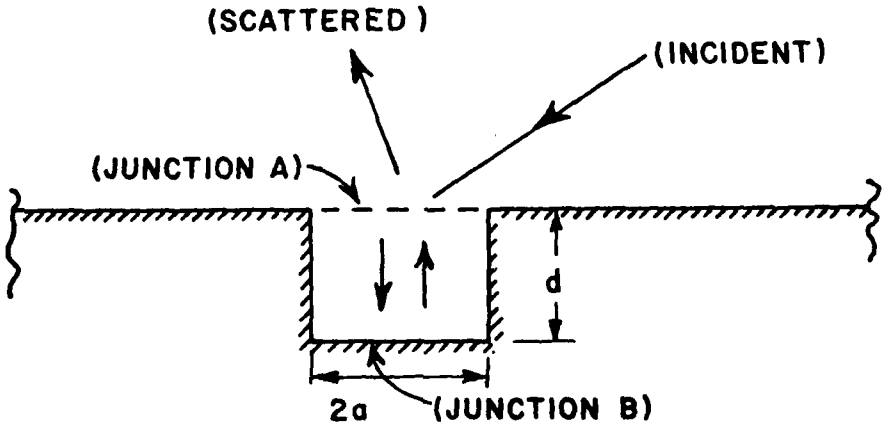

Figure B-4(b). Diffraction by a notch in a planar perfectly conducting boundary.

Presently, the problems in Figures B-4(a) and B-4(b) have been analyzed by a combination of moment-method and the multiple scattering method. The multiple scattering method isolates all the pertinent scattering mechanisms associated with the entrance and exit planes (or junctions A and B) of the aperture in a thick screen as shown in Figures B-4(a) and B-4(b); the latter feature is very useful in providing information on ways to control the scattering contributions from the different interactions. Furthermore, the multiple scattering procedure allows one to analyze the problems in Figures B-4(a) and B-4(b) via a very efficient moment method procedure which involves only "one" matrix (integral operator) inversion even though there are two junctions A and B, provided one employs a special Green's function as the kernel (within the integral operator) corresponding to the integral equation for the unknown fields over the junction C shown in Figure B-5. The special Green's function here pertains to a planar, perfectly-conducting surface of infinite extent which short circuits the aperture (junction C). This special Green's function reduces the computation of the unknown fields to only the finite extent of the aperture (or over junction C of Figure B-5); a computation of the unknown electric current (or tangential magnetic field) on the perfectly-conducting screen (of infinite extent) is thus not required. Some numerical examples illustrating the accuracy of the present approach are presented in Figures B-6 through B-8. The unknown field at junction C (Figure B-5) is expanded in terms of a set of rectangular pulse (sub-sectional) type basis functions for the calculations shown in Figures B-6 through B-8.

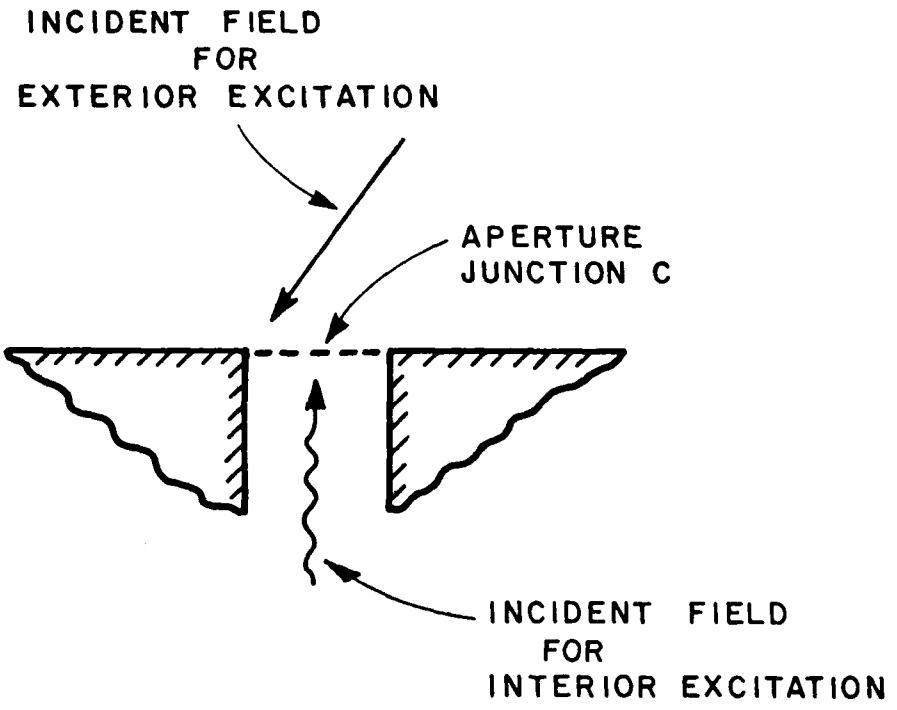

Figure B-5. Canonical problem.

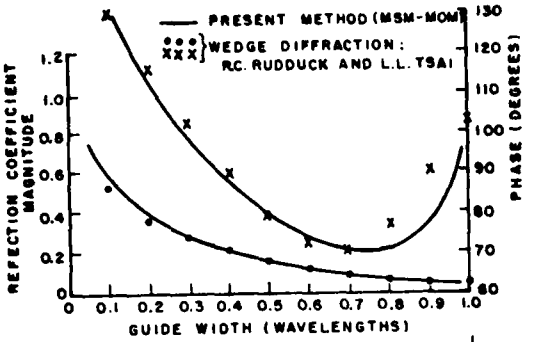

a) TEM reflection coefficient of a flanged waveguide (Note: work of Rudduck & Tsai appears in IEEE Trans. AP-16, No.1,1968).

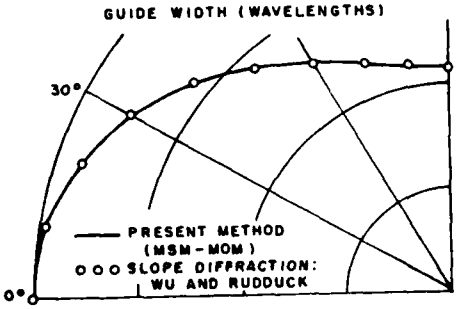

b) Radiation pattern (in dB) of a TEM-excited flanged waveguide (Note: work of Wu & Rudduck appears in OSU ElectroScience Lab. Tech. Report 1691-29, 1968).

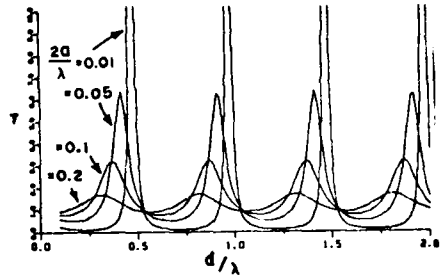

c) Transmission coefficient P_{trans}/P_{inc} for aperture of Fig. B-4(a) (Note: these results and those obtained by Harrington and Auckland in IEEE AP-28, No. 5, 1980 are almost indistinguishable).

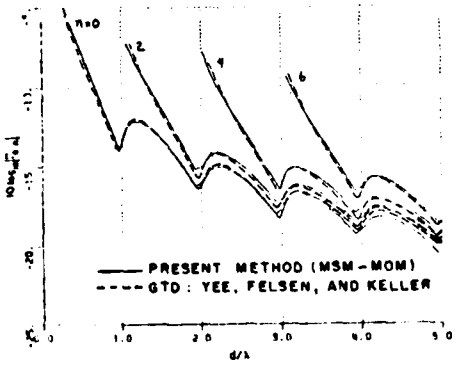

d) TM_{oo} incident to TM_{on} reflection coefficient of a flanged waveguide (Note: work of Yee, Felsen & Keller appears in SIAM J. Appl. Math, Vol. 16, Vol. 1b, No. 2, 1968).

Figure B-6. Comparison of present solution with other available solutions for special cases.

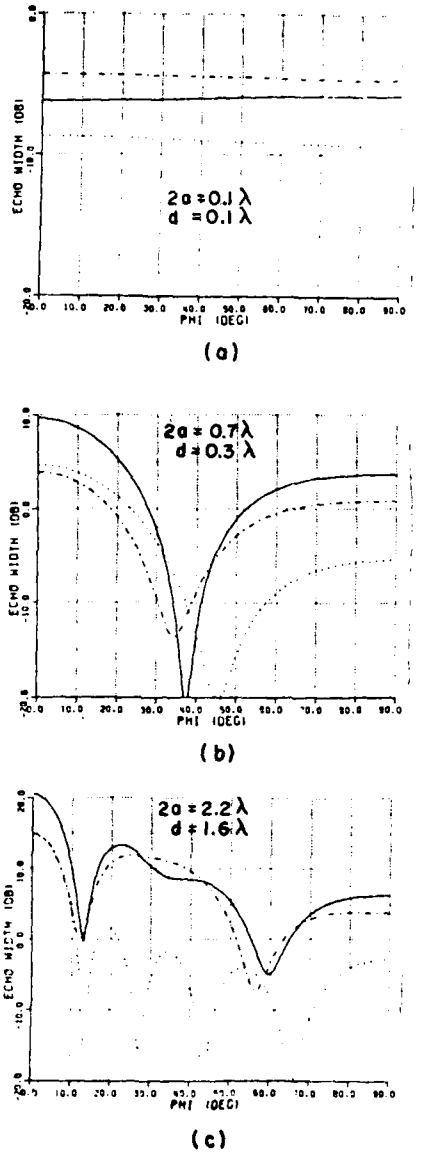

Figure B-7. Echo widths for geometry represented in Figure B-4(a).

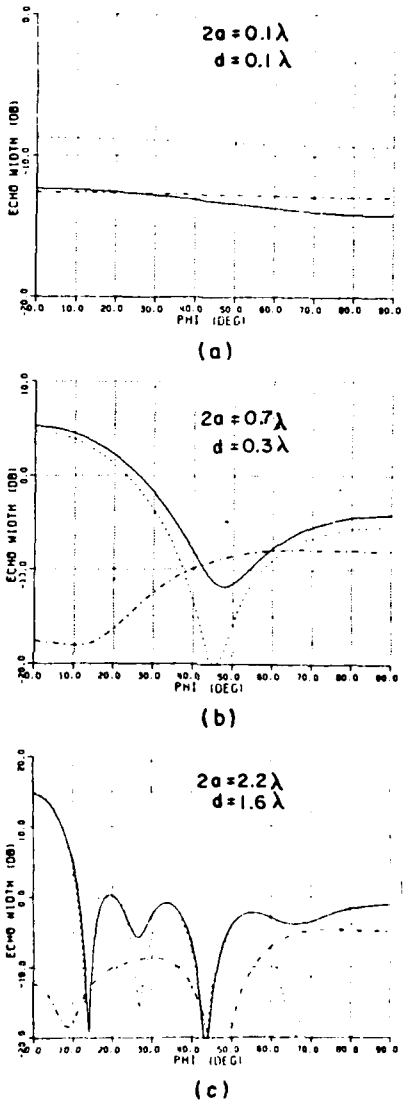

Figure B-8. Echo widths for geometry represented in Figure B-4(a).

A further reduction of the unknowns in the aperture junction C (of Figure B-5) is currently under way. Rather than expressing (or expanding) the unknown field over the entire junction C in terms of a set of subsectional basis functions (as is usually customary in moment methods), we are considering a far smaller combination of a few subsectional basis functions only near the edges of the aperture (junction C) together with ray type expansion (basis) functions elsewhere in the aperture (junction C). The form of the latter ray type basis functions is available from the high frequency uniform GTD (or UTD) solution for the diffraction by an edge [5]. Thus, the hybrid combination of GTD, moment method, and the multiple scattering method are being employed to arrive at a highly efficient, accurate, and physically appealing solution to the problems in Figures B-4(a) and B-4(b).

Publications

1. W.D. Burnside and C.W. Chuang, "An Aperture-Matched Horn Design", IEEE Transactions on Antennas and Propagation, Vol. 30, July 1982, p. 790.

References

[1] "Joint Service Electronics Program", report 710816-11, December 1981, The Ohio State University ElectroScience Laboratory, Department of Electrical Engineering; prepared under Contract N00014-78-C-0049 for Office of Naval Research, Department of the Navy.

[2] Senior, T.B.A., "The Diffraction Matrix for a Discontinuity in Curvature", IEEE Trans. Ant. and Propagation, Vol. 20, p. 326, May 1972.

[3] Chuang, C.W. and W.D. Burnside, "A Diffraction Coefficient for a Cylindrically Truncated Planar Surface", IEEE Trans. on Antennas and Prop., Vol. 28, p. 177, March 1980.

[4] Burnside, W.D. and C.W. Chuang, "An Aperture-Matched Horn Design", IEEE Trans. on Antennas and Prop. Vol. 30, p. 790, July 1982.

[5] Kouyoumjian, R.G., P.H. Pathak and W.D. Burnside, "A Uniform GTD for the Diffraction by Edges, Vertices, and Convex Surfaces", 65 pages in Theoretical Methods for Determining the Interaction of Electromagnetic Waves with Structures, ed., ∪ K. Skwirzynski, Sitjhoff and Noordhoff, Netherlands, 1981.

C. Antenna Studies

Researchers: Dr. E.H. Newman, Research Scientist (Phone: (604) 422-4999)

Dr. R.J. Garbacz, Professor

P. Alexandropoulos, Graduate Research Associate

M.R. Schrote, Graduate Research Associate

Introduction and Background

The long term goal of our work is the development of techniques for the design and analysis of antennas including their support structure. We are employing method of moments (MM) techniques, and thus the structures should be less than several wavelengths in extent. The antennas are modelled by an interconnection of straight wire segments. By properly arranging the segments, one can easily model dipoles, loops, helices, etc., and arrays of the above. The support structure is modelled as an interconnection of perfectly conducting plates. By using rectangular and/or polygonal plates, we have modelled airplanes, ships, buildings, etc. Also, to increase the generality of the solution, we allow wire to plate junctions, even near the edge of a plate. The above work is described in References [1-8].

Our existing techniques only permit the modelling of perfectly conducting support structures, since we use perfectly conducting plates. Our current work seeks to remove this limitation. Examples of finitely

conducting surfaces are a metal surface with an absorptive coating to reduce scattering (RCS), or the use of composite material to reduce weight. In choosing a technique to model the finitely conducting surfaces, we desire a solution which "fits" into the solution format used for perfectly conducting plates. Thus, treating the finitely conducting plates will be an addition, modification or generalization of the solution for perfectly conducting plates. We choose to model the finite conductivity by allowing for a surface impedance, including the case where the surface impedance on the top surface of the plate is different from that on the bottom. Below we will derive a pair of coupled integral equations for the current on a plate with surface impedance Z_T on the top surface and Z_B on the bottom surface.

Figure C-1 shows an edge view of a typical plate. The plate is shown as having a thickness t so that we can clearly define the two sides of the plate, and t will be considered as vanishingly small. Consider that the plate is illuminated by the known currents $(\underline{J}_i, \underline{M}_i)$ which produce the known incident fields $(\underline{E}_i, \underline{H}_i)$ in free space. Using the surface equivalence principal, the plate can be replaced with free space if the equivalent currents

$$\underline{J} = \hat{n} \times \underline{H} \tag{C-1}$$

$$\underline{M} = \underline{E} \times \hat{n} \tag{C-2}$$

are placed on the surface, S, of the plate. Here $(\underline{E}, \underline{H})$ are the total fields and n is the outward normal to the surface S.

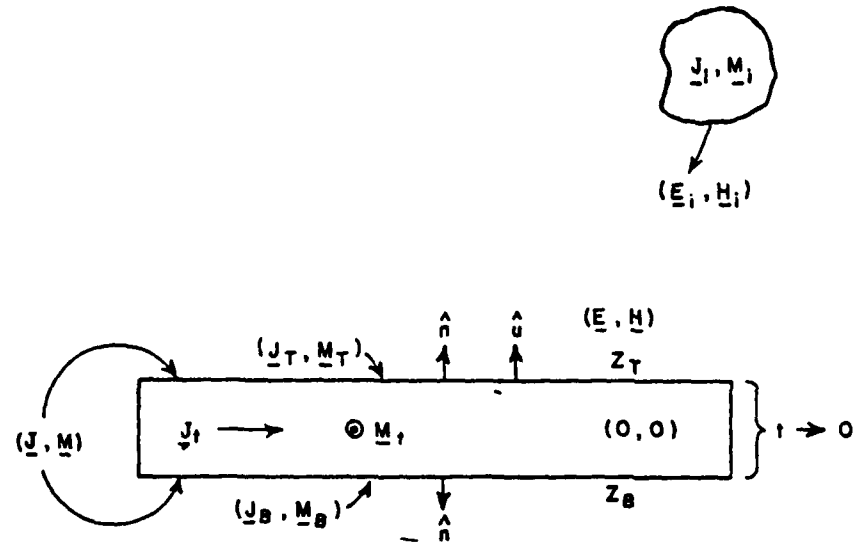

Figure C-1. Currents on a plate with surface impedance.

Since, in the equivalent problem, there is a null field interior to S, there will be zero reaction between a test source $(\underline{J}_t,\underline{M}_t)$ interior to S, and the sources $(\underline{J},\underline{M})$ and $(\underline{J}_i,\underline{M}_i)$. Thus,

$$\langle(\underline{J},\underline{M}),\ (\underline{J}_t,\underline{M}_t)\rangle + \langle(\underline{J}_i,\underline{M}_i),\ (\underline{J}_t,\underline{M}_t)\rangle = 0 \qquad \text{(C-3)}$$

or

$$\int_S \underline{J}_t \cdot (\underline{E}_s + \underline{E}_i) - \underline{M}_t \cdot (\underline{H}_s + \underline{H}_i)\, ds = 0 \qquad \text{(C-4)}$$

where $(\underline{E}_s,\underline{H}_s)$ are the scattered fields, i.e., the fields radiated by $(\underline{J},\underline{M})$ in free-space. It is clear from Equation (C-4) that if only electric test sources are used, then only the electric field boundary condition is satisfied. If only magnetic test sources are used, then only the magnetic field boundary condition is satisfied. Here we will

use electric and magnetic test sources. In this case both electric and magnetic field boundary conditions will be satisfied and we will have enough information to determine how $(\underline{J},\underline{M})$ distribute between the top and bottom surfaces of the plate.

Using reciprocity, Equation (C-4) can be written

$$\int_S \underline{E}_t \cdot \underline{J} - \underline{H}_t \cdot \underline{M}\, ds = -\int \underline{E}_t \cdot \underline{J}_i - \underline{H}_t \cdot \underline{M}_i\, dv \ , \qquad \text{(C-5)}$$

or

$$\langle(\underline{J}_t,\underline{M}_t)\ (\underline{J},\underline{M})\rangle = -\langle(\underline{J}_t,\underline{M}_t),\ (\underline{J}_i,\underline{M}_i)\rangle \ . \qquad \text{(C-6)}$$

Using the linearity of the reaction operator, Equation (C-6) becomes

$$\langle\underline{J}_t,(\underline{J},\underline{M})\rangle + \langle\underline{M}_t,(\underline{J},\underline{M})\rangle = -\langle\underline{J}_t,(\underline{J}_i,\underline{M}_i)\rangle - \langle\underline{M}_t,(\underline{J}_i,\underline{M}_i)\rangle \ . \qquad \text{(C-7)}$$

Equation (C-7) can be written as the coupled equations

$$\langle\underline{J}_t,\ (\underline{J},\underline{M})\rangle = V_J \qquad \text{(C-8)}$$

$$\langle\underline{M}_t,\ (\underline{J},\underline{M})\rangle = V_M \qquad \text{(C-9)}$$

where

$$V_J = -\langle\underline{J}_t,\ (\underline{J}_i,\underline{M}_i)\rangle \qquad \text{(C-10)}$$

$$V_M = -\langle\underline{M}_t,\ (\underline{J}_i,\underline{M}_i)\rangle \ . \qquad \text{(C-11)}$$

Using the symmetry properties of the fields of $\underline{J}_t$ and $\underline{M}_t$, it is possible to express Equations (C-8) and (C-9) in terms of the sum and difference currents. Omitting the details, the result is

$$\langle \underline{J}_t, (\underline{J}_S, \underline{M}_D) \rangle = V_J \tag{C-12}$$

$$\langle \underline{M}_t, (\underline{J}_D, \underline{M}_S) \rangle = V_M \tag{C-13}$$

Equations (C-12) and (C-13) are a new integral equation. They are different from previous equations in that they:

1. explicitly enforce electric as well as magnetic field boundary conditions
2. explicitly show the separation of current between the top and bottom surfaces of the plate
3. are applicable to assymetrically lossy (with respect to top and bottom) plates.

Equations (C-12) and (C-13) contain the four unknown vector functions $\underline{J}_S$, $\underline{J}_D$, $\underline{M}_S$, and $\underline{M}_D$. Using the concept of surface impedance, the magnetic currents can be eliminated. Again, omitting the details the result is

$$\langle \underline{J}_t, (\underline{J}_S, a\hat{u} \times \underline{J}_S + b\hat{u} \times \underline{J}_D) \rangle = V_J \tag{C-14}$$

$$\langle \underline{M}_t, (\underline{J}_D, b\hat{u} \times \underline{J}_S + a\hat{u} \times \underline{J}_D) \rangle = V_M \tag{C-15}$$

where u is a unit vector pointing up and

$$a = (Z_T + Z_B)/2 \tag{C-16}$$

$$b = (Z_T - Z_B)/2 \ . \tag{C-17}$$

There are two special cases of Equations (C-14) and (C-15) of interest.

Case 1: $Z_T = Z_B = 0$

This is a perfectly conducting plate. In this case, a = b = 0 and Equations (C-14, C-15) become

$$\langle \underline{J}_t, \underline{J}_S \rangle = V_J \tag{C-18}$$

$$\langle \underline{M}_t, \underline{J}_D \rangle = V_M \ . \tag{C-19}$$

Note that the equations uncouple. Also, when one uses electric test sources (i.e., an electric field integral formulation), one computes the sum current, while when one uses magnetic test sources (i.e., a magnetic field formulation), one computes the difference current. Since it is the sum current which radiates, electric field formulations are preferable for problems involving open surfaces. However, for closed surfaces, the interior current is zero, $\underline{J}_S = \underline{J}_D$, and magnetic field formulations are acceptable. An initial step in our research will be to

solve Equations (C-18, C-19) for $\underline{J}_S$ and $\underline{J}_D$ and from these determine $\underline{J}_T$ and $\underline{J}_B$, i.e., the top and bottom currents. This would be the first calculation, known to the author, where the currents on each side of an open surface are explicitly calculated.

Case 2: $Z_T = Z_B \neq 0$

This is a plate with symmetric surface impedance. In this case, b = 0, and Equations (C-14,C-15) become

$$\langle \underline{J}_t, (\underline{J}_S, \hat{au} \times \underline{J}_S) \rangle = V_J \qquad \text{(C-20)}$$

$$\langle \underline{M}_t, (\underline{J}_D, \hat{au} \times \underline{J}_D) \rangle = V_M \, . \qquad \text{(C-21)}$$

Note that again the equations uncouple. Equation (C-20) is comparable to the equation used by Harrington and Mautz [12] and Senior [13] for scattering from impedance surfaces.

Accomplishments

The past year's effort has involved evaluating the various reactions of Equations (C-14) and (C-15). We began with the special Case 1, $Z_T=Z_B=0$. Thus, Equations (C-18 and (C-19) were evaluated and solved for the currents on either side of a flat plate illuminated by a plane wave. The results have been submitted for publication [9]. The remaining time has been spent evaluating the various new reactions in

Equations (C-14) and (C-15). In the next reporting period, this should be accomplished and we should be able to compute the currents and scattering for a plate with surface impedance.

Publications

1. E.H. Newman and M.R. Schrote, "On the Current Distribution for Open Surfaces", submitted for publication IEEE Trans. on Antennas and Propagation.

2. "Eigenfunctions of Composite Hermitian Operators with Application to Discrete and Continuous Radiation Systems", N. Inagaki and R.J. Garbacz, reprinted in IEEE Transactions on Antennas and Propagation, AP-30, No. 4, pp. 571-575, July 1982.

References

[1] E.H. Newman and D.M. Pozar, "Electromagnetic Modelling of Composite Wire and Surface Geometries", IEEE Trans. on Antennas and Propagation, Vol. AP-26, No. 6, November 1978, pp. 784-89.

[2] E.H. Newman and D.M. Pozar, "Considerations for Efficient Wire/Surface Modelling", IEEE Trans. on Antennas and Propagation, Vol. AP-28, No. 1, January 1980, 121-125.

[3] D.M. Pozar and E.H. Newman, "Near Fields of a Vector Electric Line Source Near the Edge of a Wedge", Radio Science, Vol. 14, No. 3, May/June 1979.

[4] E.H. Newman and D.M. Pozar, "Analysis of a Monopole Mounted Near or at the Edge of a Half-Plane", IEEE Trans. on Antennas and Propagation, Vol. AP-29, May 1981, pp. 488-496.

[5] E.H. Newman and D.M. Pozar, "Analysis of a Monopole Mounted Near an Edge or a Vertex", accepted for publication IEEE Trans. on Antennas and Propagation. AP-S.

[6] E.H. Newman and P. Tulyathan, "Moment Method Solution for Polygon Plates", accepted for publication IEEE Trans. on Antennas and Propagation.

[7] E.H. Newman and P. Tulyathan, "Analysis of Microstrip Antenna Using Moment Methods", IEEE Trans. on Antennas and Propagation, Vol. AP-29, pp. 47-54, Jan. 1981.

[8] E.H. Newman, "Small Antenna Location Synthesis Using Characteristic Modes", IEEE Trans. on Antennas and Propagation, Vol. AP-27, pp. 530-531, July 1979.

D. Time Domain Studies

Researchers: D.L. Moffatt, Associate Professor (Phone: (614) 422-5749)

E.M. Kennaugh, Professor Emeritus

J. Han, Graduate Research Associate

Chun-Yue Lai, Graduate Research Associate

Ted C. Lee, Graduate Research Associate

Introduction

The optimum exploitation of the interaction of electromagnetic waves and material objects can only be achieved with a clear understanding of how the physical properties of the object in situ (size, shape and composition) are related to scattered or radiated fields. For whatever purpose, e.g., target identification, radar cross section control, specific radiation waveforms, etc., a basic understanding of the electromagnetic interactions is vital. Our research has shown that a time domain approach provides ideal insight into how such an understanding can be realized. Increasingly, solutions to radiation or scattering problems are sought over broad bandwidths. The canonical response waveforms (response waveforms to impulse, step or ramp excitations) are ideally suited for this purpose because the response to an arbitrary excitation is simply obtained using convolution.

Much of our recent research has stressed the complex natural resonances of a scatterer or radiator, that is, those complex frequencies which ellicit singularities in the transfer function relating excitation and response in a linear system. For distributed parameter systems such as scatterers and radiators, the response to an aperiodic excitation consists of, first, a forced response as the wavefront moves across the body and then a free or natural response as the wavefront moves beyond the body. For fixed time-independent residues, only the free response can be described in terms of the natural oscillation frequencies of the object.

The general goals of our research include:

1) Prediction of scattered and radiated waveforms from objects of increasing complexity for point or plane wave electromagnetic sources with arbitrary waveforms.

2) Investigation of target-dependent excitation waveforms and/or signal processing algorithms to identify and optimize electromagnetic response from specific targets.

3) Determination of the effects of system bandwidth and noise on recommended techniques for detection and identification of radar targets.

Significant progress has been made both in defining new concepts (the K-pulse) and in the refinement of basic techniques (a rational function method for extracting complex natural resonances from scattering or

radiation data). Our research is summarized in the following paragraphs. Written publications and oral presentations are listed at the end of this section. We stress here the fact that we have been extremely active in disseminating our results to the research community.

Accomplishments

Much of what has been accomplished on this program centers, in one way or another, on the complex natural resonances of radiators or scatterers. Accordingly, we continue to seek improved methods for estimating the complex natural resonances of scatterers and radiators.

1. Complex Natural Resonances and Geometrical Procedures

The K-pulse concept provides a means of relating surface waves on a structure to the complex natural resonances of the structure. Application of these ideas to the conducting sphere, conducting prolate spheroid and thin-wire were reported by Kennaugh [1]. Bagby [2] added the circular cylinder, elliptical cylinder and general wire configurations. Bagby also added the diffraction complex natural resonances of the thin circular disk. The creeping wave complex natural resonances of the thin disk have also been extracted recently. A report detailing the procedures and results of this geometrical approach to the complex natural resonances of a structure is in preparation. For solid structures with surface waves, the method for finding complex natural resonances appears to be as good as asymptotic methods such as the

geometrical theory of diffraction (GTD) can make it. For wire structures, however, results are best for very thin wires (length to diameter > 1000) and relatively poor for "fat" (length to diameter < 500) wires. Methods for improving the results for "fat" wires are still being studied.

2. Complex Natural Resonances Via Rational Function Approximants

The first attempt to extract the complex natural resonances of a scatterer from multiple frequency scattering data was by Moffatt [3] using a rational function approximation to model the transfer function of the target. This approach was largely abandoned with the advent of an eigenanalysis method suggested as an improvement of Prony's method. Recently, however, it has been found that with noisy data, better results can be obtained in the frequency domain using rational function models with somewhat less effort. Non-uniform spacing of the sampling frequencies and samples at or near the maxima and minima of the amplitude of the scattered field as a function of frequency are stressed. The most satisfactory results are obtained when a rational function model and a geometrical procedure can be applied to the same target. With correct results, the rational function model poles are correct at low frequencies and the asymptotic model poles are correct at higher frequencies. An agreement of poles from the two models for some interval of overlap is very desirable. This type of result (overlap) has been obtained for the thin disk for both the diffraction and creeping wave poles. A report on the procedures used to extract

complex natural resonances of an object from rational function models of the target's transfer function is in the early stages of preparation.

3. Cavity Structures

The last annual report on this contract noted that some early research on open and truncated circular waveguides has been done and that this research was now being pursued on another contract. The other contract has been completed with good but incomplete results. It has been demonstrated that scattering models for both loaded and unloaded guides valid in the resonance region can be built up in the time domain using low frequency approximations and high frequency asymptotic estimates. Therefore, for a general cavity configuration, GTD estimates could be combined with the results of moment method computations. The proper characteristic equation for an open circular waveguide was postulated but good estimates for the complex natural resonances of the structure were not obtained. An electric field integral equation has been formulated for a finite circular waveguide. Search procedures to extract ther complex natural resonances of this geometry are in progress. It is our contention that complex natural resonances associated with the rim of the waveguide must be identical for the finite and open circular waveguides. The even and odd modes of the somewhat simpler dipole-type modes for the finite guide have been successfully extracted. For loaded guides, finite or open, no one has successfully studied a realistic blade configuration to model some parts of a jet engine. Only planar blades have been studied. The vector

dyadic Green's function expansion for a conical shape inside a circular waveguide was not computationally tractable [5]. It now appears that a combination of the electric field integral equation already developed and used for the exterior region and a space-time integral equation for the interior region may yield better computational models. This approach will be studied once all of the complex natural resonances of the open circular waveguide have been found.

4. K-pulse Studies

Interpreted in the time domain, the K-pulse is a unique waveform of minimal duration which, as input to a specified linear system (scatterer, radiator), produces response waveforms of finite duration at all points of interest. Since derivatives of the input waveform also possess this property, uniqueness requires that the highest order discontinuity be of minimal order, as well.

Interpreted in the frequency domain, the K-pulse transform is a unique entire function (up to a multiplicative constant) whose zeros match the complex natural frequencies of the linear system which can be excited from the input terminals (directions, polarizations) of interest. Clearly, uniqueness requires that the K-pulse transform have zeros only at these match points.

Studies to date include: a) estimation of the K-pulse transform from strings of complex natural frequencies predicted by GTD aproximations for circumnavigating waves on conducting spheres, spheroids, circular and elliptic cylinders [1,2]; b) estimation of the

K-pulse waveform from specified sets of complex natural frequencies obtained by moment methods for thin wire scatterers and radiators [1]; and c) estimation of K-pulse and response waveforms for lossy and inhomogeneous transmission lines of finite length, with specified input and output terminations, obtained by combining K-pulse waveforms for uniform elements to a non-uniform line of up to 40 elements [1,4].

In electromagnetic or acoustic scattering, the K-pulse concept is an approach to factorization of transfer or reflection coefficient functions into the ratio of two entire functions which are not polynomial. It can lead to development of a simple ARMA (autoregressive moving-average) model for the scatterer which is useful in target identification or discrimination. It also separates aspect-dependent zeros and aspect-independent poles from the target response in a systematic manner. In the next contract interval, we will develop these approaches by use of theoretical concepts and available broad-band experimental scattering data.

Publications

T.W. Johnson and D.L. Moffatt, "ELectromagnetic Scattering by an Open Circular Waveguide", Radio Science, Vol. 17, No. 6, November-December, 1982.

D.L. Moffatt and C.M. Rhoads, "Radar Identification of Naval Vessels", IEEE Transactions on Aerospace and Electronic Systems, Vol. AES-18, No. 2, March 1982.

D.B. Hodge, "Electromagnetic Scatterng by a Circular Disc", accepted for publication in IEEE Transactions on Antennas and Propagation.

E.M. Kennaugh and D.L. Moffatt, Comments on "Impulse Response of a Conducting Sphere Based on Singularity Expansion Method", Proceedings of the IEEE, Vol. 70, No. 3, March 1982.

Oral Presentations

E.M. Kennaugh and D.L. Moffatt, "Improved Response Waveforms for the Circular Disk", 1982 Joint International IEEE/APS Symposium and National Radio Science Meeting, Albuquerque, New Mexico, May 1982.

D.L. Moffatt and Chun-Yue Lai, "Electromagnetic Scattering by Loaded Open Circular Waveguides", National Radio Science Meeting, Albuquerque, New Mexico, May 1982.

D.L. Moffatt and J.G. Bagby, "Approximate Characteristic Equations for Simple structures", National Radio Science Meeting, University of Colorado, January 1982.

Technical Reports in Preparation

E.M. Kennaugh, "K-pulse for Transmission Lines".

D.L. Moffatt and E.M. Kennaugh, "Transient Currents on a Sphere".

D.L. Moffatt, J.G. Bagby, and T. Lee, "A Geometrical Approach to Characteristic Equations".

References

[1] Kennaugh, E.M., "The K-pulse Concept", IEEE Trans. on Antennas and Propagation, Vol. AP-29, No. 2, March 1981.

[2] Bagby, J.G., "Natural Electromagnetic Oscillations: A Geometrical Theory", M.Sc. Thesis, The Ohio State University, August 1981.

[3] Maines, R.K. and D.L. Moffatt, "Complex Natural Resonances of an Object in Detection and Discrimination", Technical Report 3424-1, June 1974, The Ohio State University ElectroScience Laboratory, Department of Electrical Engineering; prepared under contract F19628-72-C-0203 for Department of the Air Force, Air Force Systems Command, Hanscom Air Force Base, Massachusetts.

[4] Kennaugh, E.M., "K-pulse for Transmission Lines", in preparation.

[5] Johnson, T.W. and D.L. Moffatt, "Electromagnetic Scattering by Open Circular Waveguides", Technical Report 710816-9, December 1980, The Ohio State University ElectroScience Laboratory, Department of Electrical Engineering; prepared under contract N00014-78-C-0049 for the Department of the Navy, Office of Naval Research, Arlington, Virginia, 22217.

E. Transient Signature Measurements of Radar Targets for Inverse Scattering Research

Researchers: J.D. Young, Research Scientist (Phone: (614) 422-6657)
E.K. Walton, Senior Research Associate
W. Leeper, Graduate Research Associate

Introduction

The objective of the effort is to assemble "complete" complex scattering cross section data on several canonical targets. The data are complete in the following respects:

1. Both amplitude and phase of the backscattered return are measured.
2. The data cover a 96:1 bandwidth.
3. The results are actual backscatter, i.e., precisely at 0° bistatic angle.
4. The backscatter is measured for three polarizations: vertical-vertical, horizontal-horizontal, vertical-horizontal.
5. The measurements were made at aspects of every 15° from 0° - 180°.
6. The vertical-horizontal (cross) polarized measurements were made at aspects out of the principal planes.

This report describes the frequency domain range and equipment used for the measurements; presents measured results in both the frequency and time domain for a few selected targets; compares those results to theoretical solutions; discusses the data processing utilized; and notes improvements now being made on the measurement facility.

The data bank assembled from these measurements is of interest to those doing inverse scattering research, to scattering analysts, and to those interested in the use or control of a radar target's scattering properties.

Swept Frequency System

The OSU-ESL measurement range uses the concept of background subtraction rather than background nulling [1,2]. Such a system allows for the rapid collection of target returns over a wide band of frequencies. The data collection system is shown in Figure E-1. The amplitude and phase of the return signal is recorded at discrete frequencies for each of three cases: 1) target plus background, 2) background only with no target, 3) calibration target plus background.

The calibration target is one with a known exact complex backscatter over the frequencies of interest. For the co-polarized measurements, spheres of various sizes were used as calibration targets and to provide checks in the measurement accuracy.

The measurements of target plus background (TB) are stepped through a set of pre-determined frequencies. In most cases, 201 data points

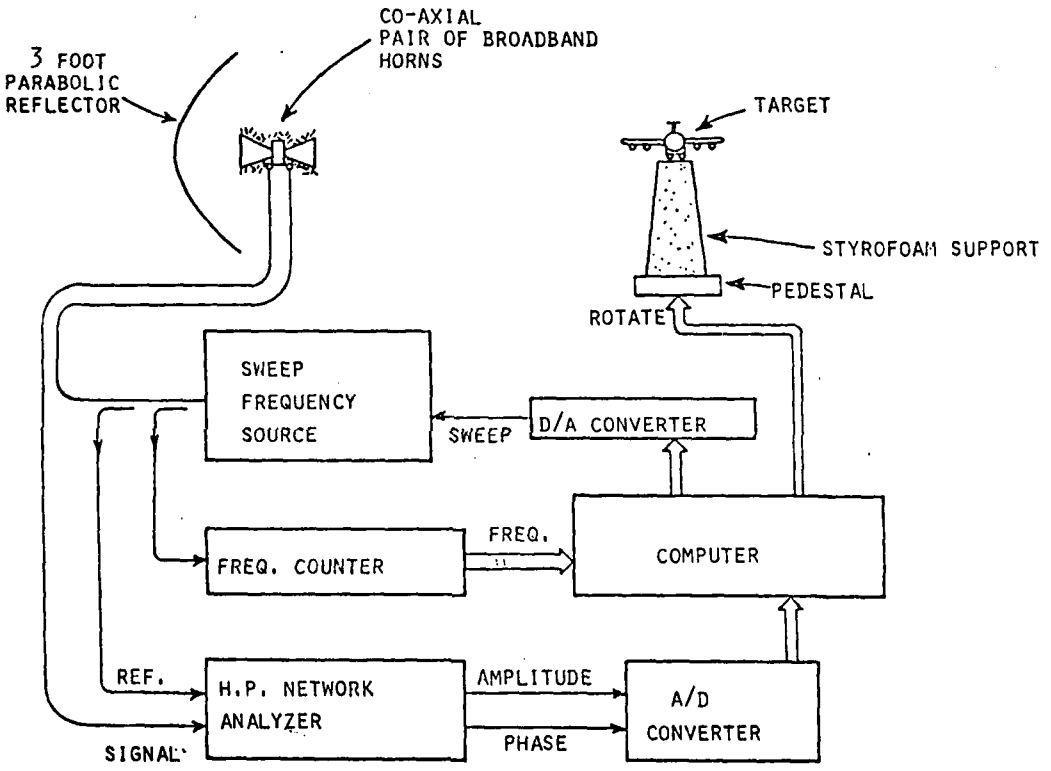

Figure E-1. Schematic diagram of the frequency domain compact scattering range implemented at OSU.

were recorded over an octave bandwidth. The measurement of background with no target (B) is then stepped through the same frequencies. The process is repeated for the calibration sphere (CB).

These three measured files are then combined with the exact sphere data (E) in the following algorithm to obtain the calibrated target response T_C:

$$T_C = (TB-B) * \frac{(E)}{(CB-B)} \quad . \qquad (E.1)$$

Since the factor $\frac{(E)}{(CB-B)}$ is a complex calibration constant at each frequency the result of the process is the complex radar cross section of the target alone.

Data acquisition is controlled by a PDP11/03 minicomputer. The oscillator is an H.P. 8690B microwave source with interchangeable octave band modules of 1-2 GHz, 2-4 GHz, 4-8 GHz, and 8-12 GHz. No external amplification was used. Output power varied from 10-70 mW. A closed loop checks the frequency of the output and corrects it within a resolution of ± 1 MHz.

The receiver is an H.P. 8410A Network Analyzer. The return signal is a vector relative to a reference signal coupled via a delay line from the transmit port. The delay line is used to minimize the number of phase branch cuts in the signal relative to reference.

The Network Analyzer provides relative amplitude and phase (50 mV/dB and 10 mV/deg) as analog voltages on separate channels. The measurement facility uses two broadband AEL microwave antennas mounted back-to-back at the focal point of a parabolic dish. Such an

arrangement allows the measurement of true backscattered target return. The transmit and receive horns are isolated with absorbing material to reduce coupling.

The AEL microwave horns operate from 1 to 12 GHz. (Results so far suggest that 1.5 GHz may be the lower limit on the focusing capability of the back-to-back horn/dish arrangement.) The targets were mounted on a 10 ft. tall styrofoam pedestal which is rotated under computer control. Measurements were made at increments of 15 degrees in the plane of symmetry for the three targets of interest: a 2:1 right circular cylinder, a 2:1 right circular cylinder with a hemispherical cap on one end, and a 2:1 prolate spheroid. For each of these targets, the frequency ranged over $0.8 \leq kL \leq 77$, where L is the object length and $k = 2\pi/\lambda$, where λ is the wavelength. In addition, spheres were measured over the same frequency spread. For the cross polarized measurements, other targets and look angles were included.

Data Processing

All experimental data are subject to errors from many sources. The processing of the data has lead to an estimate of the data accuracy and also to the development of a technique to improve the effective accuracy. It has been demonstrated that the result of all error sources is most clearly characterized as noise, a random, zero-mean variation of the measured data about the correct scattering value.

The calibration algorithm of Equation (E.1) involves the difference between two noisy signals in both the numerator and denominator. Thus,

the error due to system noise grows during calibration. A quantitative error analysis was performed which gives a complete range of reliability estimates.

A large number of data points were measured at a single frequency for each of the files; target plus background, background, and calibration sphere plus background. These points were then plotted on a polar plot to show convincingly that the phase is noisier than the amplitude of the measured data. The difference was enough to justify separate error analyses for amplitude and phase. The data points were then run through the calibration algorithm of Equation (E.1) and a standard deviation taken for amplitude and for phase. The procedure was repeated for targets with RCS ranging from 40 dBscm (0 dBSM) down to 10 dBscm (-30 dBSM).

Separate measurements were taken at several frequencies in the 2-4 GHz band and the 4-8 GHz band. The resulting error estimates ranged from ± 0.5 dB and ± 4.0° for target cross sections above +25 dBscm to ± 1.7 dB and ± 10° for target cross sections of +10 dBscm. It should be noted that these figures are for calibrated but unsmoothed data. The analysis has not yet been extended to smoothed data.

The noise floor was measured by treating a background measurement as a target and subtracting another background measurement, taken during the same data run. The result is essentially a repeatability test. This test was repeated continuously during each data session. A typical noise floor of between 0 and 5 dBscm (-40 to -35 dBSM) is shown in Figure E-2. The phase in Figure E-2 should be, and is, quite random.

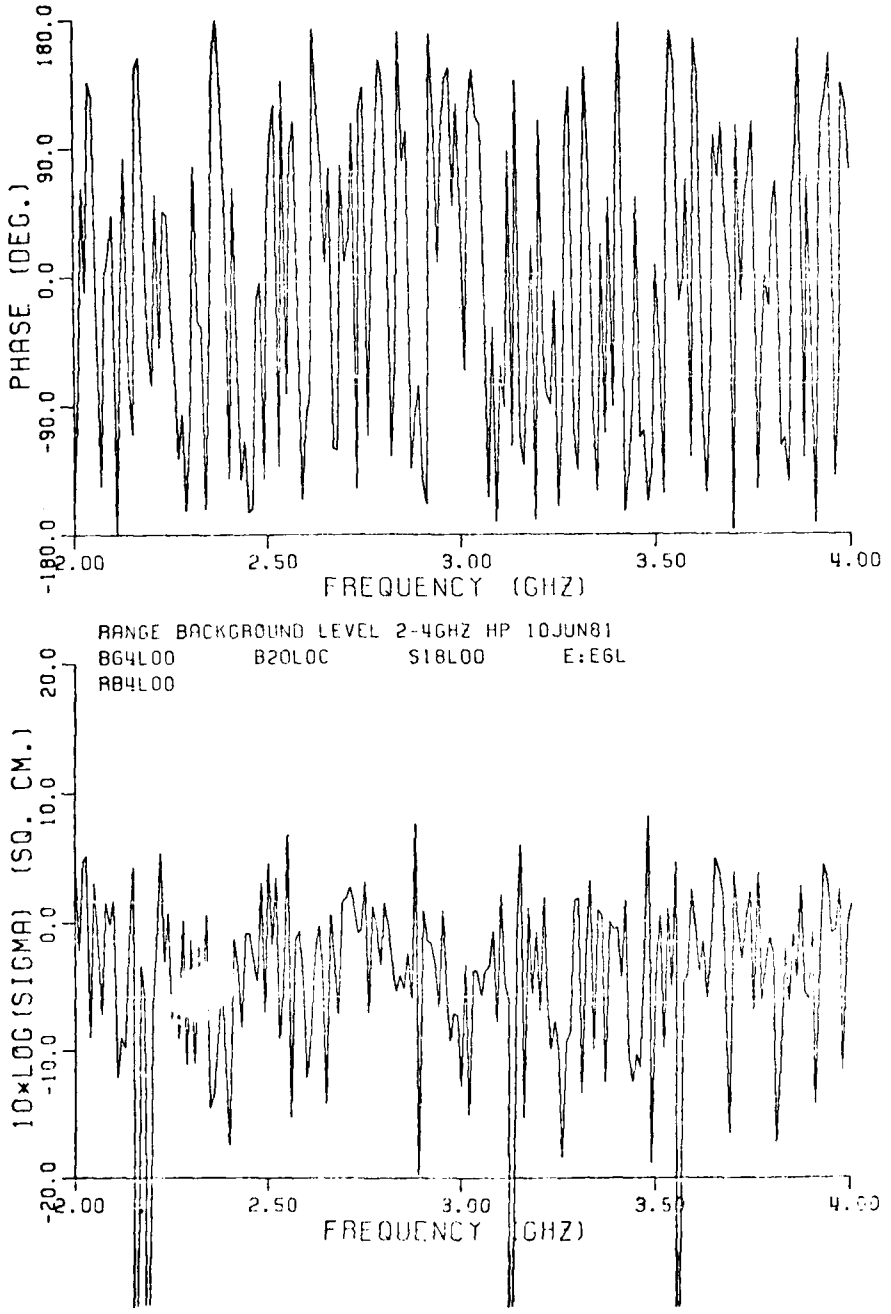

Figure E-2. Typical noise floor.

A frequency domain smoothing algorithm was adopted in the processing of all signature data in order to obtain results with improved accuracy. This is justified for several reasons. The first reason is that the original data are considerably oversampled in the frequency domain. Since the time domain transient response duration is less that 6L/C, then the frequency spectrum need only be sampled at intervals of $\omega = \frac{\pi C}{6L}$, or intervals in kL of $\pi/6$. However, these data were sampled at least 15 times that rate. Therefore, smoothing of these data is equivalent to averaging in its improvement in noise variations. Up to 15-point smoothing is permissible without degrading the target data. The second benefit of this smoothing is that there are other "clutter" returns which may have regular variations in frequency response at a rate almost equal to the sampling rate. Smoothing thus removes some clutter as well as noise from the data.

In all cases, a center of gravity type of vector smoothing was used. At each frequency, the smoothed phasor value was found by weighting the real and imaginary parts of the N adjacent vectors on either side with a cosine distribution. Such smoothing was found to give very good results for test spheres.

The two questions to be answered were: 1) where in the calibration algorithm is it best to apply the smoothing and 2) should the phase be pre-smoothed. It was attempted early on to smooth the raw data files before any background subtraction. This failed to recover the target information since, in most cases, the difference vector is very small. Subsequently, most of the data were smoothed after calibration. But

AD-A128 470 JOINT SERVICES ELECTRONICS PROGRAM(U) OHIO STATE UNIV COLUMBUS ELECTROSCIENCE LAB DEC 82 ESL-710816-12 N00014-78-C-0049 2/2

UNCLASSIFIED F/G 20/14 NL

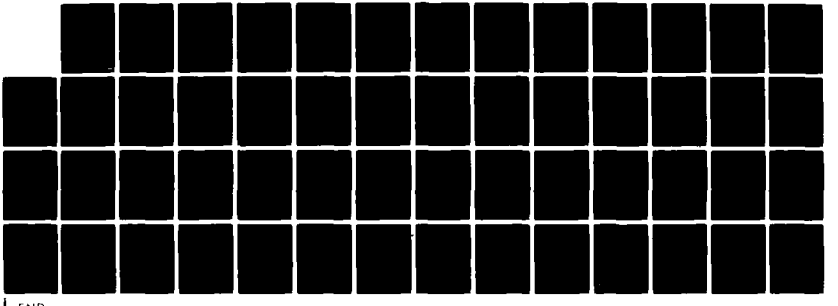

END
DATE FILMED
6-83
DTIC

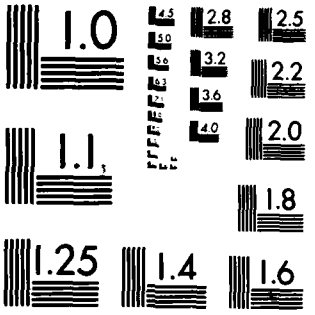

MICROCOPY RESOLUTION TEST CHART
NATIONAL BUREAU OF STANDARDS-1963-A

tests have shown that some smoothing of the difference vectors in both numerator and denominator of the calibration algorithm improves the results. It has been found that some pre-smoothing of the phase improves the results, particularly in those parts of the spectrum where phase branch cuts occur.

In all cases, the separate octave bands were smoothed separately before being combined into one kL file. Due to the fold-over necessary at the end points of each separate file, there are some discontinuities in the combined spectrum. The problem can be eliminated by combining raw files before any smoothing. This approach is currently being implemented.

Comparison of Measured and Theoretical Spectra

Measured frequency domain results were compared to theoretical solution for the spheres and the sphere-capped cylinder. The measured amplitude spectrum of a five inch diameter conducting sphere is compared in Figure E-3 to the exact Mie series solution in Figure E-4. Such checks on sphere data were used throughout the measurement process to monitor the accuracy of the measurements.

The results for the sphere-capped cylinder were compared to a first-order UTD (Uniform Geometrical Theory of Diffraction) solution. The gometry for the three-point UTD solution is shown in Figure E-5. For the sphere-capped cylinder, the sphere-capped end is 0° and the flat end is 180°. For aspects between 0° and 90°, the three high frequency diffracting mechanisms are the specular reflection from the sphere, the

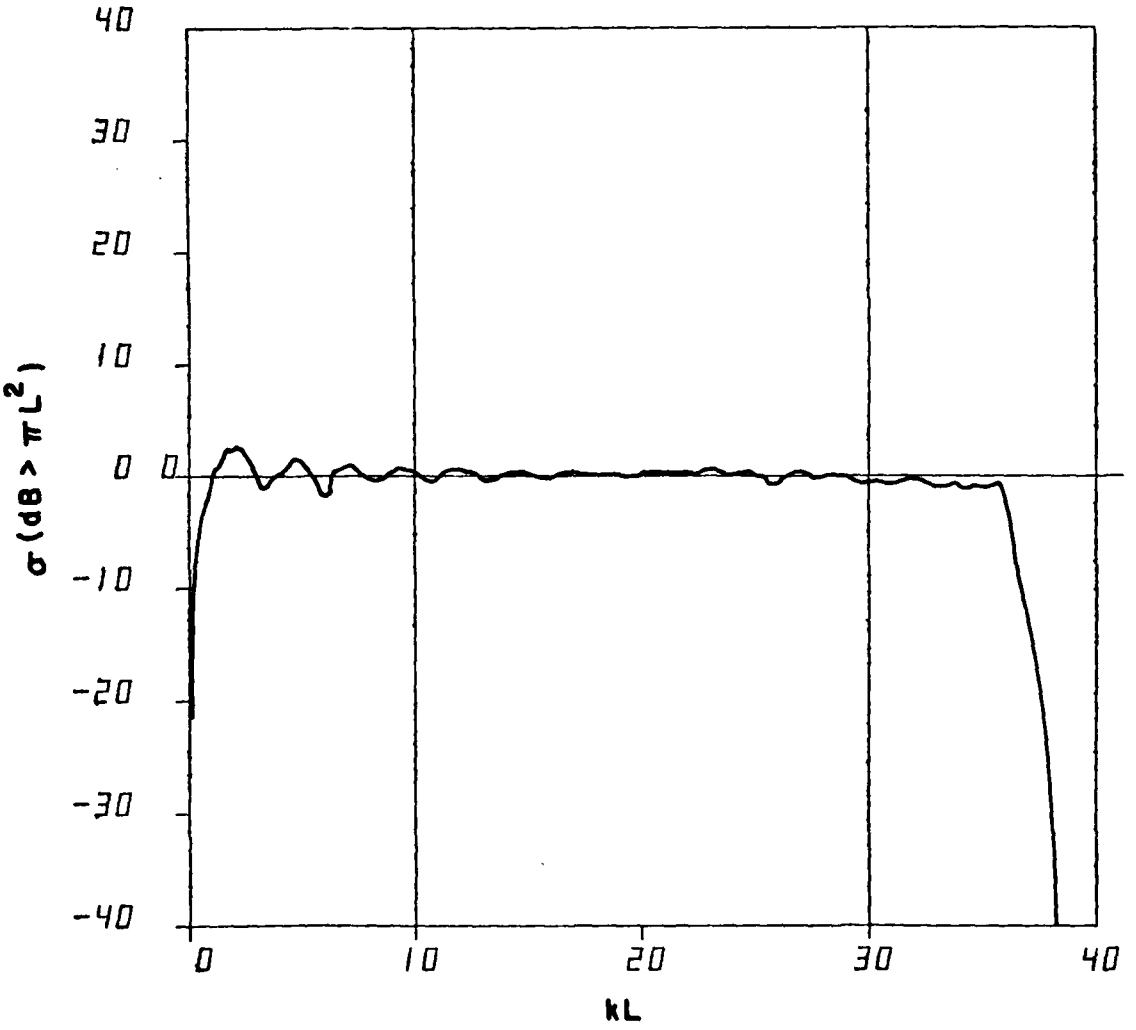

Figure E-3. Experimental spectrum for a metal sphere.

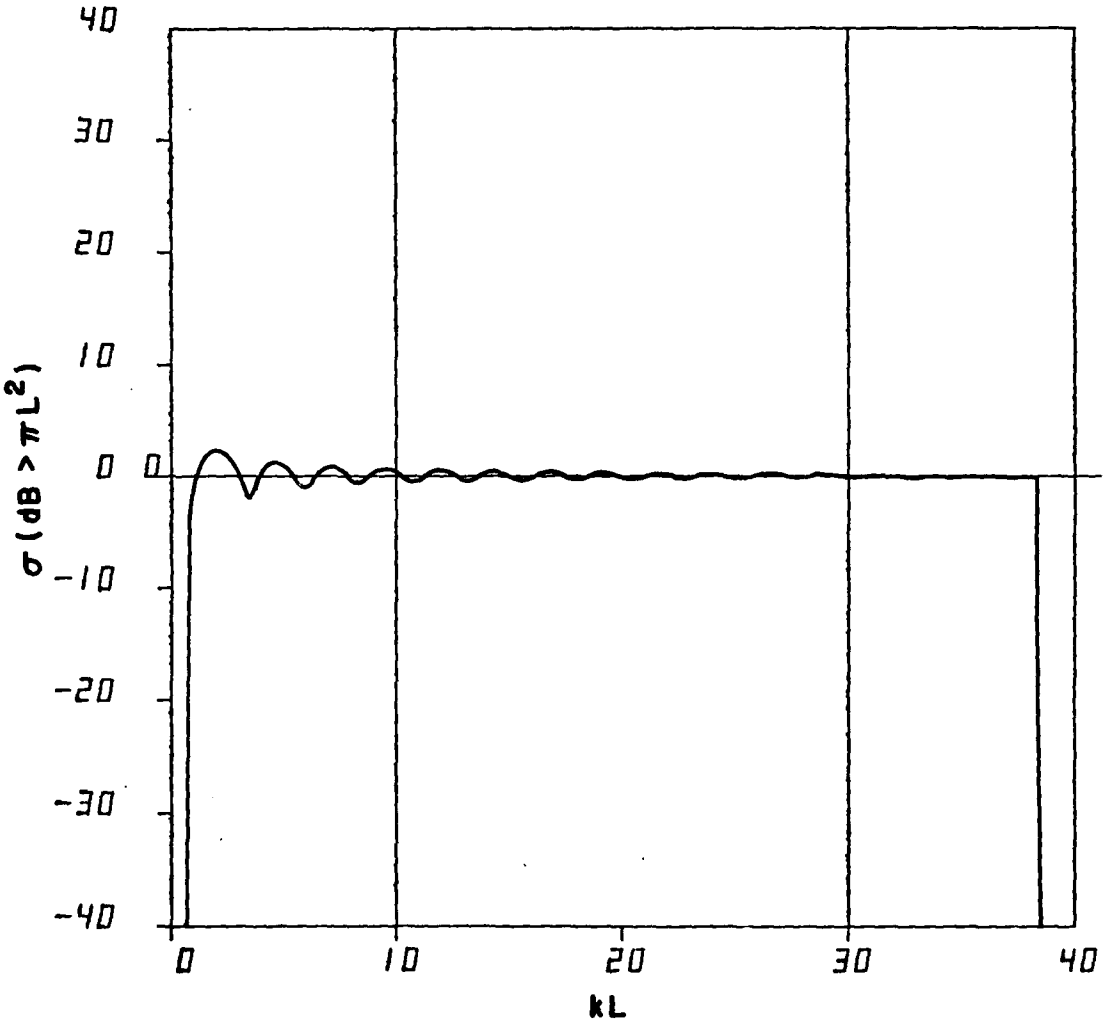

Figure E-4. Theoretical spectrum for a metal sphere.

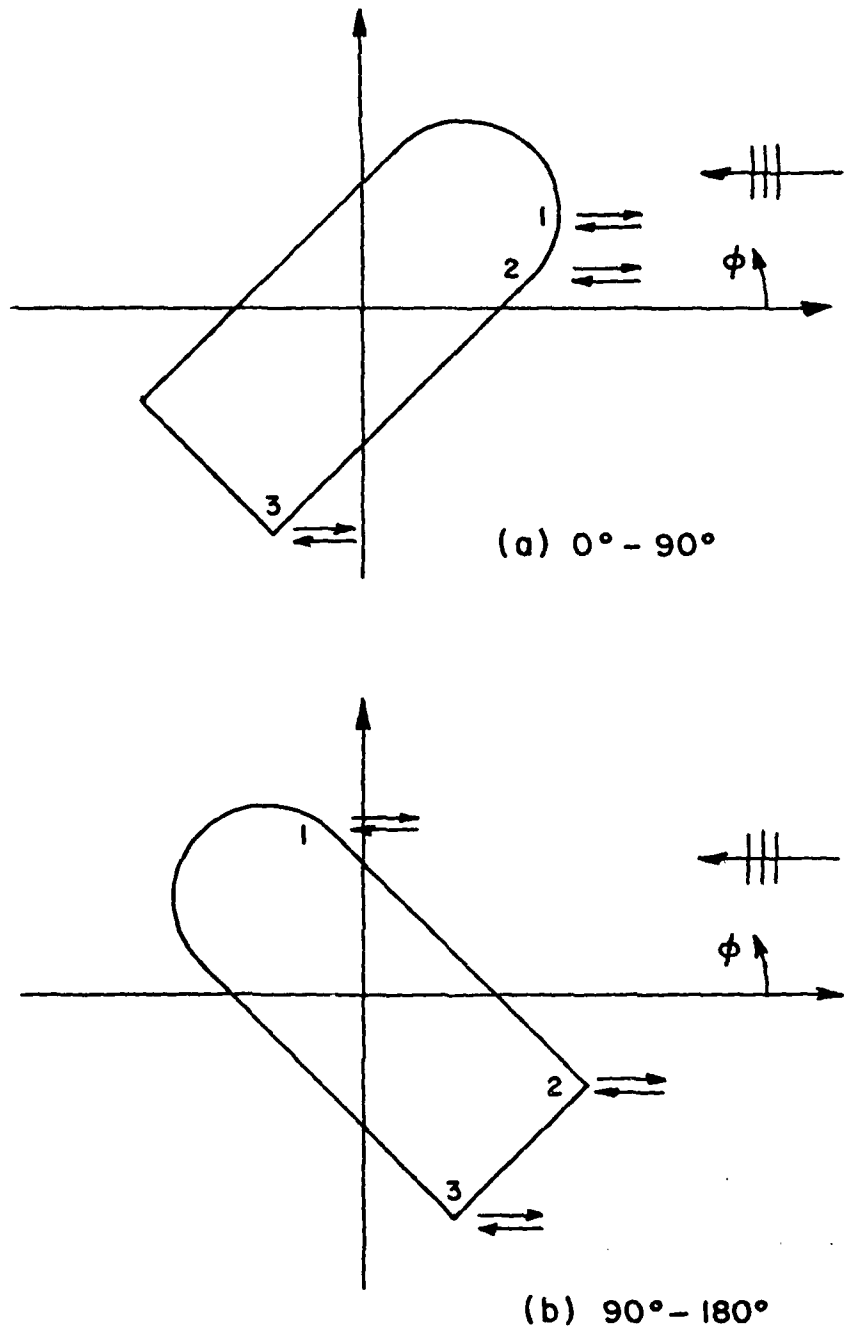

Figure E-5. The geometry for the three-point UTD solution.

curved edge on the flat end, and the curved junction at the discontinuity in curvature between the hemispherical cap and the cylinder.

For aspects between 90° and 180°, there is no reflection from the sphere but when the entire disc on the flat end is illuminated, we have two diametrically opposed stationary points re-radiating. The creeping wave around the sphere is not included in this first order solution. For a more detailed discussion of the UTD solution, see Reference 3.

The UTD solution was run for both vertical and horizontal polarizations and for values of kL from 8 to 64. The UTD amplitude spectrum for the sphere-capped cylinder at 45° is shown in Figure E-6. The incident electric field vector is in the plane of rotation (horizontal polarization). The evenly periodic resonance indicates a two point interference between the reflected specular from the spherical cap and the rear edge.

The measured amplitude spectrum is shown in Figure E-7. The flattening of the resonance indicates a more complex interaction than is predicted by the first order UTD solution. These spectra will be analyzed further in the time domain in the next section.

Time Domain Results

As noted in the introduction, the relation between the time domain backscattered waveform and the target geometry is simple and straightforward. This relation is most easily seen by scaling the time axis in

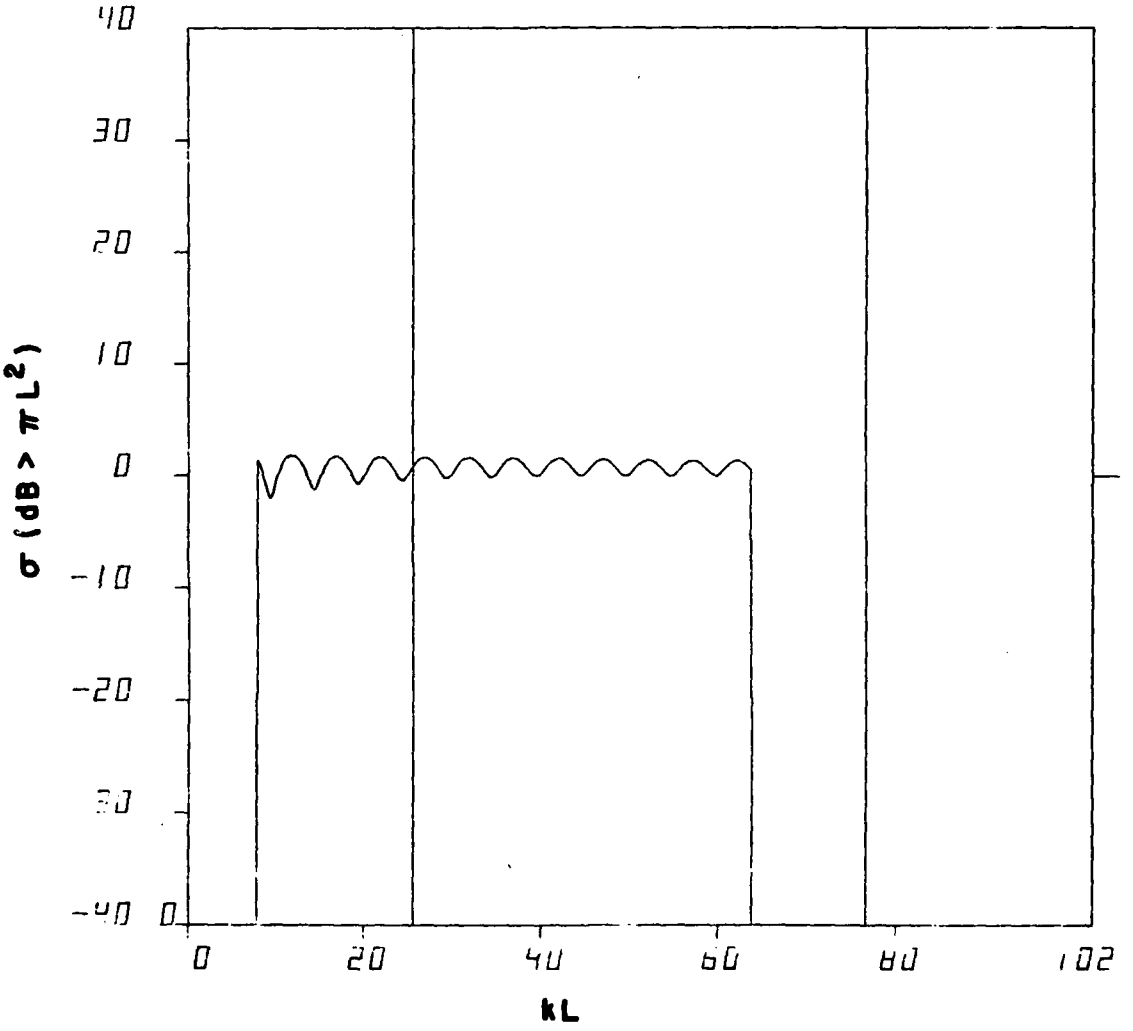

Figure E-6. UTD amplitude spectrum for sphere-capped cylinder at 45°.

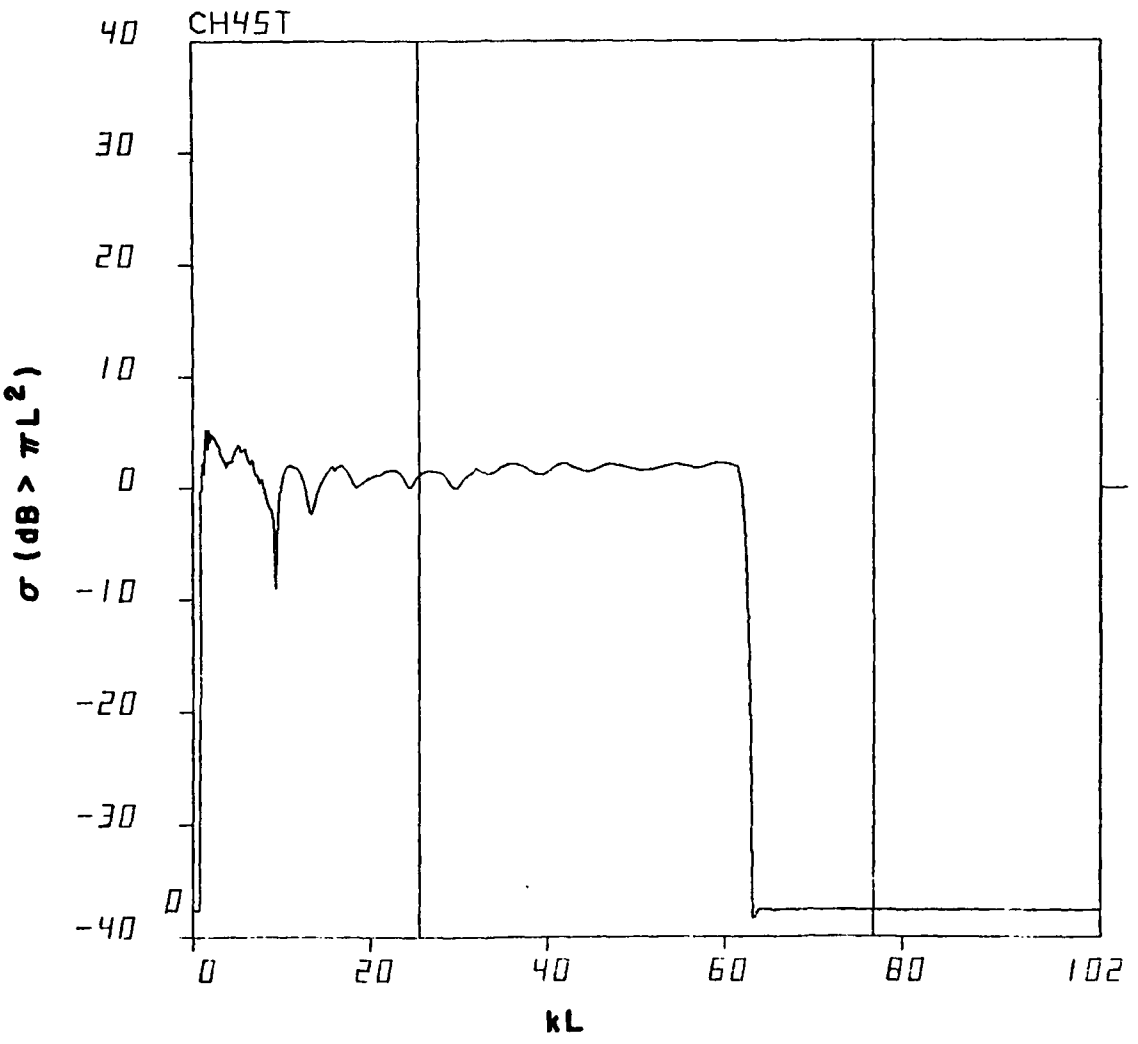

Figure E-7. Measured amplitude spectrum of sphere-capped cylinder at 45°.

units of $1/\tau$, where $\tau = L/C$ = maximum target dimension/speed of light. Time t=0 is chosen to coincide with the geometric center of the target. The time scale includes a factor of two in order to account for the two-way path of each backscattered ray.

A simple case for illustration is the impulse response of the conducting sphere. The sphere has two distinct radiating mechanisms. The specular reflection from the point nearest the source is a large negative impulse. The creeping wave around the shadowed side is a smaller and wider negative excursion. For a further discussion of the theoretical impulse response of the sphere, see References 4 and 5.

These two mechanisms are seen clearly in Figures E-8 and E-9 in which the measured and exact (band limited) sphere spectra presented in the previous section have been inverse Fourier transformed. For the sphere $\tau = 2\ a/c$ where a = sphere radius, with the sphere center at time t = 0, the specular arrives at time $t_1 = -\tau$. The free space backscatter path of the specular relative to the sphere center is -2a; time of arrival = 2 way path/c = -2 a/c = $-\tau$. The creeping wave travels an extra distance πa relative to sphere center and thus arrives at a time $t_2 = +\pi\ a/c = +\pi/2\ \tau$.

A slightly more complicated case is the sphere-capped cylinder at 0 degrees. The impulse response is shown in Figure E-10. The target has a cylinder radius of a and a total length of 5a; thus $\tau = 5\ a/c$. The specular reflection from the spherical cap arrives at time $t_1 = -\tau$ relative to target center. Up to a time equal to 2/5 τ after this initial negative impulse, the waveform is that of a sphere of radius a.

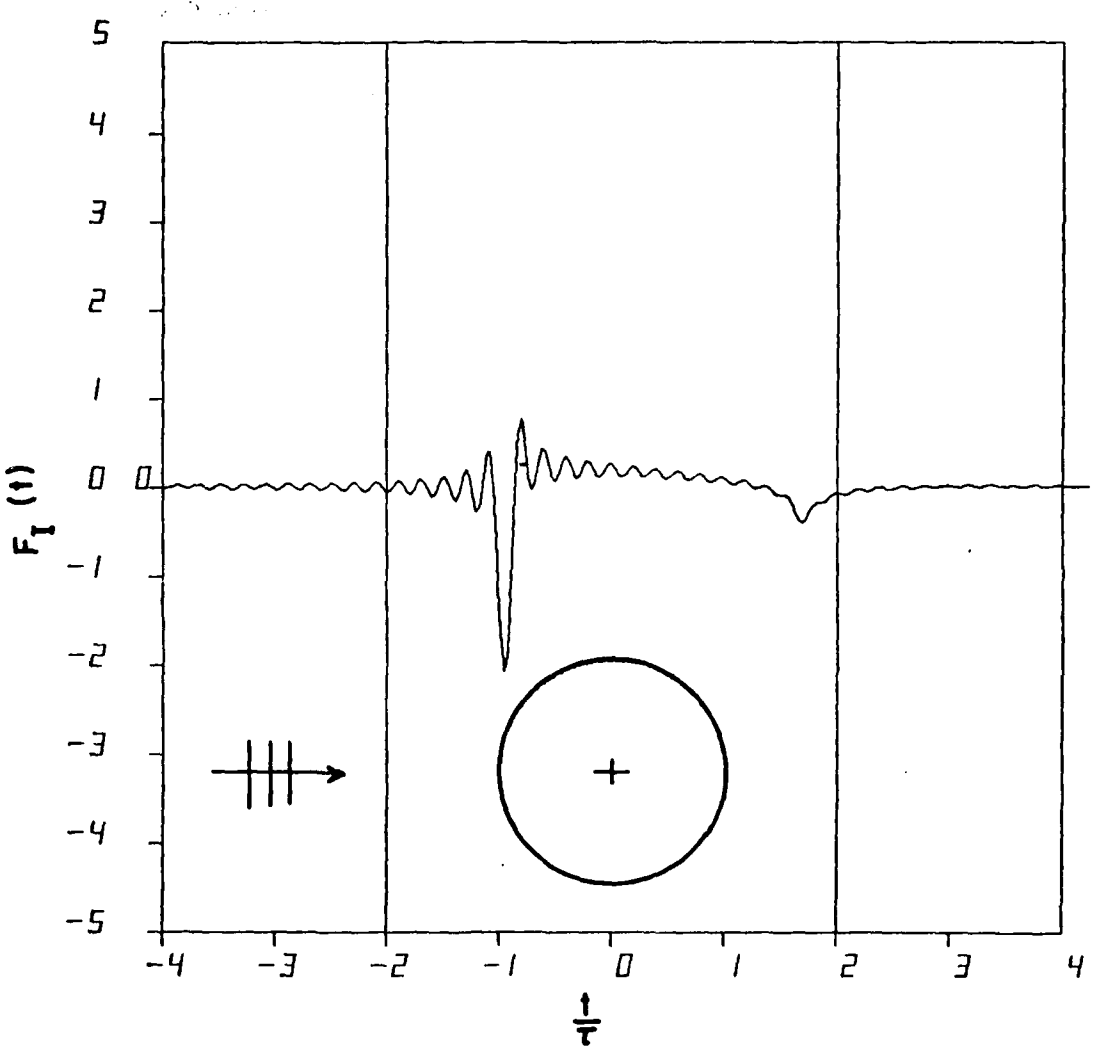

Figure E-8. Fourier transform of data in Figure E-4.

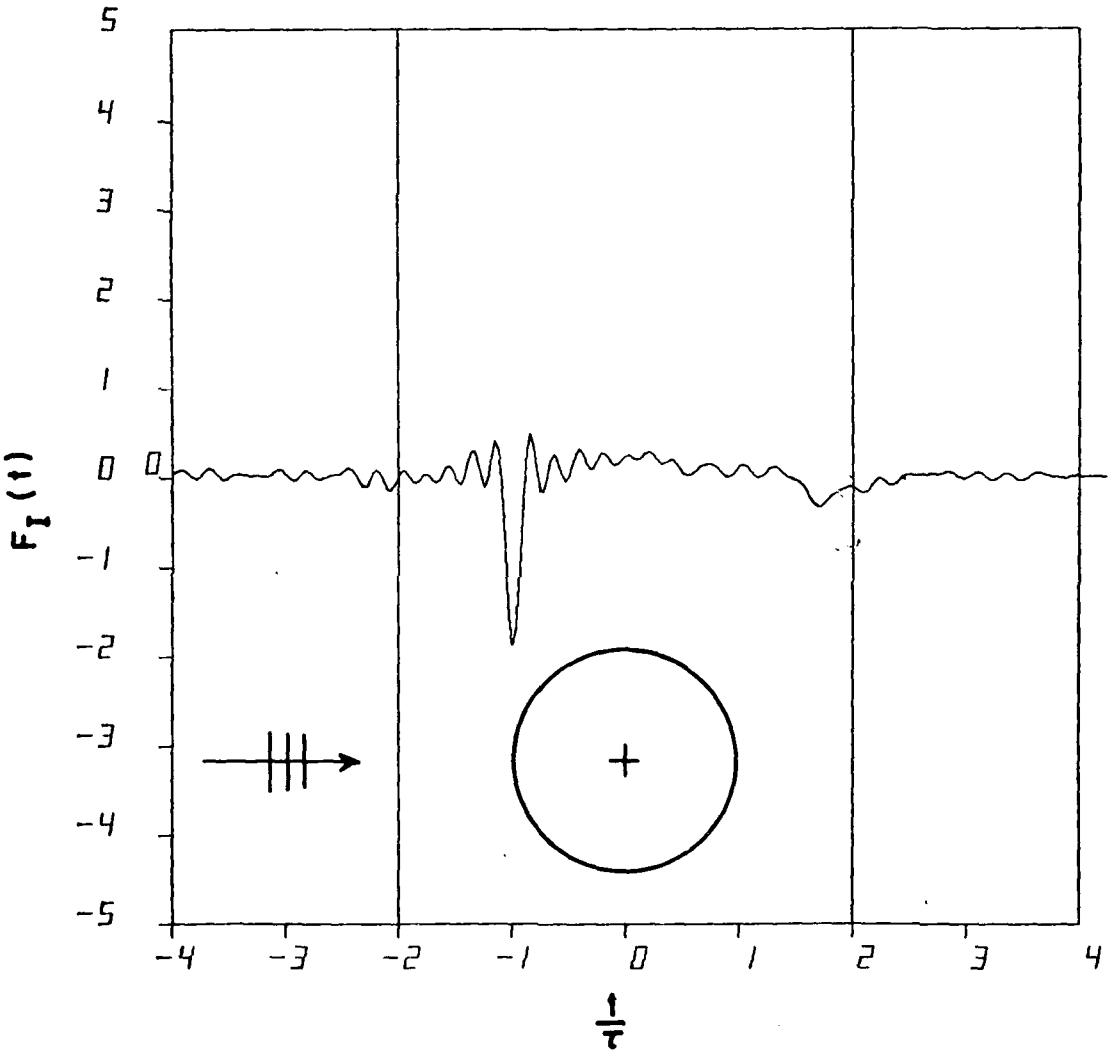

Figure E-9. Fourier transform of data in Figure E-3.

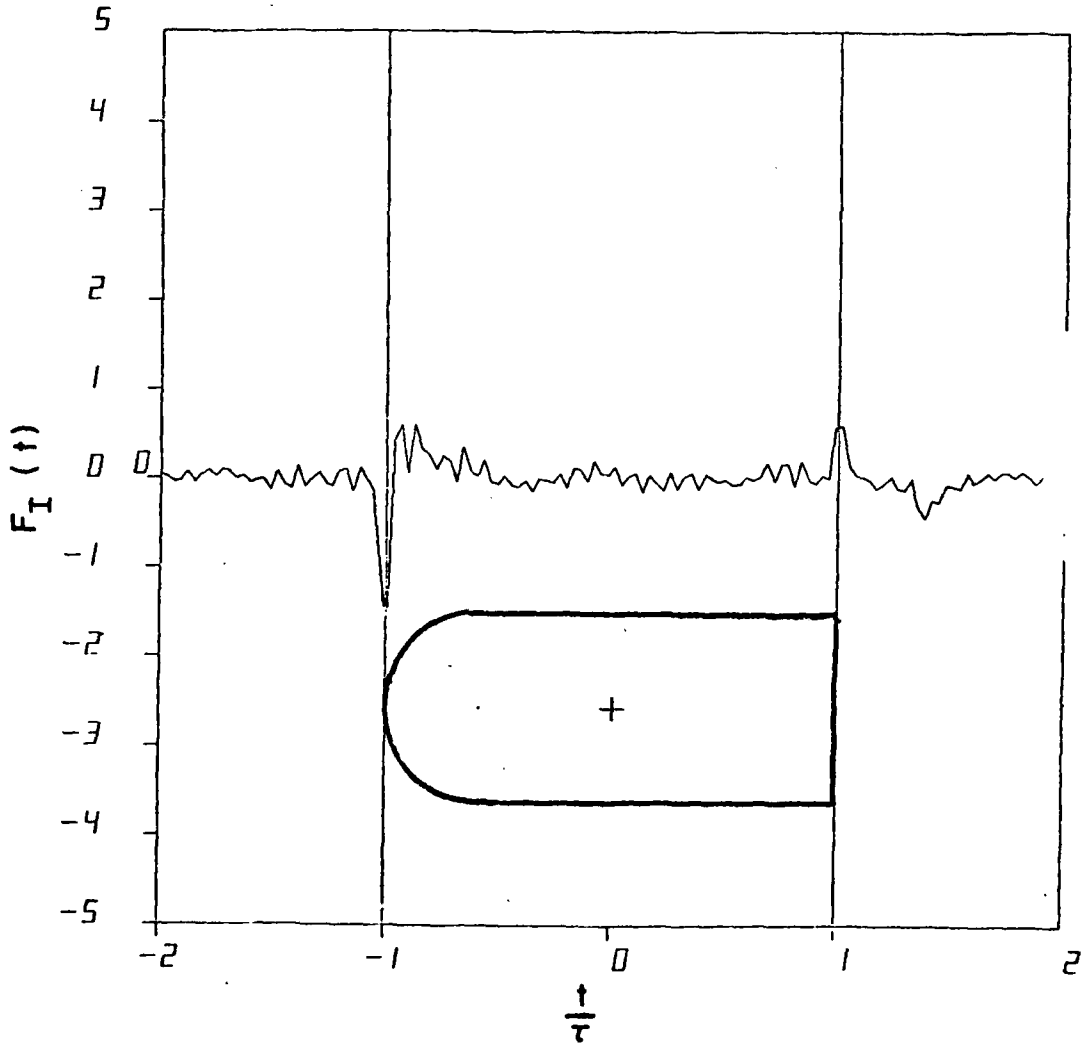

Figure E-10. Impulse response of sphere-capped cylinder at 0°.

Along the length of the cylindrical section, there are no radiating mechanisms until the rear cylinder edge. At a time $t_2=+T$, arrives a positive return which is diffracted from the cylinder edge. At a time $t_3=5/7T$, arrives a weaker negative component which is diffracted once from the rear edge, crosses the rear disc diameter, and is diffracted a second time from the cylinder edge. In its travel across the cylinder diameter, this doubly diffracted ray crosses a caustic on the cylinder axis and becomes negative. The double diffraction causes this component to be attenuated relative to the singly diffracted component. The two components from the rear edge are separated in time by $2/5T$, which is the travel time across the cylinder diameter. As can be seen from these examples, the impulse response isolates individual radiating mechanisms on the time axis in a predictable manner. As the target geometry becomes more complex it is advantageous to compare these measured data to a theoretical solution which also isolates individual radiating mechanisms. As a high frequency solution, UTD does just this.

When the UTD solution is inverse Fourier transformed into the time domain and compared to the measured impulse response, we can graphically align three valuable analytical tools: target geometry, known radiating mechanisms, and the total measured return from the target.

The first-order UTD spectrum, bandlimited to kL values from 8 to 64, has been inverse Fourier transformed with no attempt made to reduce the Gibb's phenomena. The resulting theoretical, bandlimited, first-order UTD impulse responses are shown in Figures E-11 and E-13 for the sphere-capped cylinder at an aspect of 45°.

For the cases presented so far, the polarization of the incident field has not been a factor due to the rotational symmetry of the targets at those aspects. At aspects off the axis of rotation, the cases of vertical (electric field vector perpendicular to the plane of target rotation) polarization and horizontal polarization must be treated separately.

First, considering the case for horizontal polarization, the UTD impulse response of Figure E-11 may be compared to the measured impulse response of Figure E-12. The agreement is excellent from the spherical end up to and including the initial return from the rear cylinder edge. As expected, the UTD response from this rear edge is confined to a narrow time window. The rise time and height of this feature is identical in UTD and measured waveforms. But the measured impulse response shows a significant return from the entire back edge dispersed along the time axis. Analysis of this effect is now being done and will be the subject of future publications.

Considering the case for vertical polarization, the UTD impulse response of Figure E-13 may be compared to the measured of Figure E-14. Here, too, the comparison is excellent for the front end of the target. For this polarization, the return from the stationary point at the part of the back edge nearest the radar is very small compared to that for the horizontal polarization case. It is barely discernable in either waveform. The measured impulse response shows a distinct trailing feature not, as yet, included in the first order UTD solution. This, too, is now being analyzed.

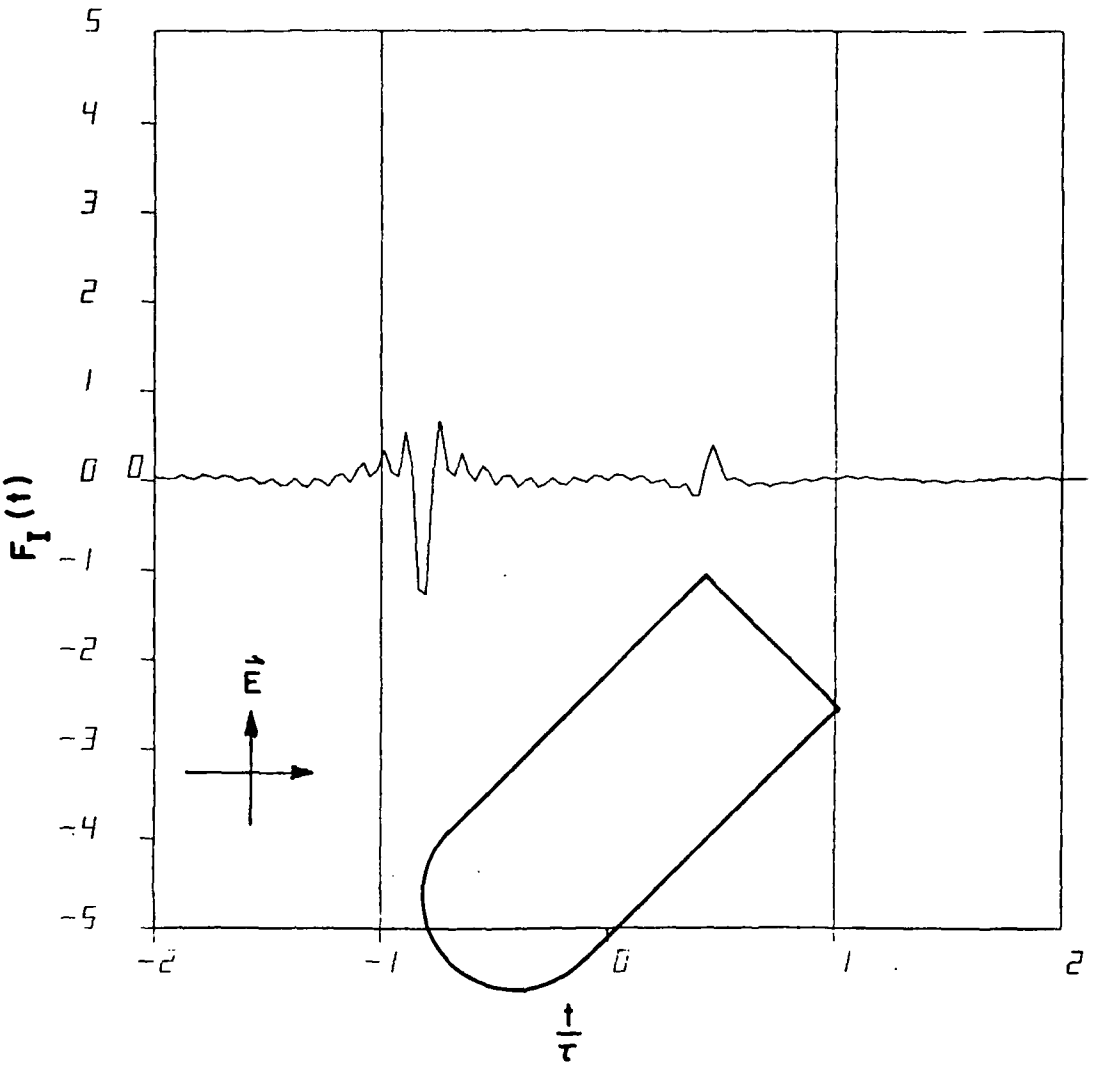

Figure E-11. First-order UTD impulse response for sphere-capped cylinder at 45°. Horizontal polarization.

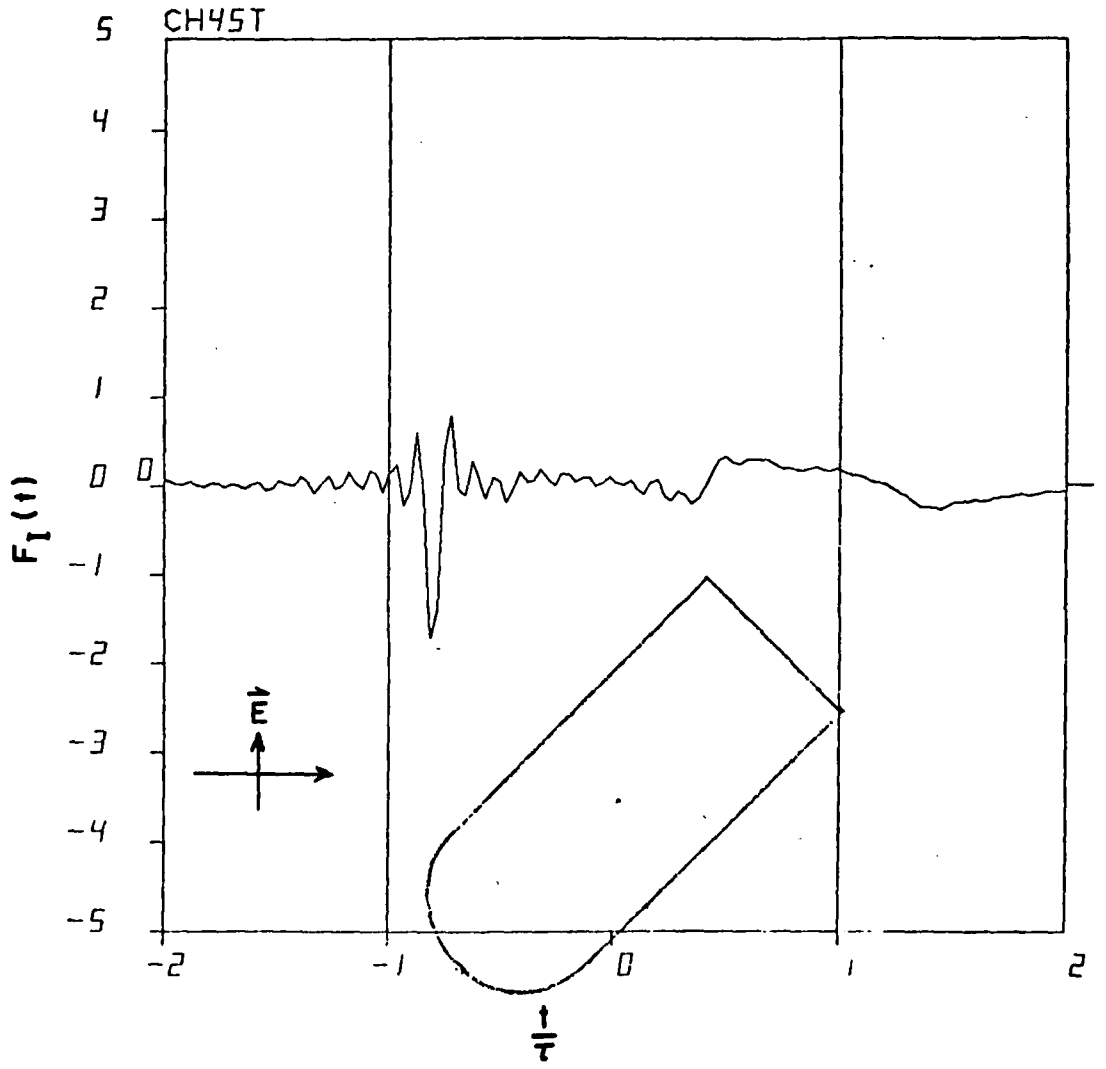

Figure E-12. Measured impulse response for sphere-capped cylinder at 45°. Horizontal polarization.

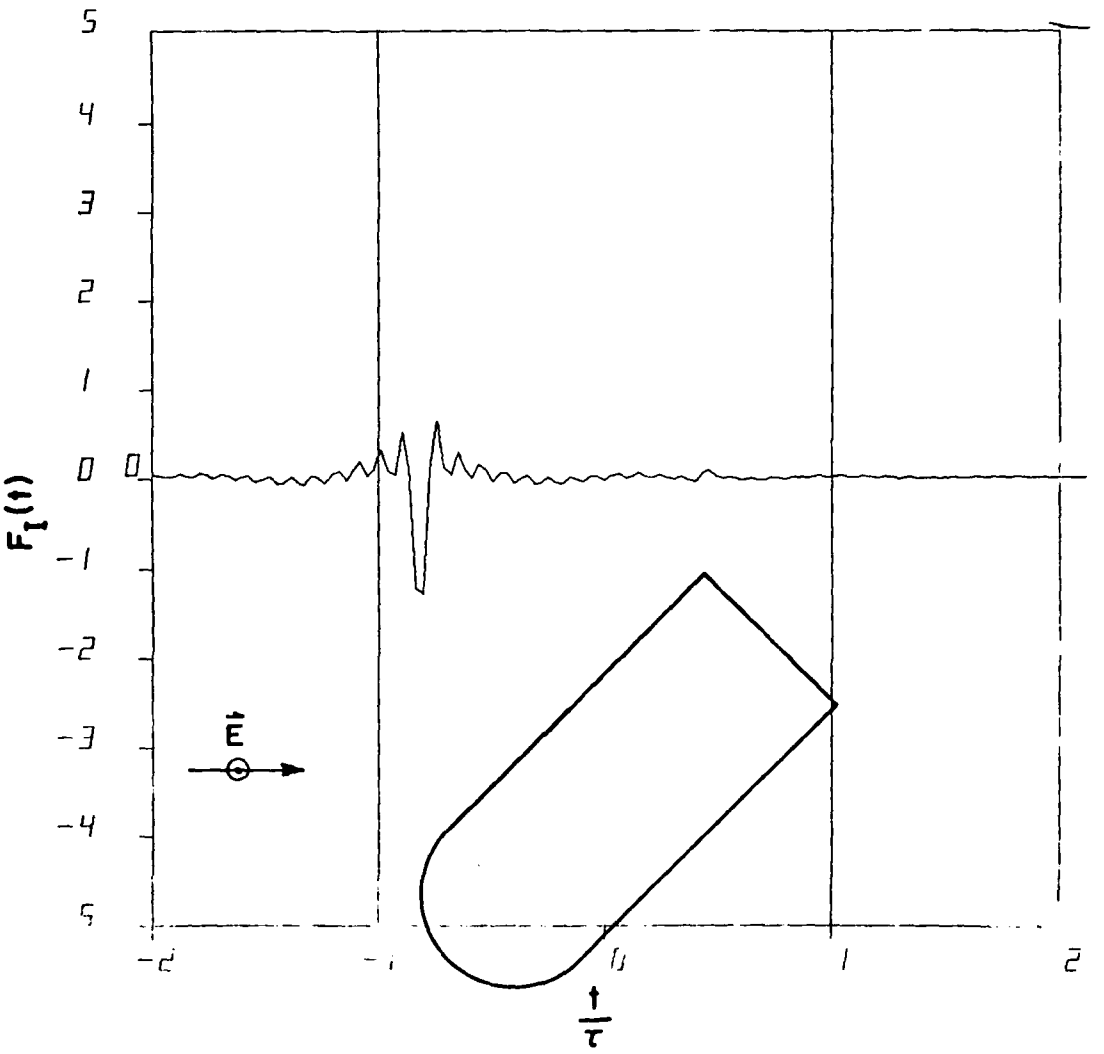

Figure E-13. First-order UTD impulse response for sphere-capped cylinder at 45°. Vertical polarization.

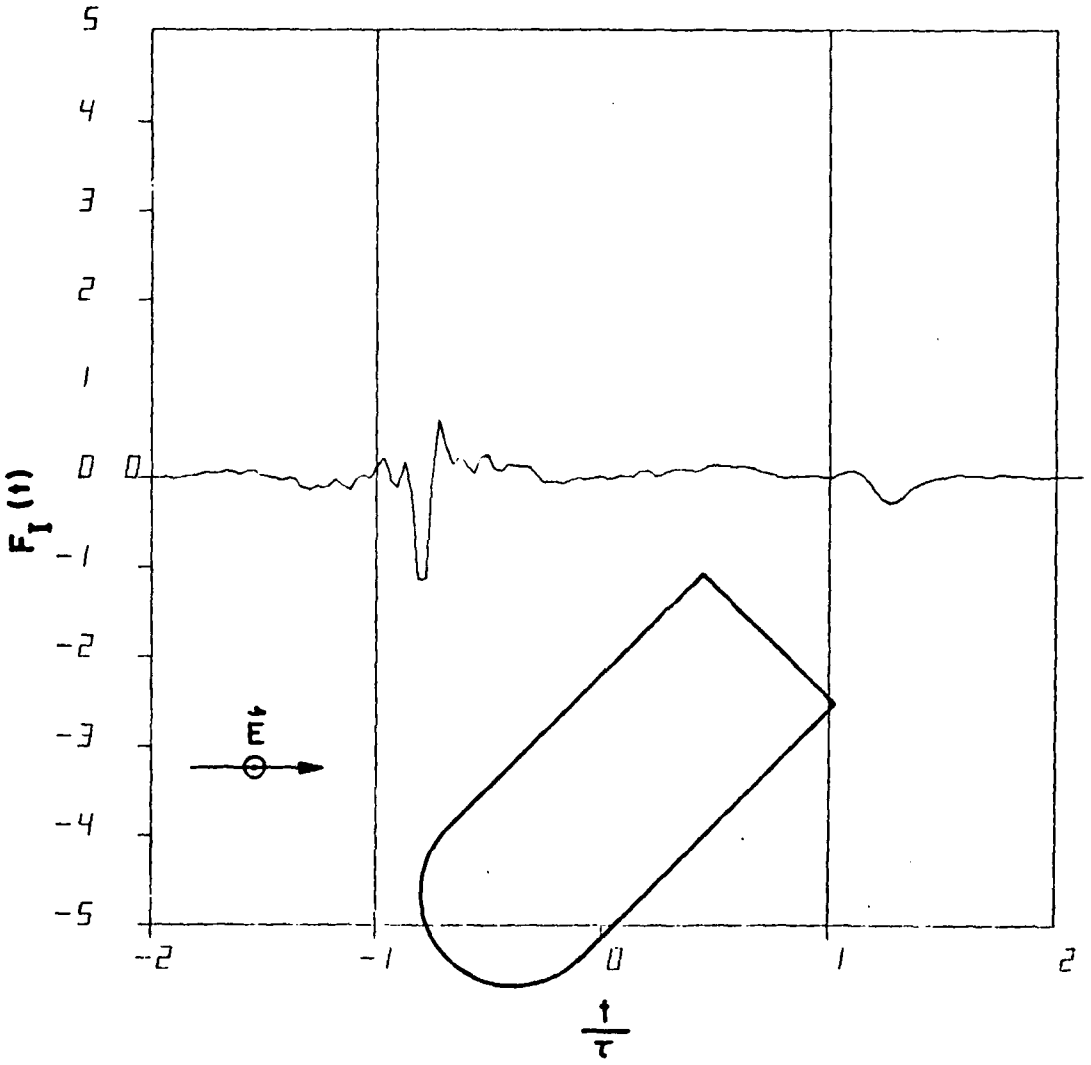

Figure E-14. Measured impulse response for sphere-capped cylinder at 45°. Vertical polarization.

Finally, if the waveforms for the two polarizations are compared, it can be seen that the target is insensitive to polarization up to the back edge, where significant differences occur. In this report we have shown a limited number of targets and aspects. Additional information about specific radiating mechanisms may be obtained simply by rotating the target or by comparing the sphere-capped cylinder to the cylinder without the spherical cap. Or, the known mechanisms in the UTD waveform may be subtracted from the measured waveform and the difference transformed back into the frequency domain. Such analyses will be the subject of a forthcoming thesis.

Up to now, this discussion has concentrated on the time domain impulse response waveforms. The other two important canonical waveforms, step resonse and ramp response, are shown in Figures E-15 and E-16 for the measured sphere-capped cylinder at 0°. These are the first and second integral of the response of Figure E-10 with consistent normalization [6].

It has been previously shown that the ramp response is proportional to object cross-sectional area vs distance along the line of sight [7] and that a synthetic object image may be derived from ramp response data [8,9]. An image of the sphere-capped cylinder at 0° is shown in Figure E-17 and for the 180° orientation in Figure E-18. The basic shape is clearly evident, and the difference in spherical and blunt end is indicated even though the physical optics approximation used in the imaging process only approximately handles the scattering phenomena in the rear, shadowed region of the target.

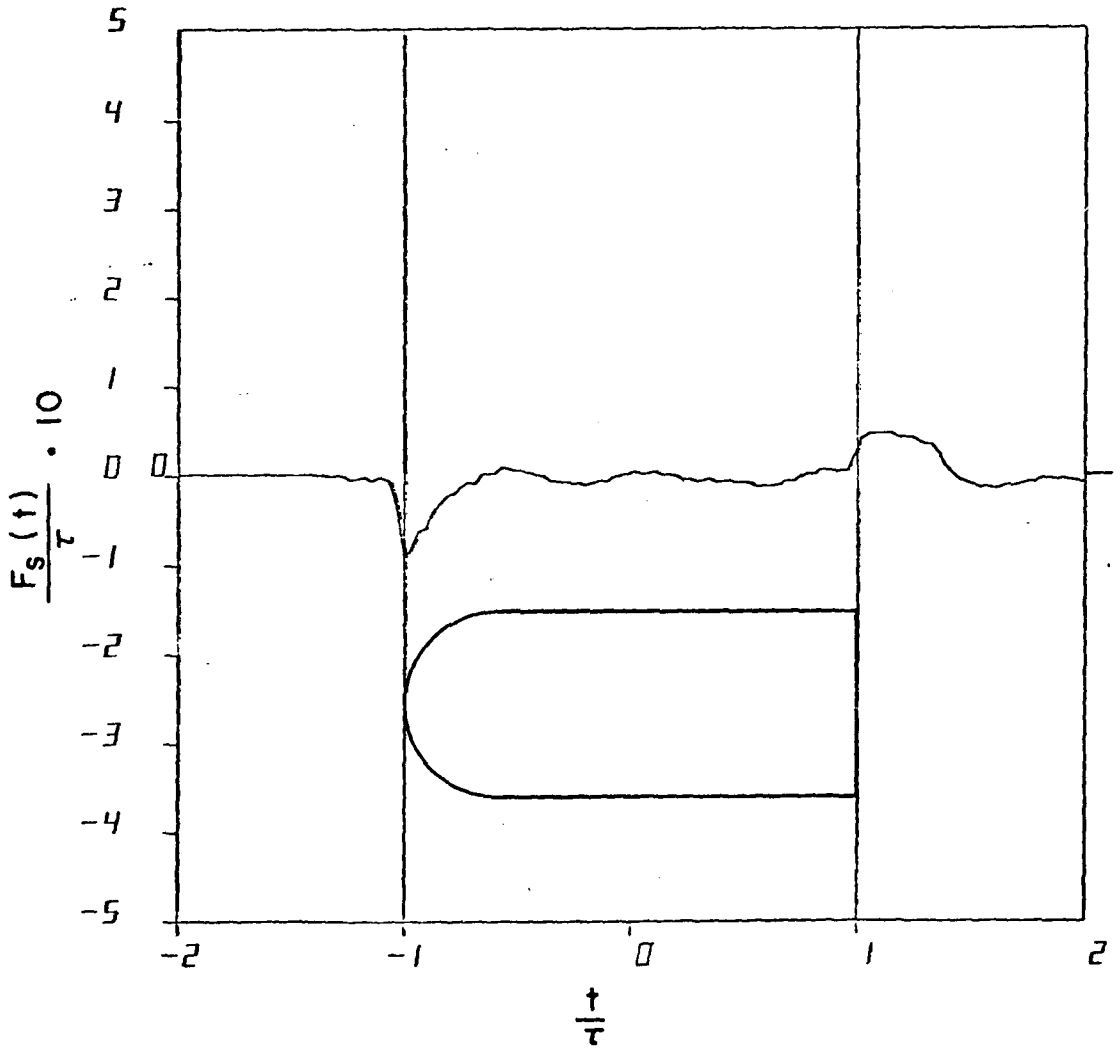

Figure E-15. Measured step response for sphere-capped cylinder at 0°.

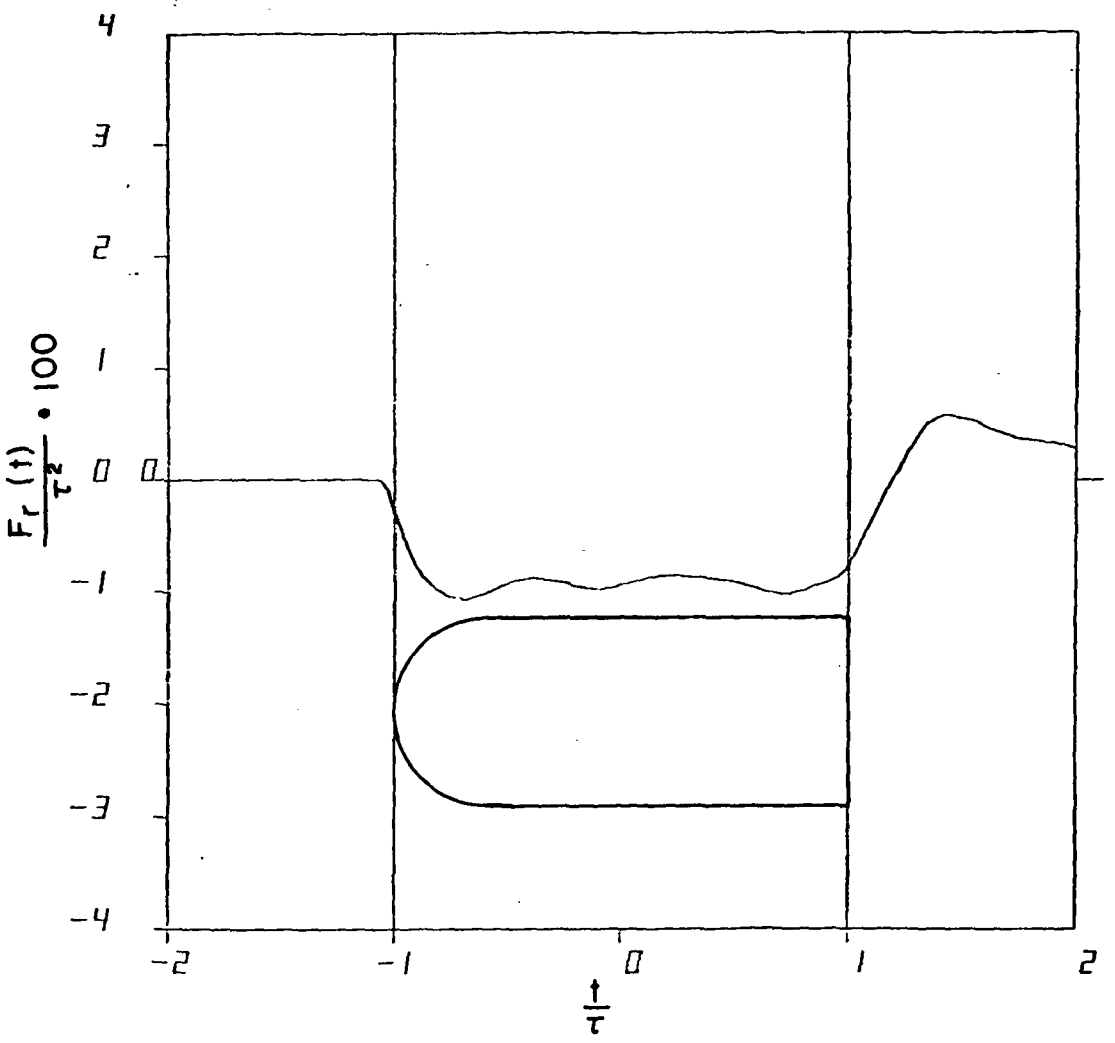

Figure E-16. Measured ramp response for sphere-capped cylinder at 0°.

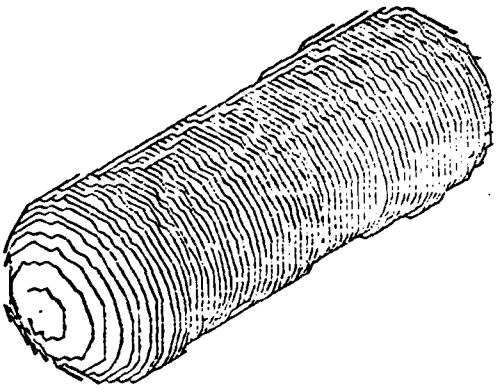

Figure E-17. Image of sphere-capped cylinder at 0°.

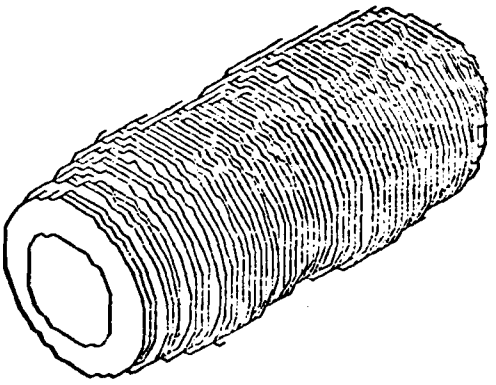

Figure E-18. Image of sphere-capped cylinder at 180°.

Cross-Polarized Measurements

In order to measure cross-polarized backscatter, it was necessary to select a suitable calibration target to replace the sphere, which has no cross-polarized return. A calibration target must satisfy the following criteria: 1) it must be broadband, i.e., not highly resonant; 2) it must have a known, readily available exact solution; and 3) it must be relatively insensitive to positioning.

A narrow, thin strip at edge-on incidence was chosen. This candidate was known to satisfy the third criterion as shown in Figure E-19 [10). It was predicted and proven that a narrow strip would be broadband. And, finally, a moment method solution was available.

At a tilt of 45° off vertical, the edge-on strip gave a cross-polarized return comparable in magnitude to the co-polarized return of our calibration spheres. The strip has a cosine sensitivity to error in the amount of tilt. Co-polarized measurements on the strip calibrated against a sphere shown in Figure E-20 verify that the narrow ($< \lambda/4$) strip is indeed broadband in both amplitude and phase.

To test the viability of obtaining cross-polarized results using the strip, the measurements were restricted to 2-4 Ghz. The targets described in the section Swept Frequency System were tilted out of the principal planes in order to ensure a cross-polarized return. In addition to these targets, several sizes of discs, flat plates and strips were included.

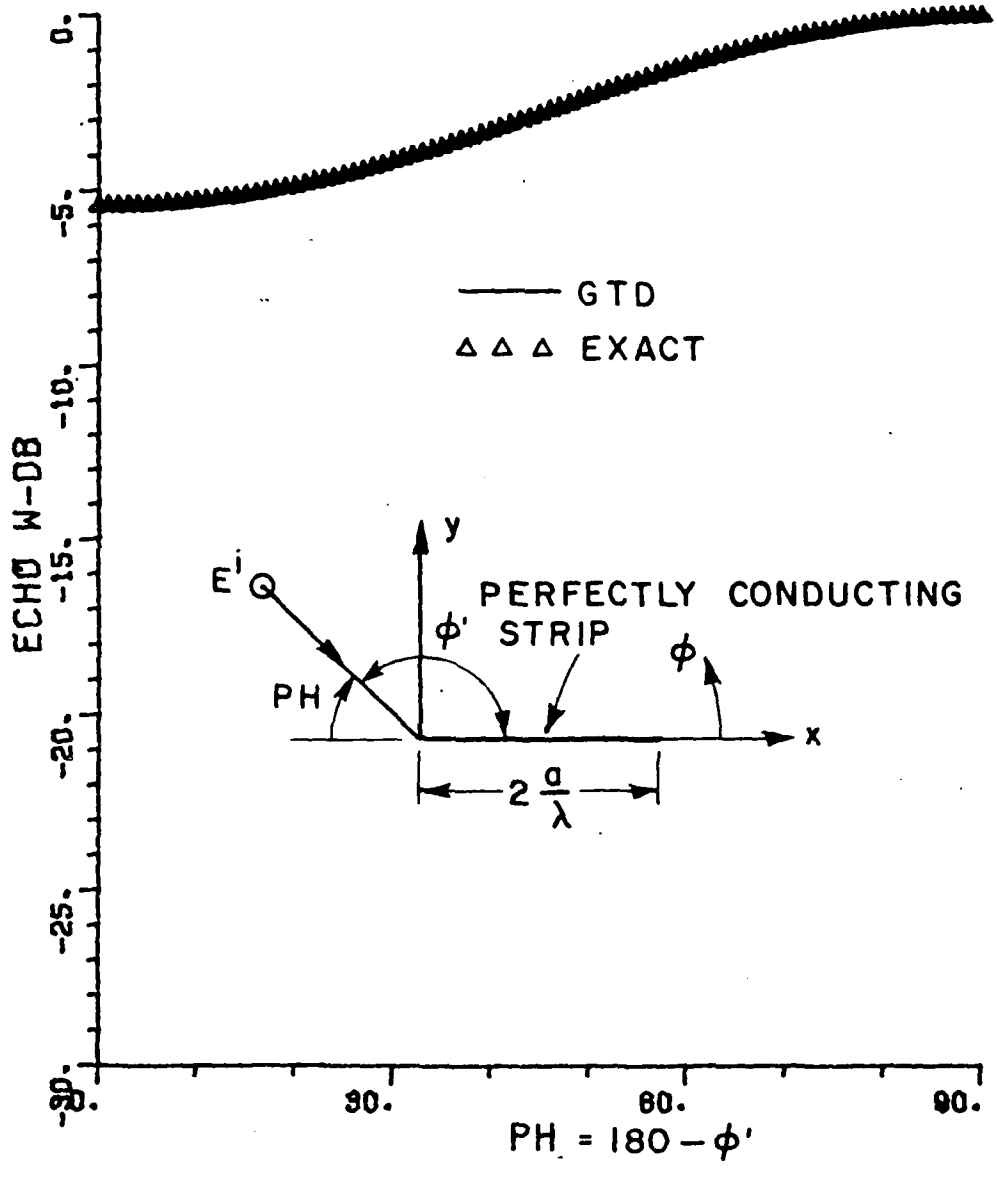

Figure E-19. H-plane echo width pattern of λ/4 wide strip.

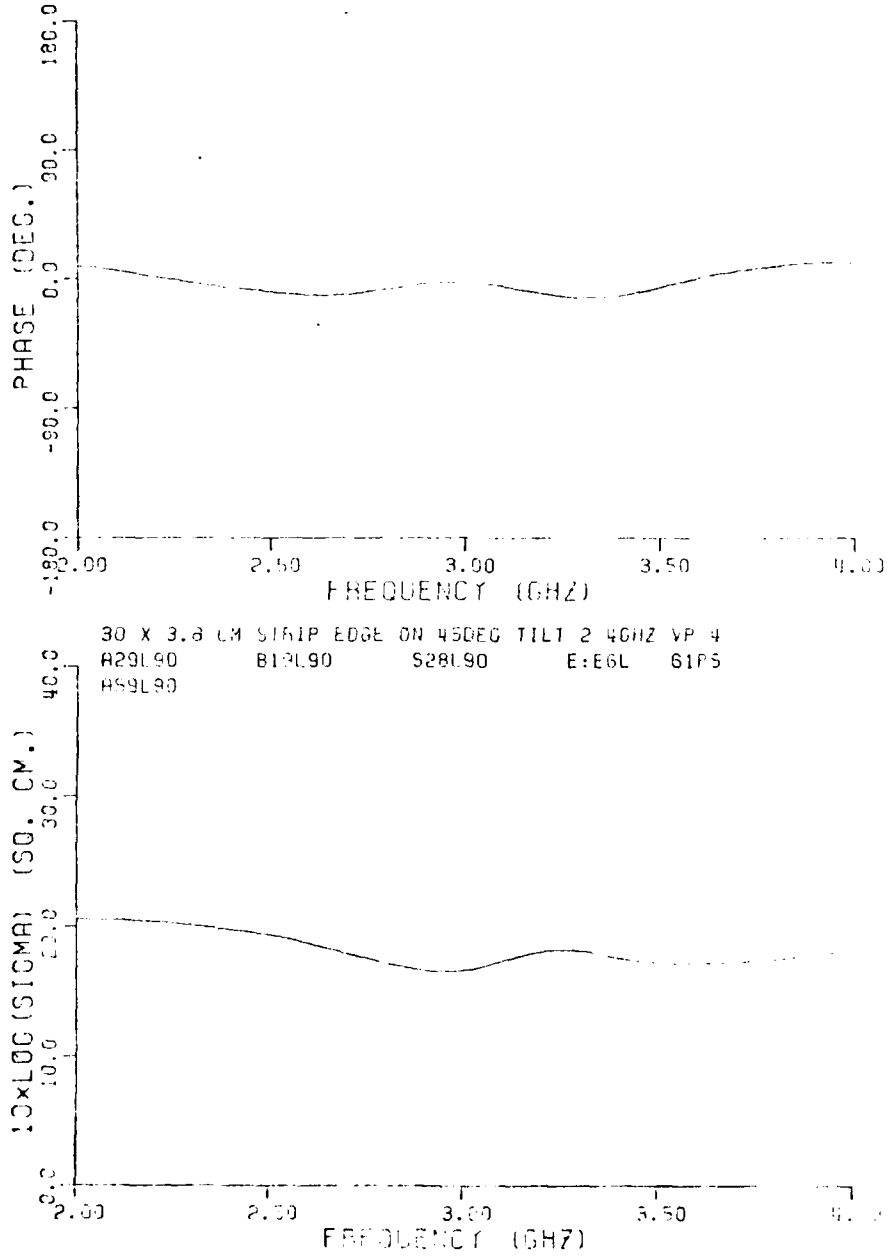

Figure E-20. Co-polarized measurements of a narrow strip calibrated against a sphere.

In Figure E-21, an exact solution by D. Hodge [11] is compared to measured cross-polarized results for a disc at edge-on incidence and a 45° tilt. The results compare very well for those portions of the spectrum above the noise floor of the system, i.e., above 0-5 dBscm.

In general, the cross-polarized return of a target will be low, and the noise floor will have to be improved in order to recover nulls below 1 cm^2.

New Equipment

During the final months of this program, some signature data on a 4:2:1 ellipsoid were recorded making use of new equipment acquired on an associated research program. This equipment consists of:

1. A Digital Equipment Corporation PDP-11-23 computer.
2. A Watkins-Johnson Model crystal stabilized source, computer-controlled through an IEEE 488 bus.
3. A Scientific Atlanta Model receiver, also IEEE 488 bus compatible.
4. A new very low cross-seciton target support pedestal with improved positioning accuracy (also computer controlled).

Performance tests of these components indicate that the effective sensitivity of the measurement system has been increased by about 15 dB. Also, measurements are faster since the whole range from 2 to 12 GHz is

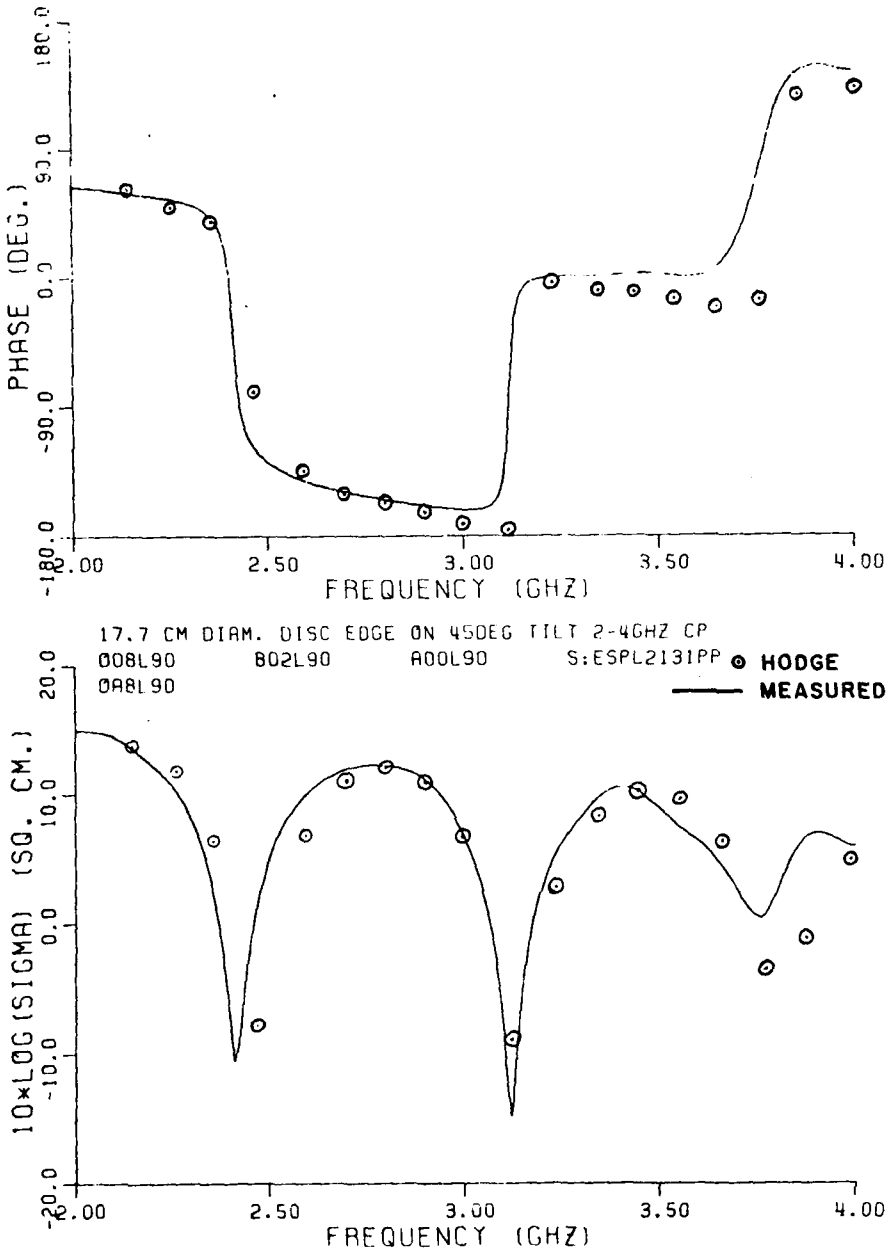

Figure E-21. Comparison of measured and theoretical (Hodge) cross-polarized response from a thin disk tilted at 45°.

acquired in one sweep, rather than plug-in change-overs taking place at 2, 4 and 8 GHz.

Backscattered cross-section data for horizontal and vertical polarization along all three principal planes of a 1.5" x 3/4" x 3/8" ellipsoid were recorded for a range from 2 to 12 GHz. A representative calibrated spectrum is shown in Figure E-22.

Conclusions

Measured data have been shown to be of sufficient accuracy and bandwidth to give complete information about a target. The data constitute complete transfer function information for the specific targets and aspects measured. Thus, the scattering response signal for any particular radar system (within the frequency band coverage) may be obtained by simply multiplying the system radiated signal complex spectrum by the complex spectral signature of the target. This should be very useful in system design for optimized target detection and discrimination involving these shapes.

The time domain waveform graphically illustrates the relation between target geometry and backscatter. These data are therefore a valuable tutorial aid in evaluating and improving the accuracy of theoretical methods.

The quality of the data already obtained is still being improved by better data processing techniques, and the quality of new data benefits from improvements in the system and range. The system has been successfully adapted to the measurement of cross-polarized backscatter.

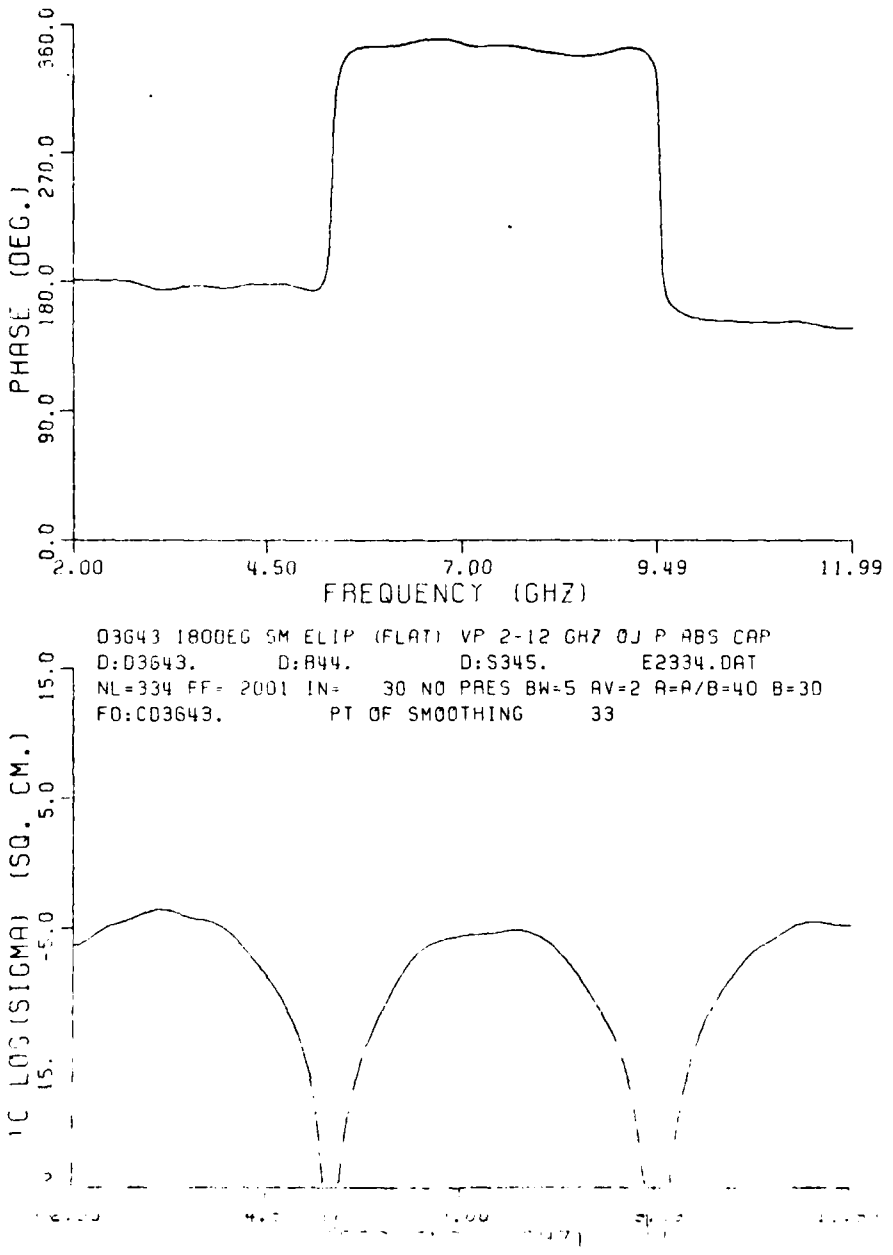

Figure E-22. Representative spectrum of backscatter from an ellipsoid.

References

[1] Weir, et al., "Broadband Automated RCS Measurement", IEEE Trans., AP-22, No. 6, November 1974.

[2] Young, "Radar Imaging From Ramp Response Signatures", IEEE Trans., AP-24, May 1976.

[3] Chu, Ph.D. Dissertation, The Ohio State Univerity, 1982.

[4] Kennaugh and Moffatt, "Transient and Impulse Response Approximations, Proc. IEEE, May 1965.

[5] Young, Moffatt, Kennaugh, "Time Domain Radar Signature Measurement Techniques", Technical Report 2467-3, July 1969, The Ohio State University ElectroScience Laboratory, Department of Electrical Engineering; prepared under contract F44620-67-C-0095 for Air Force Cambridge Research Laboratories, Bedford, Massachusetts.

[6] "Measurement and Analysis of Spectral Signatures", Rome Air Development Center, Air Force Systems Command, Griffiss Air Force Base, New York, contract RADC-TR-71-114, June 1971.

[7] Kennaugh, E.M. and D.L. Moffatt, "Transient and Impulse Response Approximations", Proc. IEEE, Vol. 53, pp. 893-901, August 1965.

[8] Young, "Radar Imaging from Ramp Response Signatures", IEEE Trans. on Antennas and Prop., Vol. AP-24, #3, pp. 276-282, May 1976.

[9] Schubert, Young, Moffatt, "Synthetic Radar Imagery", IEEE Trans. on Antennas and Prop., Vol. AP-25, #4, pp. 477-483, July 1977.

[10] Peters, "Two Dimensional Applications for Bodies with Edges", The Ohio State University - ElectroScience Laboratory Short Course Notes, Vol. I.

[11] Hodge, D.B., "The Calculation of Far Field Scattering by a Circular Metallic Disk", Technical Report 710816-2, February 1979, The Ohio State University ElectroScience Laboratory, Department of Electrical Engineering; prepared under contract N00014-78-C-0049 for Department of the Navy, Office of Naval Research, Arlington, Virginia 22217.

APPENDIX I

PROJECT TITLES AND ABSTRACTS

Project 784652 An Advanced Prototype System for Locating and Mapping Underground Obstacles

The objective of this program is to develop a portable video pulse radar system for locating and mapping underground objects to a depth of 10-15 feet. The emphasis is on improving signal processing techniques and optimizing system performance to improve target resolution.

Project 784673 Advanced Numerical Optical Concepts

The objective of this program is the development of the technology for optical computing systems.

Project 710816 Block Funded Support for Electromagnetic Research

This is research in the area of electromagnetic radiation and scattering including: (1) extension of the Geometric Theory of Diffraction (GTD) for convex surfaces, edges, vertices and time domain

solutions; (2) the GTD combined with the Method of Moments (MM); (3) extension of the MM codes utilizing polygon surface current patches and wire-patch attachment modes; (4) transient electromagnetic phenomena including target identification, radar imagery, K-pulse techniques and scattering from a thin, circular disk; and (5) improving the free space scattering range at The Ohio State University ElectroScience Laboratory to obtain accurate polarization matrix information on selected reference targets.

Project 710964 Analysis of Ariborne Antenna Patterns

The objectives of this program are to: (1) improve the aircraft model for far field pattern computations by considering a more realistic vertical stabilizer; (2) study various ways to model more general antenna types such as a monopole in the presence of directors; (3) examine various flat plate simulation codes; and (4) compare various calculated results with measurements supplied by NASA (Langley).

Project 711639 Superdirective Arrays

The objective of this study is the development of computer codes to analyze the performance of a circularly disposed superdirective array with the appropriate feed network.

Project 711679 Jam Resistant Communications Systems Techniques

The objectives of this program include (1) development and testing of a bit-synchronous time-division multiple-access digital communications system suitable for use by a large number of small (airborne) terminals in conjunction with larger ground stations, (2) the application of adaptive arrays for up-link antijam protection of this system, and (3) development of techniques, circuits and components for increased data rates, digital control, and interference rejection in high speed digital communications systems.

Project 711930 Radar Cross Section Studies

The objective is to establish the GTD techniques required to treat the radar cross section of missile and aircraft bodies.

Project 711964 Electrically Small Antennas

This three-year program of research into electrically small antennas has three phases: Phase 1 - a basic study to develop the theory, techniques and computer codes for electrically small antennas mounted on a general structure; Phase 2 - a study to develop the theory, techniques and computer codes for printed circuit antennas; and Phase 3 - a study to compare the K-Pulse concept with more conventional techniques for increasing the maximum data rate in pulse communications using small antennas.

Project 712242 Formulate Quasi-Optical Techniques for Antennas at UHF

The goal of this program is to increase the electromagnetic effectiveness of Navy ships by developing low cost, integrated, systematic EM design procedures.

Project 712257 Application of Optical Computing Techniques to Jet Engine Control

This program involves the following tasks: (1) survey and document control requirements for jet engines using information supplied by sponsor; (2) survey and document the field of optical computing as applied to jet engine controls; (3) generate a report listing the various schemes and comparing them for speed, information processing capability, and ability to withstand the necessary environmental conditions; and (4) make recommendations as to the scheme most likely to satisfy the requirments stated in (1).

Project 712742 Radar Measurement of Rain Cells

The purpose of this effort is to obtain a statistical characterization of the distribution of rain attenuation along earth-space paths. This is to be accomplished through the simultaneous measurement of path attenuation and radar backscatter. Supporting measurements of the path radiometric temperature and the ground rain rate are also proposed. The resulting data are to be analyzed to yield information which will permit a more accurate conversion of point rain rate staistics to path attenuation statistics.

Project 712861 Coal Pile Electromagnetic Sensing Research

This project involves a research program in electromagnetic subsurface remote sensing as applied to accurate estimation of the quantity of coal in a large coal pile. This problem is important to inventory control at coal fired generating stations in the electric power industry. Coal quantity depends on both density and volume of the pile, and means for remote sensing of both of these parameters is sought.

Project 712949 Leaky Ported Coaxial Cable Embedded at a Uniform Depth in a Lossy Half Space

It is the purpose of this research to complete our theory appropriate for a planar interface and the extension of our computer code to obtain numerical results for the associated propagation constants and field configurations.

Project 713169 EO Device Signature Reduction

This is a classified program.

Project 713176 Xenon Probe Laser for Atmospheric Studies

The objective is to construct and test a versatile laser, rugged enough for field operation and tunable to various lines in the 2-11.3 μm range, for use as an atmospheric probe laser.

Project 713206 Advanced RCS Reduction

This is a classified program.

Project 713302 Design of Dual Band Antennas

The Navy frequently has need for antennas which will operate at more than one band of frequencies. This project addresses the design of a dual band reflector antenna utilizing a dichroic surface design that is based on extensive experience at the ElectroScience Laboratory with transparent metallic surfaces.

Project 713303 On-Aircraft Antennas

The objectives of this program are: 1) to develop the capability to analytically synthesize the aperture distribution of a complex antenna array given its free space near field antenna pattern; 2) to test the technique developed in item 1 by using simple antenna arrays; and 3) to investigate the accuracy of the Geometrical Theory of Diffraction as applied to a curved surface in terms of low scattering levels associated with side lobe illumination of such structures.

Project 713381 Electromagnetic Reradiation Theoretical Prediction for Complex Building Structures

The purpose of this program is to develop a model of a building with sufficient structural detail to allow predictin or radio direction finding errors for roof-top antenna systems against any specified HF signal.

Project 713402 Microstrip Analysis Techniques

This study extends the state of the art in microstrip analysis techniques by considering mutual coupling between microstrip antennas on a flat strip and on a cylinder.

Project 713533 Engineering Calculations for Satellite Systems Planning

The objective of this program is to enhance the computational capability of NASA/Lewis Research Center for calculating the performance of proposed communications satellite systems. In particular, the effort addresses the potential interference between services sharing a common frequency band.

Project 713581 Development of Computer Models of Large Reflectors

The objective of this study is to develop computer models to provide design information for space-borne reflector antennas.

Project 529622 Gas Leak Detection

The objective of this program is to develop electromagnetic techniques for the location of leaks in underground gas pipes.

Project 529623 Terrascan Improvement

The objective is the development of an improved Terrascan unit for the location of buried pipes. Two areas are being addressed: 1) improvement of the sensor head (antenna) and 2) improvements in the ease of operation of the unit and its adaptability to a wide range of soil conditions.

Project 713603 Sophisticated Jammers and Adaptive Arrays

The objective of this research is to obtain a quantitative understanding of the effectiveness of several types of jamming that could be used against an adaptive array and, time and funds permitting, attempt to develop a strategy for dealing with such jamming.

Project 713645 MX Physical Security System

The objective of this program is to develop electromagnetic techniques for determining the electrical parameters of soil in situ.

Project 713656 Study of Meteorological Factors in Earth Satellite Propagation

The objectives of this program are to 1) conduct gain degradation measurements on Comstar D/4 28.56 Ghz synchronous satellite beacon and 2) conduct path diversity measurements using two 28 Ghz radiometers separated by approximately 12 Km.

Project 713671 Conduct Exploratory Development of Millimeter Wave (MMW) Systems Using the Targeting Systems Characterization Facility (TSCF)

The objective of this study is to assess the effects of target and background signatures, meteorological conditions, and sensor-to-target geometries of the TSCF on MMW radar and radiometric measurements, to recommend appropriate design modifications and calibration procedures and to provide technical and computer software support for TSCF MMW measurements.

Project 713711 Program Planning Measurement of Surface Ship Radar Backscatter at HF for Target Identification Studies

The objective of this program is to plan for methods to measure radar backscatter from ships. The computer controlled radar cross section measurement system is to be configured for the task of measuring the radar cross section of ship models.

Project 713712 Evaluation of Design Candidate Antenna

The objective of this study is to analyze the performance of a design candidate antenna with a tunnel. Computer models are to be developed for the scan plane so that worst case performance can be predicted.

Project 312688 Geophysical Research

The objective of this program is to determine the state-of-the-art in underground exploration using electromagnetic techniques and define a program for an electromagnetic exploration system (EMES).

Project 713715 Construction of Vehicle Tracking System

This contract provides for the construction of a ground-based optical vehicle tracking system. This system will use three Reticon digital line scanning cameras to track a number of light sources moving over a portion of the Vehicle Dynamics Area of the Transportation Research Center of Ohio. The output of the cameras will be processed in a computer to determine the position, velocity and acceleration of each light source as a function of time. Position accuracy of ±1.5" will be obtained for stationary light sources and an accuracy of better than ±0.75" will be achieved for moving light sources. Vehicle heading and articulation angles will be computed from the positions of pairs of lights.

Project 713731 Data Processing of Radar Measurements

The objective of this program is to digitize a collection of data on radar backscatter from moving tactical ground vehicles and store the data on computer compatible tape files for future processing.

Project 713758 Basic Computer Code Development

The objective of this program is to extend the ESL basic scattering code to include higher-order scattering effects and impedance loaded surfaces.

Project 713768 A Theoretical and Experimental Study of a Potential Mobile System for Evaluating Electrical Parameters of the Earth

The objective of this study is to evaluate a novel approach for rapidly estimating the electrical parameters of the earth over a broad frequency band.

Project 713774 The Effects of Atmospheric Water Vapor on Infrared Propagation

The objective of this program is to make measurements of the absorption of infrared radiation by pure and pressure-broadened water vapor samples at several different frequencies using a frequency-doubled CO_2 laser. Results of these measurements are to be incorporated into an analysis of continuum absorption as wings of strong absorption lines.

Project 713971 Computation of the Performance of an Element Antenna Array Mounted on an Aircraft

The objective of this program is to compute the radiation patterns of a specified set of antenna elements and a specified frequency range to insure adequate SINR (signal to interference plus noise ratio) over a specified field of view. Array performance is simulated to represent an adaptive mode of operation.

Project 714100 Navigation System Simulation

The objective of this program is to evaluate the simulation and performance of the GPS/JTIDS Adaptive Multifunction Array antenna design.

Project 714119 Support Services of Electromagnetic Design of RAM/RAS and Non-Specular Scattering

This is a classified program.

Project 714152 Frequency Sensitive Surface (FSS)

The purpose of this program is to design a frequency sensitive surface (FSS) to be comprised of two or three loaded dipole arrays sandwiched between an appropriate number of dielectric slabs.

Project 714190 Resonant Structure NCTR

The objective of this research project is to measure the complex polarization scattering matrix of resonant structures.

Project 714215 Research on Near Field Pattern Effects

This study consists of the following: (1) develop a near field solution for the volumetric pattern of an antenna mounted on a 3-dimensional fuselage structure; (2) extend the present numerical analysis for near field principal plane patterns to treat multiple plates; (3) using these improved solutions, examine their validity and usefulness in analyzing various complex airborne antenna problems; and (4) compare results with measured results.

Project 714258 Advanced SATCOM ECCM Techniques

This is a classified project.

Project 714259 Low RCS SATCOM Antennas

This is a classified project.

Project 714349 Radar Cross Section of Aircraft/Avionics Systems

This is a classified project.

Project 714381 Electromagnetic Reradiation Theoretical Prediction for Complex Building Structures

The purpose of this research project is to develop building models with sufficient structural detail to allow prediction of phase and gain patterns for rooftop-mounted antenna systems against any specified HF Signal.

Project 714414 Construction of Vehicle Tracking - Phase II

This project provides for the construction of a ground-based optical tracking system. This system will use three Reticon digital line scanning cameras to track a number of light sources moving over a portion of the Vehicle Dynamics Area of the Transportation Research Center of Ohio.

Project 714428 Radar Cross-Section Controls

This project seeks to develop design parameters for slotted metallic radomes and RCS control of OSR antenna assembly.

Project 714505 Advanced Adaptive Antenna Techniques

The objective of ths research program is to study the effect of frequency hopping on the performance of an adaptive array and the performance of the Frost algorithm with multiple constraints for use in communications systems.

Project 714541 Hybrid Metallic Radome

The purpose of this study is to perform a computer analysis of a hybrid metallic radome of unique structural composition.

Project 312145 DBS Antenna Measurements

The purpose of this program is to measure the performance of candidate antennas for DBS application.

Project 714614 Radar Cross Section Studies

This is a classified program.

Project 714861 On-Aircraft Antennas

This is a classified program.

APPENDIX II
ELECTROSCIENCE LABORATORY SPONSORING AGENCIES

OHIO STATE UNIVERSITY - ELECTROSCIENCE LABORATORY ACTIVE PROJECTS DURING OCTOBER 1981 - OCTOBER 1982

PROJECT ENGINEER	PROJECT NUMBER	SPONSOR	CONTRACT OR GRANT NUMBER	STARTING DATE	ENDING DATE	AWARD AMOUNT	SOURCE
	Facilities Contract		AF 33(600)-31168				
CALDECOTT	784652	EPRI	RP7856-1	01-01-77	12-31-83	800K	03
COLLINS	784673	BMDSC	DASG60-77-C-0045	03-01-77	05-31-82	249K	02
WALTER	710816	ONR	N00014-78-C-0049	10-01-77	09-30-83	1987K	01
BURNSIDE	710964	NASA/Langley	NSG 1498	01-16-78	02-28-83	249K	02
NEWMAN	711639	NSA	MDA904-79-C-0407	10-24-78	12-31-81	178K	03
KSIENSKI/BURNSIDE	711679	RADC	F30602-79-C-0068	12-04-78	05-30-82	873K	02
PETERS/BURNSIDE	711930	NASA/Langley	NSG 1613	05-01-79	04-30-83	352K	02
RICHMOND/WALTER	711964	ARO	DAAG29-79-C-0082	05-01-79	10-30-82	154K	02
MARHEFKA/RUDDUCK	712242	NOSC	N00123-79-C-1469	08-01-79	10-31-82	375K	02
COLLINS	712257	NASA/Lewis	NSG 3302	08-01-79	07-30-83	280K	02
PATHAK	712661	ESD/Hanscom AFB	F19628-80-C-0056	04-01-80	03-01-82	147K	02
LEVIS	712742	Intelsat	INTEL-066	03-20-80	03-19-82	168K	01
YOUNG	712861	TVA	TVA-53983A	04-17-80	09-30-82	163K	01
RICHMOND/GARBACZ	712949	Waterways Exp. Stat.	DACA39-80-K-0001	05-01-80	03-31-82	105K	01
DAMON	713169	ASD/WPAFB	F33615-80-C-1072	08-01-80	02-01-83	193K	01
DAMON	713176	NRL	N00173-80-C-0416	08-01-80	07-31-82	50K	03
MUNK	713206	ASD/WPAFB	F33615-80-C-1086	08-25-80	08-24-83	300K	02
MUNK	713302	NRL	N00173-80-C-0367	09-30-80	12-31-82	98K	03
RUDDUCK	713303	NADC	N62269-80-C-0384	09-22-80	09-30-82	100K	03
NEWMAN	713381	Southwest Research	P.O. 105317SW	10-23-80	02-26-82	71K	02
NEWMAN	713402	ARO	DAAG29-81-K-0020	11-01-80	10-31-82	102K	02
LEVIS	713533	NASA/Lewis	NAG 3-159	01-20-81	07-13-84	113K	01
RUDDUCK	713581	Martin Marietta	RH1-092665	01-21-81	09-30-82	92K	03
YOUNG	529622	Gas Research Institute		01-19-81	01-19-82	101K	02
YOUNG	529623	Gas Research Institute		01-26-81	01-26-82	125K	02
COMPTON	713603	NASC	N00019-81-C-0093	03-23-81	03-22-82	80K	02
YOUNG	713645	Boeing Aerospace	F55411	03-05-81	12-31-81	160K	02
LEVIS	713656	Jet Prop. Lab	NO. 956013	03-12-81	03-31-83	255K	02
LEVIS	713671	ASD/WPAFB	F33615-81-C-1437	04-01-81	07-31-82	47K	01
KSIENSKI/WALTON	713711	ONR	N00014-81-K-0491	04-01-81	07-31-82	50K	02
RUDDUCK	713712	Aerospace Corp	P.O. 27809-AN	04-01-81	12-31-83	105K	02
WALTER	312688	Terra Research		03-15-81	Indefinite	10K	03
SVOBODA/POIRIER	713715	NHTSA	OSU-81-0032	03-01-81	09-30-82	76K	02
KSIENSKI/WALTON	713731	ASD/WPAFB	F33615-81-C-1490	05-01-81	01-01-82	71K	02
WALTER/MARHEFKA	713758	Lockheed	DA5006340F	04-22-81	12-15-81	24K	03
PETERS	713768	NSF	ECS-8020636	05-01-81	04-30-83	60K	01
DAMON/LONG	713774	ARO	DAAG29-81-K-0084	06-01-81	05-31-83	200K	01
KSIENSKI	713971	Forsvarets Materielverk	FK 82463-80-409-23-001	07-06-81	01-31-82	30K	02

PROJECT ENGINEER	PROJECT NUMBER	SPONSOR	CONTRACT OR GRANT NUMBER	STARTING DATE	ENDING DATE	AWARD AMOUNT	SOURCE
KSIENSKI	714100	Analytic Sciences	10300	09-01-81	09-30-83	95K	02
MUNK	714119	McDonnell Douglas	P.O. Z10104	09-04-81	09-30-82	35K	03
MUNK	714152	Ford Aerospace	SP-720849-AX	07-16-81	12-07-81	30K	02
YOUNG/MOFFATT/ WALTON	714190	ONR	N00014-82-K-0037	10-01-81	09-30-82	360K	01
BURNSIDE	714215	NASC	N00019-81-C-0424	10-01-81	09-30-82	65K	02
KSIENSKI	714258	RADC	F30602-82-C-0009	02-04-82	08-03-84	750K	02
MUNK	714259	ESD/AFSC	F19628-82-K-0027	02-01-82	09-30-82	59K	02
PETERS/BURNSIDE	714349	Rockwell	L2XN-11455-915	01-25-82	09-30-82	150K	02
NEWMAN	714381	Southwest Research	PO: 15044-SW	02-27-82	02-26-83	75K	01
SVOBODA	714414	NHTSA	OSU-82-0039	01-01-82	09-30-82	29K	03
MUNK	714428	Boeing	BE5591	03-22-82	12-15-82	25K	02
COMPTON	714505	NASC	N00019-82-C-0190	04-28-82	04-27-83	80K	02
MUNK	714541	General Electric	211-000575FK036	05-17-82	10-29-82	7K	02
DAMON	312145	Stolle	547928	04-30-82	08-20-82	16K	01
PETERS/BURNSIDE	714614	Naval Air Station	N0429A-82-C-0396	06-15-82	06-14-83	100K	02
RUDDUCK	714861	NADC	N62269-82-C-0375	09-07-82	09-06-83	35K	03

APPENDIX III

REPORTS PUBLISHED BY ESL OCTOBER 1981 TO OCTOBER 1982

784673-3 ADVANCED NUMERICAL OPTICAL CONCEPTS - SEMIANNUAL, S.A. Collins, Jr. and Jack Ambuel, February 1982.

784673-4 ADVANCED NUMERICAL OPTICAL CONCEPTS - SEMIANNUAL, S.A. Collins, Jr. and Jack Ambuel, March 1982.

784673-5 ADVANCED NUMERICAL OPTICAL CONCEPTS - SEMIANNUAL, S.A. Collins, Jr., C.Y. Yen, M.T. Fatehi and K.C. Wasmundt, March 1982.

784673-7 ADVANCED NUMERICAL OPTICAL CONCEPTS - FINAL, S.A. Collins, Jr., May 1982.

529622-2 IDENTIFICATION OF LEAKS RESEARCH - QUARTERLY, J.D. Young, December 1981.

529622-3 IDENTIFICATION OF LEAKS RESEARCH - QUARTERLY, J.D. Young, February 1982.

529623-1 LOCATION OF BURIED PIPE -- DEVELOPMENT OF AN IMPROVED TERRASCAN* UNIT, J.D. Young, October 1981.

529623-2 LOCATION OF BURIED PIPE -- DEVELOPMENT OF AN IMPROVED TERRASCAN* UNIT, J.D. Young, December 1981.

529623-3 LOCATION OF BURIED PIPE -- DEVELOPMENT OF AN IMPROVED TERRASCAN* UNIT, J.D. Young, January 1982.

529623-5 DEVELOPMENT OF AN IMPROVED RADAR-BASED UNDERGROUND PIPE LOCATION - ANNUAL, J.D. Young, March 1982.

710816-11 JOINT SERVICES ELECTRONICS PROGRAM - FOURTH ANNUAL, December 1981.

710964-10 ANALYSIS OF AIRBORNE ANTENNA PATTERNS - SEMIANNUAL, R.G. Rojas, E.H. Newman and W.D. Burnside, September 1982.

710964-11 A GENERALIZED METHOD FOR DETERMINING RADIATION PATTERNS OF APERTURE ANTENNAS AND ITS APPLICATINO TO REFLECTOR ANTENNAS, J.R. Paknys, September 1982. Thesis.

711353-4 EXTENDING THE GEOMETRICAL THEORY OF DIFFRACTION USING THE MOMENT METHOD - 1 September 1978 to 31 August 1981 - FINAL R.G. Kouyoumjian, August 1981.

711639-5 SUPERDIRECTIVE ARRAY OPTIMIZATION CODE - FINAL, E.H. Newman and M.R. Schrote, January 1982.

711639-6 SUPERDIRECTIVE ARRAY ANALYSIS CODE - FINAL, E.H. Newman and M.R. Schrote, January 1982.

711679-3 A WEIGHT STORAGE AND RECALL SYSTEM FOR USE IN AN EXPERIMENTAL ADAPTIVE ARRAY, H.S. Eilts and W.G. Swarner, February 1981.

711679-4 ANGLE OF ARRIVAL ESTIMATION, B.V. Andersson, April 1981.

711679-8 PREDICTION OF ADAPTIVE ARRY PERFORMANCE IN A MULTIPLE JAMMER ENVIRONMENT, I.J. Gupta and A.A. Ksienski, December 1981.

711679-9 THE SINR PERFORMANCE OF CASCADED ADAPTIVE ARRAYS, H.S. Eilts, March 1982.

711679-11 JAM RESISTANT COMMUNICATIONS SYSTEMS TECHNIQUES - FINAL, A.A. Ksienski, May 1982.

711930-2 UTD ANALYSIS OF ELECTROMAGNETIC SCATTERING BY FLAT PLATE STRUCTURES, F.A. Sikta and L. Peters, Jr., December 1981. Dissertation.

711930-5 ELECTROMAGNETIC SCATTERING FROM INLETS AND PLATES MOUNTED ON ARBITRARY SMOOTH SURFACES, J.L. Volakis, August 1982. Dissertation.

711964-5 ELECTRICALLY SMALL ANTENNAS - SEMIANNUAL, J.H. Richmond and C.H. Walter, January 1982.

711964-6 ELECTRICALLY SMALL ANTENNAS - SEMIANNUAL, J.H. Richmond and C.H. Walter, June 1982.

712242-9 QUASI-OPTICAL TECHNIQUES FOR ANTENNAS AT UHF - QUARTERLY, R.C. Rudduck and R.J. Marhefka, April 1981.

712242-10 QUASI-OPTICAL TECHNIQUES FOR ANTENNAS AT UHF - QUARTERLY, R.C. Rudduck and R.J. Marhefka, July 1981.

712661-1 ANALYSIS OF EM BACKSCATTER FROM A JET INTAKE CONFIGURATION, P.H. Pathak and C.C. Huang, July 1981.

712684-9 ADVANCED ADAPTIVE ANTENNA TECHNIQUES - FINAL, R.T. Compton, Jr., April 1981.

712742-3 RADAR MEASUREMENTS OF RAIN CELLS -- EFFECTIVE PATH LENGTH AND RAIN EXTENT, C.B. Sun and D.B. Hodge, August 1981.

712831-1 MICROWAVE OVEN - WORST CASE PROBING ANALYSIS - FINAL, E.H. Newman and D.M. Pozar, November 1980.

712949-4 PROPAGATION OF SURFACE WAVES ON A BURIED COAXIAL CABLE WITH PERIODIC SLOTS, J.H. Richmond, May 1982.

712949-5 COMPUTER PROGRAM FOR SURFACE WAVES ON A BURIED COAXIAL CABLE WITH PERIODIC SLOTS, J.H. Richmond, July 1982.

713206-2 THE BROADBAND FREQUENCY RESPONSE OF PERIODIC SURFACES, C.J. Larson, December 1980. Dissertation.

713302-1 A COMPACT SATCOM ANTENNA FOR X- AND Q-BAND - FINAL, S.J. Lin, L. Henderson, K. Miller and B.A. Munk, April 1982.

713303-2 THE DETERMINATION OF THE APERTURE DISTRIBUTION OF A LINEAR ARRAY THROUGH NEAR FIELD MEASUREMENTS, R.F. Backhus, June 1982. Thesis.

713321-4 NEAR FIELD ANALYSIS OF AIRBORNE ANTENNAS - FINAL, W.D. Burnside and N. Wang, December 1981.

713402-4 MICROSTRIP ANALYSIS TECHNIQUES - SEMIANNUAL, E.H. Newman, June 1982.

713603-4 A METHOD OF CHOOSING ELEMENT PATTERNS IN AN ADAPTIVE ARRAY, R.T. Compton, Jr., January 1982.

713603-5 ADAPTIVE ARRAY BEHAVIOR WITH SINUSOIDAL ENVELOPE MODULATED JAMMING, A.S. Al-Ruwais and R.T. Compton, Jr., March 1982.

713603-6 SOPHISTICATED JAMMERS AND ADAPTIVE ARRAYS - QUARTERLY, R.T. Compton, Jr., June 1982.

713603-7 THE EFFECT OF RANDOM STEERING VECTOR ERRORS IN THE APPLEBAUM ADAPTIVE ARRAY, R.T. Compton, Jr., June 1982.

713645-1 BOEING FINAL REPORT, D. Moffatt, J.H. Richmond, P. Hayes and J.D. Young, October 1981.

713656-1 AN IMPROVED EMPIRICAL MODEL FOR DIVERSITY GAIN ON EARTH-SPACE PROPAGATION PATHS, D.B. Hodge, September 1981.

713656-2 METEOROLOGICAL FACTORS IN EARTH-SATELLITE PROPAGATION - ANNUAL, C.A. Levis, R.C. Taylor, R. Leonard, K.T. Lin, B. Pigon and A. Weller, March 1982.

713671-1 A COMPARISON OF SEVERAL SYSTEMS FOR TRANSMISSION MEASUREMENTS AT 94 GHz, O.M. Buyukdura and C.A. Levis, August 1981. Thesis.

713774-1 THE EFFECTS OF ATMOSPHERIC WATER VAPOR ON INFRARED PROPAGATION - SEMIANNUAL, R.K. Long and E.K. Damon, January 1982.

713712-1 THE EXCITATION OF SURFACE WAVES IN PLANAR DIELECTRIC LAYERS, C.H. Chan, October 1982. Thesis.

713810-1 ANALYSIS OF AIRBORNE ANTENNA PATTERN DISTORTION EFFECTS USING FINITE FLAT PLATE SIMULATIONS - FINAL, R.J. Marhefka and W.D. Burnside, April 1982.

714152-1 THREE FREQUENCY SENSITIVE SURFACES FOR 20/30 GHz - FINAL, B.A. Munk, K.T. Ng, L.W. Henderson and E.K. English, November 1981.

APPENDIX IV

PAPERS PUBLISHED BY ESL OCTOBER 1981 TO OCTOBER 1982

*ANALYSIS OF A MONOPOLE MOUNTED NEAR AN EDGE OR A VERTEX, D.M. Pozar and E.H. Newman, Reprinted in IEEE *Transactions on Antennas and Propagation*, AP-30, No. 3, pp. 401-408, May 1982.

*AN ANALYSIS OF DIFFRACTION AT EDGES ILLUMINATED BY TRANSITION REGION FIELDS, R. Tiberio and R.G. Kouyoumjian, Reprinted in Radio Science, Vol. 17, No. 2, pp. 323-336, March-April 1982.

*THE ANALYSIS OF THE RF RESPONSE OF A SOLID WIRE EXCITED BY A FOCUSED LASER BEAM, K.R. Demarest and J.H. Ricmhond, reprinted in IEEE Transactions on Antennas and Propagation, AP-30, No. 2, pp. 177-182, March 1982.

*ANTENNA SHAPE SYNTHESIS USING CHARACTERISTIC MODES, R.J. Garbacz and D.M. Pozar, Reprinted in IEEE Transactions on Antennas and Propagation, AP-30, No. 3, pp. 340-350, May 1982.

*COMMENTS ON "IMPUSLE RESPONSE OF A CONDUCTING SPHERE BASED IN SINGULARITY EXPANSION METHOD", E.M. Kennaugh and D.L. Moffatt, Reprinted in Proceedings of the IEEE, Vol. 70, No. 3, pp. 294-295, March 1982.

DEPENDENCE OF ADAPTIVE ARRAY PERFORMANCE ON CONVENTIONAL ARRAY DESIGN, I.J. Gupta and A.A. Ksienski, Reprinted in IEEE Transactions on Antennas and Propagation, AP-30, No. 4, pp. 549-553, July 1982.

*THE EFFECT OF A PULSED INTERFERENCE SIGNAL ON AN ADAPTIVE ARRAY, R.T. Compton, Jr., Reprinted in IEEE Transactions on Aerospace & Electronics Systems, AES-18, No. 3, pp. 297-309, May 1982.

*EIGENFUNCTIONS OF COMPOSITE HERMITIAN OPERATORS WITH APPLICATION TO DISCRETE AND CONTINUOUS RADIATION SYSTEMS, N. Inagaki and R.J. Garbacz, Reprinted in IEEE Transactions on Antennas and Propagation, AP-30, No. 4, pp. 571-575, July 1982.

FIELD OF SEPARABLE ELECTRIC SOURCE CURRENT DISTRIBUTION IN FREE SPACE, J.H. Richmond, Reprinted in Radio Science, Vol. 16, No. 6, pp. 1299-1301, November-December 1981.

---

*Papers supported all or in part by JSEP.

A HYBRID MM-GTD TECHNIQUE FOR THE TREATMENT OF WIRE ANTENNAS NEAR A CURVED SURFACE, L.W. Henderson and G.A. Thiele, Reprinted in Radio Science, Vol. 16, No. 6, pp. 1125-1130, November-December 1981.

*A METHOD OF CHOOSING ELEMENT PATTERNS IN AN ADAPTIVE ARRAY, R.T. Compton, Jr., Reprinted in IEEE Transactions on Antennas and Propagation, Ap-30, No. 3, pp. 489-493, May 1982.

MOMENT METHOD ANALYSIS OF FINITE RECTANGULAR WAVEGUIDE PHASED ARRAYS, A.J. Fenn, G.A. Thiele and B.A. Munk, Reprinted in IEEE Transactions on Antennas and Propagation, AP-30, No. 4, pp. 554-564, July 1982.

*RADAR IDENTIFICATION OF NAVAL VESSELS, D.L. Moffatt and C.M. Rhoads, Reprinted in IEEE Transactions on Aerospace and Electronics Systems, AES-18, No. 2, pp. 182-187, March 1982.

*RAY ANALYSIS OF MUTUAL COUPLING BETWEEN ANTENNAS ON A CONVEX SURFACE, P.H. Pathak and N. Wang, Reprinted in IEEE Transactions on Antennas and Propagation, AP-29, No. 6, pp. 911-922, November 1981.

SCATTERING FROM CYLINDRICAL INHOMOGENEITIES IN A LOSSY MEDIUM, L. Peters, Jr., and J.H Richmond, Reprinted in Radio Science, Vol. 17, No. 5, pp. 973-987, September-October 1982.

SPREAD SPECTRUM IN A FOUR-PHASE COMMUNICATION SYSTEM EMPLOYING ADAPTIVE ANTENNAS, J.H. Winters, Reprinted in Transactions on Communications, COM-30, No. 5, pp. 929-936, May 1982.

*A SURFACE PATCH MODEL FOR POLYGONAL PLATES, E.H. Newman and P. Tulyathan, Reprinted in IEEE Transactions on Antennas and Propagation, AP-30, No. 4, pp. 588-593, July 1982.

*THE TRIPOLE ANTENNA: AN ADAPTIVE ARRAY WITH FULL POLARIZATION FLEXIBILITY, R.T. Compton, Jr., Reprinted in Transactions on Antennas and Propagation, AP-29, No. 6, pp. 944-952, November 1981.

ON WAVE MODULATION BY A ROTATING OBJECT, C.W. Chuang, P.H. Pathak and C.C. Huang, Reprinted in IEEE Transactions on Antennas and Propagation, AP-30, No. 3, pp. 486-489, May 1982.

*PHASE LINEARIZATION OF A BROAD-BAND ANTENNA RESPONSE IN TIME DOMAIN, J.L. Volakis and J.D. Young, IEEE Transactions on Antennas and Propagation, Vol. AP-30, No. 2, March 1982.

---

*Papers supported all or in part by JSEP.

*THE EFFECT OF RANDOM STEERING VECTOR ERRORS IN THE APPLEBAUM ADAPTIVE ARRAY, R.T. Compton, Jr., IEEE Transactions on Aerospace and Electronic Systems, Vol. AES-18, No. 5, pp. 392-400, July 1982.

*AN APERTURE-MATCHED HORN DESIGN, C.D. Chuang and W.D. Burnside, IEEE Transactions on Antennas and Propagation, Vol. 30, p. 790, July 1982.

---

*Papers supported all or in part by JSEP.


DATE
IL ME